



CHALMERS
UNIVERSITY OF TECHNOLOGY



Geotechnical response of an axially loaded floating pile in soft soil

An analysis in evaluating pile response at static load, including a prediction event for practising engineers

Master of Science Thesis in the Master's Programme Infrastructure and Environmental Engineering

FREDRIK EDVARDSSON
JOHANNES PETTERSSON

MASTER'S THESIS 2018:ACEX30-18-92

Geotechnical response of an axially loaded floating pile in soft soil

An analysis in evaluating pile response at static load, including a
prediction event for practising engineers

FREDRIK EDVARDSSON
JOHANNES PETTERSSON



CHALMERS
UNIVERSITY OF TECHNOLOGY

Department of Civil and Environmental Engineering
Division of Geology and Geotechnics
Geotechnical Engineering
CHALMERS UNIVERSITY OF TECHNOLOGY
Gothenburg, Sweden 2018

Geotechnical response of an axially loaded floating pile in soft soil
An analysis in evaluating pile response at static load, including a prediction event
for practising engineers
FREDRIK EDVARDSSON
JOHANNES PETTERSSON

© FREDRIK EDVARDSSON & JOHANNES PETTERSSON, 2018.

Examiner: Jelke Dijkstra, Division of Geology and Geotechnics
Supervisor: Mats Karlsson, Division of Geology and Geotechnics

Master's Thesis 2018:ACEX30-18-92
Department of Civil and Environmental Engineering
Division of Geology and Geotechnics
Geotechnical Engineering
Chalmers University of Technology
SE-412 96 Gothenburg
SWEDEN
Telephone +46 31 772 1000

Cover: Caption of the static loading test performed April 10 2018. Including the
Authors and their supervisors at Peab Anläggning.

Typeset in L^AT_EX
Printed by [Teknologtryck]
Gothenburg, Sweden 2018

Geotechnical response of an axially loaded floating pile in soft soil
An analysis in evaluating pile response at static load, including a prediction event
for practising engineers
FREDRIK EDVARDSSON
JOHANNES PETTERSSON
Department of Civil and Environmental Engineering
Chalmers University of Technology

Abstract

The design process of long floating piles relies mainly on the empirical data from static loading tests made during the 1960s and 1970s. To evaluate the validity of two of the most used techniques in Sweden, the α - and β -method, a 50 m long floating pile was tested during a static loading test. Practising engineers from all over the world were invited to predict a load- movement response curve for the loading test, along with the predicted pile capacity based on their interpretation of the term. The results from the static loading test show that the short term ultimate resistance calculated using recommended α -method is 6% higher than the short term soil failure load of the loading test. The long term ultimate resistance from the β - method is 97% of the post-peak stabilization load which correlates well with the long term ultimate resistance derived from the short term loading test of 70-80%. The long term results from the α - and β - method differ with only 2%. The compiled predictions also presents large differences, both regarding capacity and the behaviour of the pile, which indicates wide interpretations of both soil and pile data, along with different design methods used. An analysis of the force distribution in the test pile shows that the last 10 m of the pile, 17% of the total pile length, carried 55% of the maximum pile load before soil collapse.

Berförmågeberäkningar för långa kohesionspålar grundar sig i empiriska försök utförda under 1960- och 1970-talet. För att utvärdera validiteten för två av de mest använda metoderna för geoteknisk bärförmåga för pålar i Sverige, α - och β -metoden, provtrycktes en 50m lång testpåle under statisk belastning. Verksamma ingenjörer från hela världen bjöds in för att beräkna en last- rörelse- responskurva för provbelastningen, samt deras tolkning av pålens geotekniska bärförmåga. Resultatet från den statistiska provtryckningen visar att korttidsbärförmågan från α - metoden är 6% högre än korttidsbrottet från provtryckningen. Långtidsbärförmågan från β - metoden är 97% av stabiliseringslasten efter jordbrott vilken i sin tur överensstämmer väl med den härledda långtidsbärförmågan från korttidsbrottslasten i provbelastningen på 70- 80%. Långtidsbärförmågorna från α - och β - metoden skiljer endast 2% med givna α och β . De sammanställda beräkningarna från de externa ingenjörerna visar på stora skillnader, både gällande kapacitet och pålens sättningens beteende, vilket indikerar breda tolkningar av jord- och påldata samt skilda beräkningsmodeller. En analys av kraftdistributionen i testpålen visar att de sista 10 m av testpålen, 17% av pålens totala längd, bar 55% av pålagd maxlast före brott.

Keywords: Floating piles, Ultimate resistance, Force distribution, Prediction event, Alpha method, Beta method, Gothenburg clay, Static loading test, Cohesion soil, t-z- curve.

Acknowledgements

First and most, we want to thank our tireless mentors Michael Sabattini and Johnny Wallgren at Peab Anläggning for their support, ideas, and never ending explaining of various geotechnical mechanics and phenomenons. Michael and Johnny were the original promoters for the loading test, and this thesis would never have been possible without their initiative and driving force. A special thanks to Marcus Jonsson, geotechnical consultant at Peab Anläggning for taking the time to elaborate ideas and sharing his immense knowledge in the field.

We want to target great appreciation to Dr. Bengt H. Fellenius, whose extensive experience in prediction events along with his immeasurable knowledge about geotechnics were crucial for this thesis. The large network of Dr. Fellenius played a great role in the spread of the event.

Furthermore we want to acknowledge our gratitude to our examiner and supervisor Jelke Dijkstra and Mats Karlsson at Chalmers University of Technology for their guidance and critical approaches to our aims and methods, along with providing us with further knowledge in our quest to find the results.

In addition, we want to thank the following persons for their invaluable contributions and support to our work:

- Victor Karlovskis, Peab Anläggning - For his consulting concerning geotechnics in general, and pile design in particular.
- Peter Alheid, Hercules Grundläggning - For taking the time to meet with us to discuss pile design methods, and supporting our work.
- Magnus Ruin, Oskar Lynxén, Robin Kihlén, ÅF - For delivering excellent test data from the test pile , along with providing great company during the whole testing procedure.
- Peab Grundläggning - For an outstanding performance regarding pile installation and successfully keeping measuring instruments intact.
- Jesper Johansson, Peab Grundläggning - For the excellent work during the assembly of the test rig.
- Svenska Geotekniska Föreningen (SGF) - For helping us spread our prediction event.
- Various personnel at the Peab anläggning office for the support and provided knowledge.

Finally we want to address our gratitude to all anonymous participants who took their time to provide us with their pile testing predictions. This material plays a big role in our thesis, and we are very grateful for their contribution.

Fredrik Edvardsson Johannes Pettersson. Gothenburg, May 31 2018



Contents

List of Figures	xiii
List of Tables	xv
1 Introduction	1
1.1 Background	1
1.2 Aims	2
1.3 Implementation and thesis outline	3
2 Literature review	5
2.1 Floating piles	5
2.1.1 Load transfer between pile and soil	7
2.1.2 Action and resistance effect	8
2.2 Shear strength of soft soils	10
2.3 Effects of pile driving	12
2.4 Ultimate resistance	12
2.4.1 α -method	13
2.4.2 β -method	15
2.5 Static loading tests	15
2.6 Axial pile performance- t - z curves	17
3 Methodology	21
3.1 Ultimate resistance calculations	21
3.2 Static loading test	22
3.2.1 Test setup	22
3.2.2 Test instruments	24
3.2.3 Assessment	28
3.2.4 Strain and load interpretation	29
3.3 Prediction survey	30
3.4 t - z implementation	30
4 Project properties and site description	31
4.1 Soil properties	31
4.2 Pile properties	35
5 Results	37
5.1 Ultimate resistance evaluation	37
5.1.1 α - method	37
5.1.2 β - method	38

5.2	Static loading test	40
5.2.1	Load-movement response at pile head	44
5.2.2	Force distribution	45
5.3	Prediction event	46
6	Analysis	49
6.1	Loading test observations and error sources	49
6.1.1	Overall impression of the loading test	49
6.1.2	Correction with regard to uneven pressure at pile head	49
6.1.3	Impact of surrounding support piles	50
6.2	Rate of settlement and post peak response	51
6.3	Theoretical and empirical load movement response and Capacity	54
6.3.1	Predicted responses with empirical result	54
6.3.2	t - z response of pile head movement	56
6.3.3	Ultimate resistance compilation	61
6.3.4	Force distribution and resistance effect	62
6.3.5	Ultimate resistance (α - method) and shear strength	66
6.3.6	Ultimate resistance (β - method)	69
7	Conclusion	71
	References	73
A	Appendices	I
A.1	Prediction event invitation	II
A.2	Test site location	IX
A.3	Soil tests	XII
A.4	Shear strength evaluation	LXVI
A.5	Stress distribution evaluation	LXVIII

List of Figures

1.1	Predicted and actual load-movement curves of the pile head, from 3rd Bolivian International Conference on Deep Foundations (B. Fellenius, 2016). Blue lines indicate predicted load- movement curves and red line is test result from a static loading test	2
2.1	Shaft bearing Pile (Olsson & Holm, 1993)	6
2.2	Force distribution, and load- movement relationship along a floating pile (B. Fellenius, 2018)	8
2.3	Action- and Resistance effect on a single pile (Alén, 2009)	9
2.4	Load distribution at pile exposed to negative skin friction (B. Fellenius, 2017a)	10
2.5	Mohr- Coulombs soil failure criteria, (Briaud, 2013)	11
2.6	Conceptual model of stress- strain relationship of the clay- pile interface (Poulos, 1971)	11
2.7	Adhesion factor α (Tomlinson, 1970)	14
2.8	Correction factor κ_T (Eriksson, Jendeby, Olsson, & Svensson, 2004)	15
2.9	Capacities set from given load-movement curves submitted via survey (B. Fellenius, 2017a)	16
2.10	Illustration of a principal spring model from (Karlsruud, Nadim, et al., 1990)	17
2.11	Example of a typical axial loaded pile t - z curve. (API, 2007).	18
2.12	t - z curves proposed by (Karlsruud, 2014) compared with (API, 2007).	19
3.1	Test setup in 2D	22
3.2	Test setup in 3D	23
3.3	Footage from test setup, April 2018	23
3.4	Footage from the test setup, wooden frame protecting the test pile measuring instruments	24
3.5	Hydraulic jack between the test pile and support beams	25
3.6	Compressor with measuring equipment	25
3.7	Dial indicator for pile head movement	26
3.8	Prisms for the total station	26
3.9	Geokon Vibrating wire Rebar Strain Meter, close up	27
3.10	Strain meters placement in test pile	27
3.11	Computers for collection of test data	28
4.1	Shear strength compilation	32
4.2	Map of test pile area	34
4.3	Project location in Gothenburg (Google Maps)	34
4.4	Profile of test pile	35

5.1	Shear strength evaluation. Black line is the over all trend. Green and blue is local DSS and red is the used, adjusted evaluation.	37
5.2	Resistance effect of the test pile based on ultimate resistance	38
5.3	Evaluated graph for determining β (NGF, 2012).	39
5.4	Footage from the static loading test preformed April 10 2018	40
5.5	Footage from the static loading test preformed April 10 2018	41
5.6	Footage from the static loading test preformed April 10 2018	42
5.7	Footage from the static loading test preformed April 10 2018	43
5.8	Load- movement response curve of the full test. Red circles indicates, from the left, peak shear (τ_m) and steady state (τ_s)	44
5.9	Pile head movement over time	45
5.10	Force distribution at every applied load	46
5.11	Countries participating in the prediction event	46
5.12	Predicted load- movement curves from the prediction survey	47
6.1	Skewing of surface between hydraulic jack and supportive beam	50
6.2	Cracks in the concrete slab, spreading out from one of the supportive piles .	50
6.3	Pile head creep after re-stabilization at 1435 kN	51
6.4	Instantaneous vertical settlements with increased load	52
6.5	Pile head creep during the last 3 minutes of each loading step	52
6.6	Pile head movement compared to prediction survey	55
6.7	$t-z$ - curve proposed by (Karlsrud, 2014).	56
6.8	$t-z$ - curve proposed by (API, 2007).	56
6.9	Evaluated load- movement- response based on t-z - analysis with the API and Karlsrud approach, excluding pile compression.	56
6.10	[Pile length affected by stress at every loading step, API approach.	58
6.11	Pile length affected by stress at every loading step, Karlsrud approach. . . .	59
6.12	Evaluation of average stress	59
6.13	Stress distribution for applied load 728 kN. Segment length 30m.	59
6.14	Load- movement- response from $t-z$ analysis along with loading test result.	60
6.15	Compiled ultimate resistances of the test pile from predictions, compared with the static loading test, and the α - and β - methods	61
6.16	Assessed movement at predicted pile capacity	62
6.17	μ -strains registered from every sister bar mounted on level -2, -11 and -19.5m from ground surface.	63
6.18	μ -strains registered from every sister bar mounted on level -39.5 and -48m from ground surface.	64
6.19	Adjusted and pre-calculated alpha together with force distribution from the loading test result	65
6.20	Shear strength evaluation	67
6.21	Back calculated mobilized shear strength with c_u trend lines and used, adjusted c_u	68
6.22	Force distribution, and load- movement relationship along a floating pile. <i>Fellenius 2018, Development of t-z curves</i>	68

List of Tables

2.1	Loading time adjustment factor κ_t , (Eriksson et al., 2004)	13
2.2	α - values according to swedish practise (Byggnorm, 1983)	14
3.1	Properties for hydraulic jack	25
3.2	Thermal coefficient K for Steel and Concrete	29
4.1	Compiled density from CPT probe test performed by Bohusgeo AB 2011-04-12, see appendix A.3	33
4.2	Pile properties, concrete	35
4.3	Pile properties, reinforcement bars	35
5.1	Adjusted α with factor κ depending on diameter, shape and time	37
5.2	Ultimate resistance result from α - method	38
5.3	Ultimate resistance result with β from Norsk Peiliveiledning (NGF, 2012)	39
5.4	Number of drop hammer impacts and associated force	45
6.1	Evaluated α shear strength values over depth, adjusted for loading test result of 1820 kN	58
6.2	Pile compression at loading steps of the Karlsruds approach	60
6.3	Pile compression at loading steps of the API approach	60
6.4	Loading time adjustment factor κ_t , (Eriksson et al., 2004)	66
6.5	β calculated from test result	69

1

Introduction

E45, Lilla Bommen-Marieholm is an ongoing project in central Gothenburg where the main road is lowered 6 meters below ground level. The construction is scheduled to be completed in 2021 and it will then include a 400 meter-long-tunnel starting at Lilla bommen to enable for future housing and office areas at ground level. Directly below the construction site lays a more than 90 meters deep clay layer. To enable the forthcoming tunnel, roads and buildings, 3000 floating piles with a length of 65 meters have been installed in the clay. In connection to the project, the contractor is performing a static loading test on one of these piles which is located away from the construction area and it will not be a part of the final construction.

The test pile was installed in September 2017 and is instrumented with strain gauges with temperature sensors attached to the reinforcing bars at 5 levels in the pile. A hydraulic jack will incrementally apply loads up to more than 3000 kN on the pile head, and the instrumentation will provide an insight of the pile response.

By also measuring the displacement of the pile head during the loading test, a load-movement- response- curve can be obtained. To show the difficulties of predicting the pile head movements of a deep foundation, practicing geotechnical engineers from all over the world was invited to take part of the loading test information, and predict load- movement- curves with their own methods and interpretations. These were compared with the actual test result.

1.1 Background

A pile is a vertical structural element of a deep foundation, driven or bored into the ground. The deep foundation transfers the loads of the super structure either to underlying rock or soils with greater strength, in order to reduce settlements at ground level. Depending on the soil characteristics, different types of piles and shapes are used.

Early pile design consisted of strong wood elements driven into the soil, and the oxygen-free environments ensured long life spans without rot. Differing ground water levels and heavier constructions demanded other types of piles, and today steel or reinforced concrete piles are standard. The area where the city of Gothenburg is located consists several valleys between solid rock peaks, filled with mostly loose post glacial saturated clay. Here, reinforced concrete piles of varying lengths and widths is the most commonly used type for the cohesive soil.

The methods for designing a deep foundation today are mainly based on empirical data

from static loading tests carried out during the 1960s and 1970s (Jendeby, 1986; Eriksson et al., 2004). One key aspect of the deep foundation design is the relationship between the load and the pile head displacement. Previous static load tests that included prediction events indicates large differences in calculated behaviour of the pile, see Figure 2.5. The presence of many methods leads to the variety of results and yields that no general and relevant method have been proposed yet. An overestimate of the movement or ultimate resistance results in larger material usage and more expensive geotechnical solutions. An underestimate might result in construction failure. By further investigation of the pile-soil relationship, a more accurate design can be obtained.

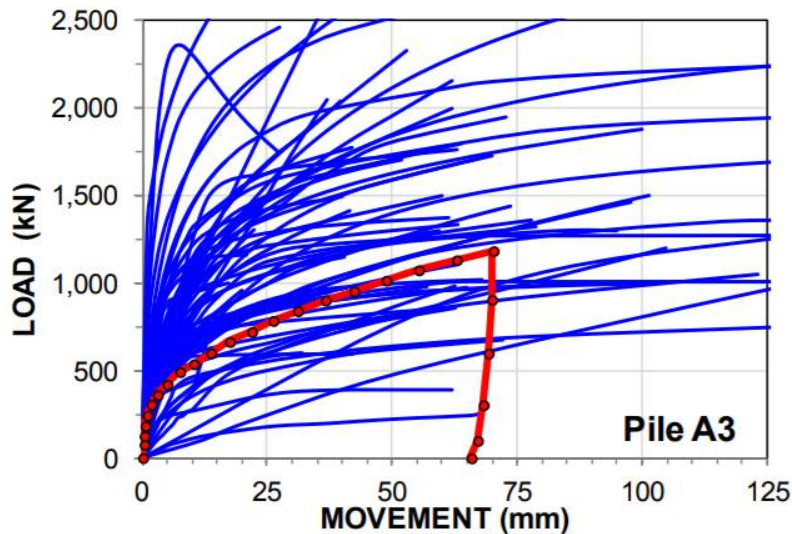


Figure 1.1: Predicted and actual load-movement curves of the pile head, from 3rd Bolivian International Conference on Deep Foundations (B. Fellenius, 2016). Blue lines indicate predicted load- movement curves and red line is test result from a static loading test

The term capacity or ultimate resistance might be somewhat diffuse terms when describing floating piles. When the loading on such is increased, it moves or compresses, i.e. the pile head moves. The question is how much can the pile be allowed to move (depending on super structure), and how much load can it carry before this displacement is reached. The question is also if and when the load- movement- curve *peak*, if this is the geotechnical capacity.

1.2 Aims

The Master thesis will investigate the result of a static loading test of a single floating pile in soft soil. The test result will be analyzed and compared with:

- Predicted load- movement response curves from practicing professional geotechnical engineers
- Common Swedish calculation methods for ultimate resistance - the α - and β - method
- Two established t - z approaches

The empirical data on which the current calculation methods are based on are mainly obtained from essentially shorter piles (Jendeby, 1986; Eriksson et al., 2004). By comparing the α - and β - method to the result from the loading test, the validity of these methods for longer piles can be investigated.

The aim is to increase understanding of the interaction between pile and soil, and to investigate force distribution in a single pile exposed to static load. Furthermore, the thesis also aims to show on the complexity of foreseeing this type of geotechnical problem.

1.3 Implementation and thesis outline

The master thesis is made up of five parts. A litterateur review, static loading test, a prediction event, hand calculations, and a result analysis. Each part with a different purpose but essential for the overall report.

A methodology chapter explains how each in going section of the thesis will be preformed and carried out. It includes how methods for ultimate resistance is use, and also how to interpret the test result from the static loading test.

The literature review initiates the thesis, it includes all theory that the calculations, assumptions and phenomenons are based on, along with providing tools for the reader to get an overall understanding of the soil and pile mechanics treated in the thesis. The chapter is based on facts and everything can be referred to the bibliography. Since the report is focusing on floating piles in soft soil in central Gothenburg/ Sweden, the literature will mostly consist of elements treating that area.

The second part is a static loading test of a floating pile implemented during the early spring of 2018. The test is a part of a research study made by Peab Anläggning and financiers. It is a major part of the master thesis and a lot of focus is given to successfully implement and analyze the test and test result.

Along with the the static loading test, the master thesis provides an opportunity for other geotechnical engineers to predict a load- movement curve at the pile head during static load, this is part number three of the thesis. An invitation to participate is sent out to Engineers in Sweden, Norway, Finland, Denmark and Canada. Each participant is provided with geotecnical data and asked to submit a load- movement curve though a given excel template. They are also asked to send the invitation to friends and colleagues to further reach out to more participants all over the world. The predictions is made with full confidentiality.

The thesis will also include hand calculated pile ultimate resistances and load movement responses using different methods and approaches. This forth part is based on theoretical calculation methods and will be compared with test result from the static loading test and submissions from the prediction event.

Part number five is an analysis and compilation of the result from the static loading test , hand calculations and prediction event. This last part constitute basis for discussion and conclusions.

2

Literature review

In deep foundation design in cohesive soils, analysis of how the axial load from completed construction transfers from piles to soil is of most importance. The following chapter consists of literature based theory, and everything can be referred to the bibliography with a purpose to provide tools for understanding of soil and pile mechanics.

2.1 Floating piles

Floating piles, piles made for clay, defines as piles with a bearing capacity derived mainly from adhesion of the soil in contact with the pile shaft. The purpose is to transfer load from buildings, bridges etc. to deeper clay layers though mainly skin friction (Eriksson et al., 2004). Toe resistance is considerable smaller, hence it is often omitted in dimension design. Figure 2.1 illustrates a general case of a shaft bearing pile exposed with vertical load Q . The stresses are mobilized along the pile at the interface between pile and soil. Further, simplified technical bearing capacity of the pile can be expressed with equation 2.1 (Alén, 2009)

$$R = Q_m + Q_s = f_m * A_m + f_s * A_s \quad (2.1)$$

where

R = Geotechnical bearing capacity

Q_m = Shaft resistance

Q_s = End resistance at pile toe

f_m = Average shaft friction

A_m = Area of the shaft

f_s = Nominal compressive strength of the soil at the toe at ground failure

A_s = Area of the pile section at the toe

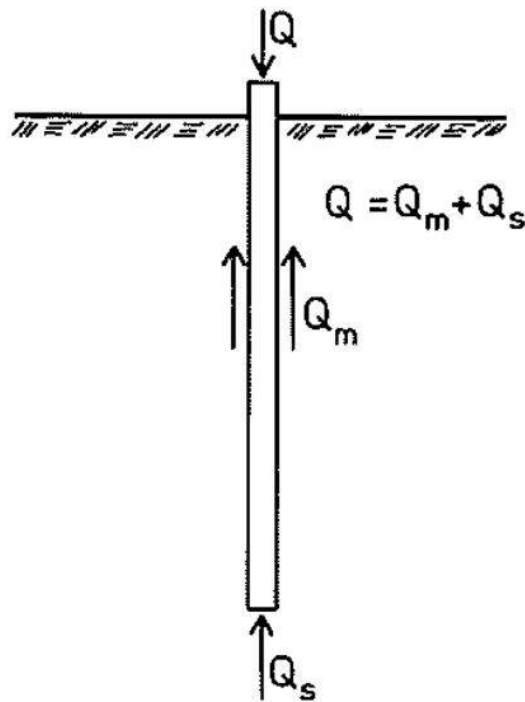


Figure 2.1: Shaft bearing Pile (Olsson & Holm, 1993)

Described in equation 2.1 the capacity of the pile can be seen as the sum of shaft and toe resistance. However, the term "capacity" is an *"imprecise concept"* according to Dr. Bengt H. Fellenius, a professional engineer specializing in foundation design. *"In many cases, an ultimate shaft resistance value does not exist"*. In an ideal environment, all movement after the elastic deformation is irrelevant, the magnitude of force needed to go beyond elastic deformation is equal to the carrying capacity (B. Fellenius, 2017a). But since toe and shaft resistance both mobilize during movement, this can be a response to applied vertical load or due to down drag, see Chapter 2.5, follows that the *capacity* in terms of total soil collapse will in most cases not be reached. Dr. Fellenius means that pile design should be based on settlement and construction deformation rather than *capacity*.

Dimension prerequisites for a geotechnical construction must contain the most critical combinations of load effect and geotechnical bearing capacity (Olsson & Holm, 1993). Risk for corrosion, local and regional settlement and pile fracture has to be evaluated in the calculations. The generalized requirement for Ultimate limit state pile design is:

$$R_d \geq S_d \quad (2.2)$$

Where

S_d is dimensioned load effect

R_d is dimensioned bearing capacity from equation 2.1

2.1.1 Load transfer between pile and soil

The response of a cohesion pile to an applied axial load is to transfer it to the soil via shaft and toe resistances, which both increase with increased relative movement. (*Fellenius - Report 380, 2017*) The resistances depends on among other things the surrounding stress, expressed as overburden effective stress, and shear stiffness. That is, the shaft resistance along a specific pile element or toe resistance for a pile toe element are functions of the effective overburden stress and the relative movement between the pile and the soil at the element considered.

When applying Hooke's law on both the pile and the soil, it is evident that an applied load on a floating pile results in movement of the pile head. This is a combination of the pile compressing due to axial stress, and soil deformation due to shear stress, in simplified terms.

$$\epsilon = \sigma/E \quad (2.3)$$

$$\gamma = \tau/G \quad (2.4)$$

where

ϵ = Strain

σ = Stress

E = Elasticity modulus (Young's modulus)

γ = Shear strain

τ = Shear strength

G = Shear modulus

Due to varying shear stiffness and effective stresses with the depth, the settlement of the pile head is a result of different mechanics in different depths. In the uppermost part of the pile, the shear strength and effective stresses of the soil is lower than in greater depths, hence the pile can slide more easily along the soil. This, combined with negative skin friction, results in no net resistance down to the neutral plane (further explained in chapter 2.1.2). In the lowermost part, under the neutral plane, the shear strength is large enough to withstand all the loads carried down via the pile, and the pile foot is at a start practically still. These mechanisms results in a compression of the pile between the head and neutral plane due to applied loads, and a settlement of the pile below the neutral plan when large enough loads are applied. This is also dependent of load magnitude, since lower loads indeed can be transferred to the soil in the upper part with the lower pile unaffected by these.

As can be seen in Figure 6.22, it is suggested (Fellenius 2018, Development of t-z curves) that plastic deformation is reached along the pile at different loads. I.e. the upper part of the pile might have reached its bearing capacity while the lowermost part hardly mobilized any stresses at all.

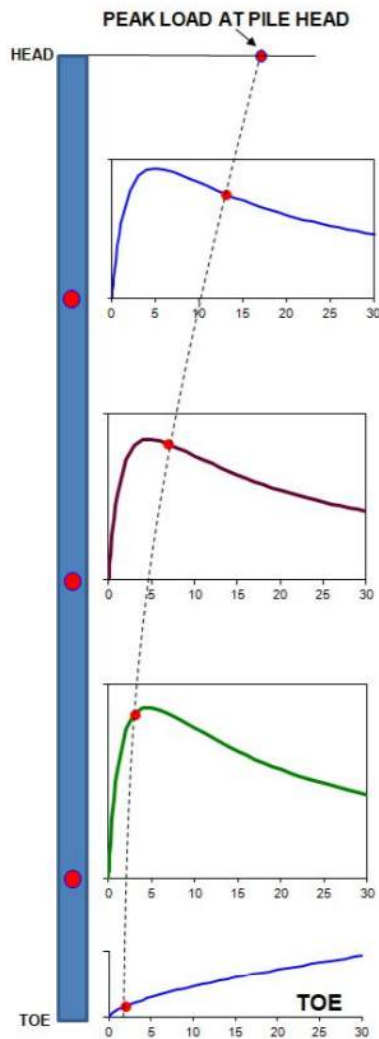


Figure 2.2: Force distribution, and load- movement relationship along a floating pile (B. Fellenius, 2018)

The design process of deep foundations normally involves the prediction of both capacity and settlement. Since noticeable movement of the pile is needed to mobilize resistance of the lowermost part, the predicted settlements may affect its design (Bradshaw, Haffke, & Baxter, 2012). Advanced models for computing the load- movement behavior of deep foundations are based on a load transfer method. The “t-z curve” defines the load transfer relationship along the shaft of the foundation and “q-z curve” defines the relationship at the toe where t is the mobilized unit shaft resistance, q is the mobilized unit toe resistance, and z is the vertical movement of a point on the pile."Both shaft and toe resistance are usually just referred to by a strength value, a certain proportionality coefficient called alpha, or beta times the effective stress or shear strength, acting at the element. However, that value is not meaningful unless the movement at which it is mobilized is also noted and moreover, also the shape before and after this resistance- movement point on the curve. (B. Fellenius, 2017b)

2.1.2 Action and resistance effect

During operating conditions, the pile is affected by a permanent, (or *dead*) load, a variable (*live*, or *transient*) load and an additional down drag caused by settlements of surrounding soil, negative skin friction. Even if the settlements are small or unnoticeable, this is an always occurring phenomenon based on the relative movement between pile and adjacent soil due to consolidation and creep (B. Fellenius, 2017a). It can be translated into an action effect on the pile, see figure 2.3 and is calculated with equation 2.5.

$$E = Q_p + \int_0^z f_m dA \quad (2.5)$$

To counteract this action effect, the pile has a resistance effect, figure 2.5, calculated using equation 6.3.4.

$$R = R_{toe} + \int_z^{L_p} f_m dA \quad (2.6)$$

where

Q_p = Dead load

L_p = Length of pile

f_m = Average shaft friction

A = Pile circumference area

R_{toe} = Toe resistance

z = Depth

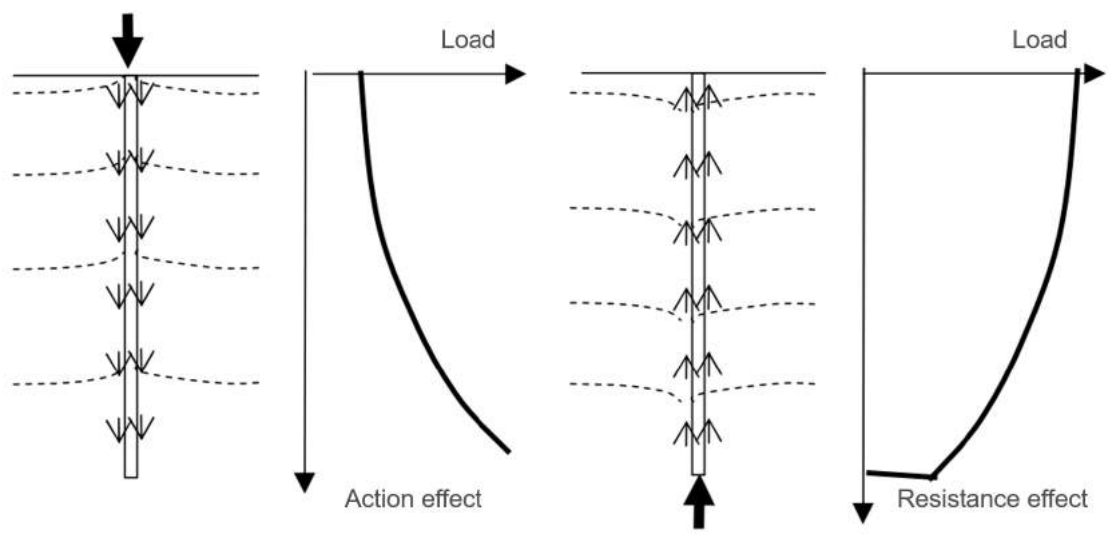


Figure 2.3: Action- and Resistance effect on a single pile (Alén, 2009)

Even though Negative skin friction is an always occurring phenomenon, it can be hard to estimate the rate of settlement if the effective stress σ' is less than pre consolidation pressure σ'_c , hence it is assumed the creep, and down drag, is neglected if $\sigma' \leq 0.8\sigma'_c$ (Eriksson et al., 2004). In conclusion negative skin friction is only considered along the pile, where the verticle effective stresses are greater than $0.8\sigma'_c$.

Combining the action load effect with the resistance effect of the pile, the load distribution on a single pile can be estimated, this is illustrated in Figure 2.4. The point where action effect and bearing capacity (or resistance effect) collide indicates a force equilibrium called neutral plane, it is the depth of where shear stress along the pile converges from negative skin friction to positive shaft resistance.

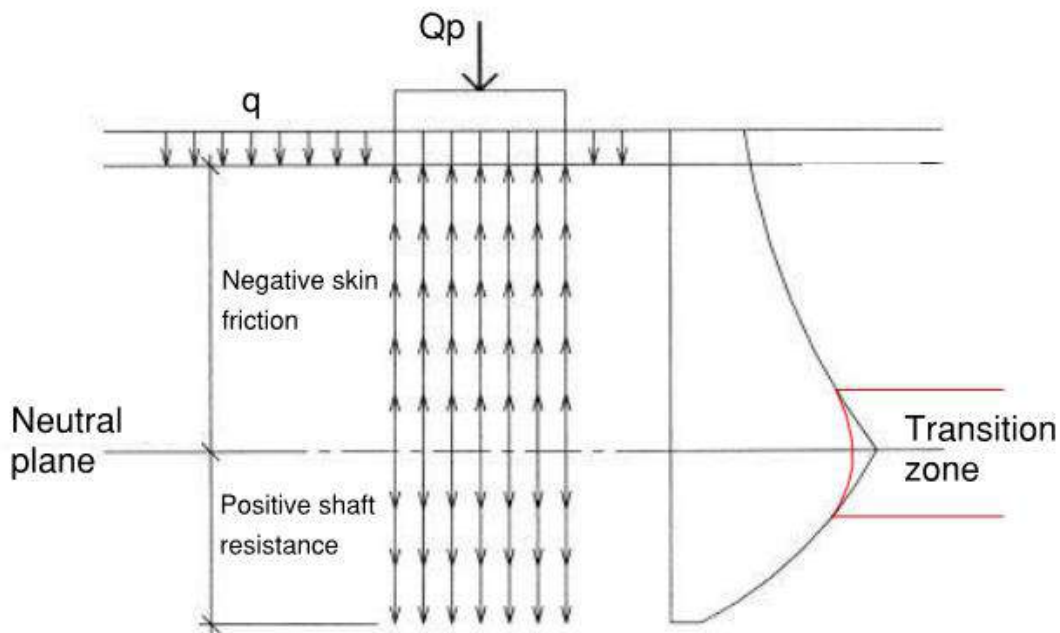


Figure 2.4: Load distribution at pile exposed to negative skin friction (B. Fellenius, 2017a)

Settlements above the neutral plane consist of mainly compression of the pile due to the permanent load and negative skin friction, but since the pile is stiff, this deformation is often small and can in many cases therefore be neglected. However, the longer the pile, the greater the compression, and since *Swedish* piles in general are long and slender, compression and buckling can be a larger contributor to pile head movement. Settlements from under the neutral plane is mainly due to pile movements relative to the soil, and stands for the majority of the plastic settlements of the pile. The relative movement between soil and pile at the neutral plane is zero and therefore the neutral plane is also the *settlement- and strain equilibrium*. However, the transition between negative skin friction and positive shaft resistance is in reality a smooth transition and not a fix point, or plane (B. Fellenius, 2017a). The *Transition zone* can vary in length depending on type of soil, and shaft friction. Increased toe resistance makes for a lower depth for the neutral plane and higher load make for a shallower. In general, the neutral plane is set under the middle point of the pile, depending on pile length.

2.2 Shear strength of soft soils

Fine grained soils such as clay is soils with a grain size is less than $1/256$ mm. Because of its structure, in addition to frictional forces there is a molecular attractive force between the particles, cohesion force. Together they make for the soil shear strength. Shear strength is defined as the amount of shear stresses that a soil can sustain. It can typically be described and defined using the Mohr- Colombs failure criterion, based on Mohr ´s circle where σ_1 and σ_3 are major and minor principal stresses respectively, and τ is the shear strength. (Smith, 1982)

$$\tau = (\sigma_1 - \sigma_3)/2 \quad (2.7)$$

Soil failure occurs where Mohr's circle tangent Mohr's failure envelope line, see Figure 2.5

$$\tau = c' + \sigma' \tan \phi' \quad (2.8)$$

The failure envelope line represents technical mechanics of the soil in terms of apparent cohesion c' , effective stress σ' and internal friction angle ϕ' (Briaud, 2013)

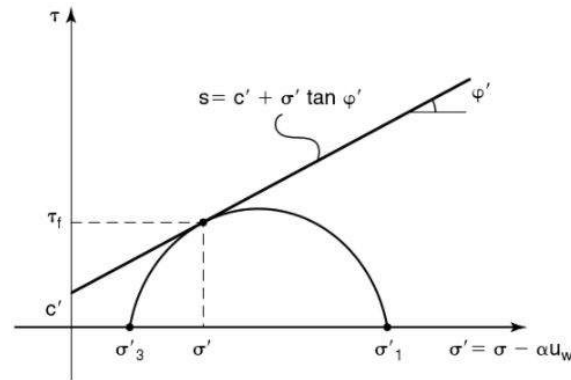


Figure 2.5: Mohr- Coulombs soil failure criteria, (Briaud, 2013)

Applied loads and increment of the stresses in the soil, results in an axial or shear strain. Figure 2.6 illustrates a typical stress strain relationship of clay where the strains eventually leads to soil failure where the curve peaks. This is the maximum shear strength value τ_{max} .

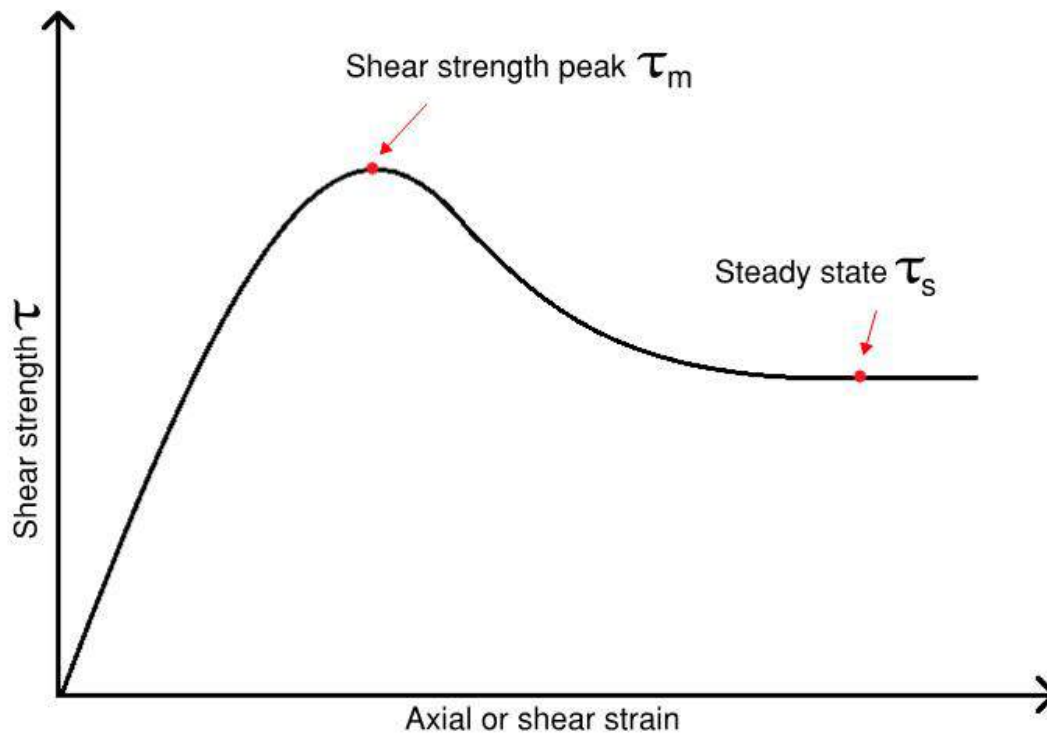


Figure 2.6: Conceptual model of stress- strain relationship of the clay- pile interface (Poulos, 1971)

Shear strength of clay (c_u) is time dependent (Torstensson, 1973), meaning that the appearance of the curve changes depending of loading time. Faster loading time allows for a higher resistance (higher peak) with a steeper inclination of the first part of the curve and vice verse. Other factors which matter for the shape of the first part of the curve is initial structure, state, and methods of loading (Poulos, 1971). The initial state and structure of the soil is altered after maximum shear, until steady state deformation is reached, τ_s . This steady state phenomenon can also be seen as a long term shear state. In a doctoral study made at Chalmers university of technology in Sweden, short and long term testing were made on short pre-cast concrete pile elements. The relationship between steady state and maximum shear, τ_m/τ_s were approximately 70% (Yannie, 2016). 70% is also an accepted assumption in Sweden when calculating ultimate resistance of floating piles in long term loading, (Eriksson et al., 2004), see Chapter 2.4.1 (κ_t).

2.3 Effects of pile driving

In short terms, the process of driving and installing a displacement pile in soil consists of exposing the pile to a series of vertical short duration impacts on its head. This is forcing it to penetrate the soil and overcome the the dynamic soil resistance, causing vertical movement. Clay and other low permeability soils exposed to this type of structural disturbance entail large displacement and properties changes. This stress strain response varies over time from instillation changes to long term effects. The process can be derived into three stages, installation, equalization and loading (Ottolini, Dijkstra, & van Tol, 2014).

During the pile installation, the pile toe penetrates through the soil, remoulding the layer closest to the pile. The adjacent soil is displaced perpendicular to the pile, resulting in increased mean total stresses in surrounding soil (Ottolini et al., 2014). Since the soil is often regarded as untrained (no volume change), the total stress is accommodated by increased excess pore pressure (Karlsrud, 2014).

Over time, the excess pore pressure will dissipate, increasing the effective stresses and re-consolidation of surrounding soil begins. The loss of shear strength due to remolding is slowly regained, increasing the theoretical geotechnical bearing capacity (Skov & Denver, 1988). The loading phase consist of load transfer between pile and soil, see Chapter 2.1.1.

2.4 Ultimate resistance

Equation 2.1 is a simplified expression of the geotechnical bearing capacity of a floating pile. The average shaft friction f_m is expressed in different ways when developing the equation depending on calculation method. In Sweden, the calculation is often based on undrained soil conditions. Exceptions are made (often with over consolidated clays) where drained conditions are used instead. These two ways of calculating the geotechnical bearing capacity are characterized using adhesion factor α and β respectively and are consequently called α - and β - method. There are more ways of determining the bearing capacity, however, the thesis will only treat the α - and β - method due to its commonness and usage in Sweden. Both methods are using the skin resistance part of Equation 2.1:

$$R_{skin} = f_m * A_m \quad (2.9)$$

This can also be written as:

$$R_{skin} = \int_{L_p} f_m \theta dz \quad (2.10)$$

where:

θ = Circumferential area

L_p = Pile length

2.4.1 α -method

The α -method is based on total shear strength analysis and expressed as a function of undrained shear strength c_u . Therefore, the result from the α - method is directly dependent on *good* c_u investigations. Initially, the skin resistance of floating piles were proposed by Tomlinson, (Tomlinson, 1970), using undrained cohesion c_u , adhesion factor α , lateral earth pressure coefficient K , effective average vertical stress \hat{q} and effective friction angle δ :

$$f_m = \alpha c + \hat{q} K \tan \delta \quad (2.11)$$

This is however not generally used, rather it was simplified so that the shaft friction using the α -method is (Bowles, 1997):

$$f_m = \alpha * c_u \quad (2.12)$$

The pile toe resistance can be expressed with a load factor N_s , (usually between 6-9) times shear strength (Alén, 2009):

$$f_s = N_s * c_u \quad (2.13)$$

Chapter 2.1 explains how shear strength of soil is depending of the increment time. Higher loading rate results in a stiffer behavior whereas a slower phase loading equals a less stiff behavior. Due to this, the shear strength c_u can be corrected with a loading time factor κ_t , (Eriksson et al., 2004).

$$C_{corr} = \kappa_t * C_{uncorr} \quad (2.14)$$

Table 2.1: Loading time adjustment factor κ_t , (Eriksson et al., 2004)

Duration	Example of load types	κ_t
"Minute"	Shear strength testing with wing test, Wind load, by- passing cars etc.	1.0
"Day"	Short time material setup etc.	0.9
"Month"	material stocking, high tides etc.	0.8
"Long time"	Dead load, stocking etc.	0.7

Combining Equations 2.1, 2.10, 2.13 and 2.12 gives a final equation for the geotechnical bearing capacity with the α method, it can be written as:

$$R = \int_{L_p} \alpha c_u \theta dz + N_s c_u A_s \quad (2.15)$$

Where α is an adhesion factor of the undrained shear strength and c_u is the shear strength of the soil at the point of interest. Figure 2.7 illustrates the relation between α and undrained shear strength c_u (or s_u) proposed by (Tomlinson, 1970). It shows a value between 0.5 and 1.1 depending on source. α -value used in Swedish practice depending on pile material are shown in table 5.2 (Byggnorm, 1983). Kjell Karlsrud gathered other methods for α -interpretations in his report (Karlsrud, 2014). It insinuates that more parameters besides shear strength are needed to evaluate alpha.

Proposed by the Swedish pile commission, report 100, assume an $\alpha_{uncorrected}$ (α_{uncorr}), $\alpha=1$. This value is then adjusted with factor κ depending on:

- κ_ϕ - Diameter. 0.9 for *normal piles* ($D_p \approx 0.3m$)
- κ_f - Shape. Equal to 1 when using a constant cross section.
- κ_T - Time after installation, see figure 2.8

In conclusion, adhesion factor α can be calculated as:

$$\alpha = \alpha_{uncorr} * \kappa_\phi * \kappa_f * \kappa_T \tag{2.16}$$

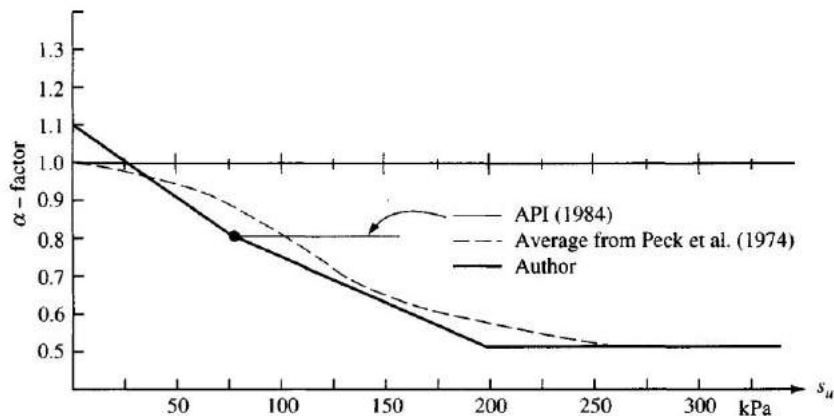


Figure 2.7: Adhesion factor α (Tomlinson, 1970)

Table 2.2: α -values according to Swedish practice (Byggnorm, 1983)

Pile material	α -value
Wood	0.8
Concrete	0.7
Steel	0.7

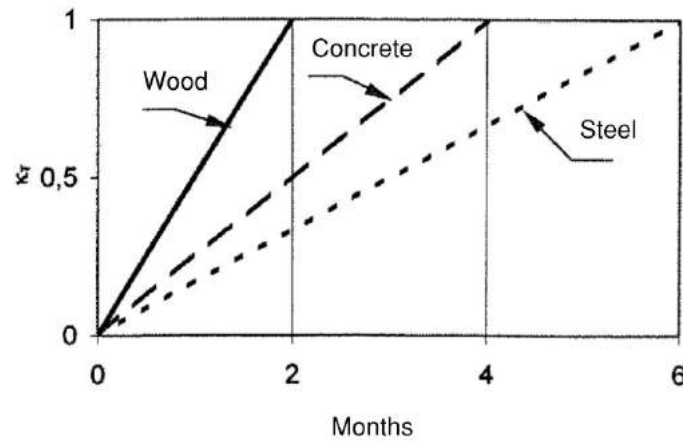


Figure 2.8: Correction factor κ_T (Eriksson et al., 2004)

2.4.2 β -method

The β method is used to calculate the long term ultimate resistance (Wrana, 2015), and relates the skin resistance to effective stresses in the soil (Chandler, 1968) (Burland, 1973). The geotechnical bearing capacity R is expressed as a function of adhesion factor β and effective stress σ'_o (Olsson & Holm, 1993). β contains both friction angle ϕ' and earth pressure coefficient K' .

$$R = \beta * \sigma' \quad (2.17)$$

$$\beta = K' * \tan\delta \quad (2.18)$$

$$K' = 1 - \sin\phi' \quad (2.19)$$

$$\tan\delta = \tan\phi' \quad (2.20)$$

The β - factor can also be empirically evaluated without the friction angle and earth pressure coefficient. See chapter 5.1.2 for evaluation of β . With a changing effective stress along the pile, R can be evaluated by integrating σ' times the circumferential area of the pile, θ , over the length of the pile L_p , see equation 2.21.

$$R = \int_{L_p} \beta \sigma'_o \theta dz \quad (2.21)$$

2.5 Static loading tests

One may argue that a prediction of movement due to a static loading test has very little to do with the design phase of a deep foundation. What is evident though is the range of interpretations made from different actors when trying to predict the behaviour of the pile, Figure 2.9 illustrates result from a previously made prediction event arranged by Dr. Fellenius, (B. Fellenius, 2017a). With or without a prediction event connected to the test, it provides important information about the soil- structure interface between the pile and

soil. Load tests are usually short events, between a few hours up to a few days. This short duration procedure fails to examine the long term behaviour of the pile, but gives an useful insight of the direct response of the applied load. For most projects the main purpose of pile testing is either to validate the design before construction and/or to check compliance with the specification during construction. However pile testing is also used in research to provide better solutions, and for design development.

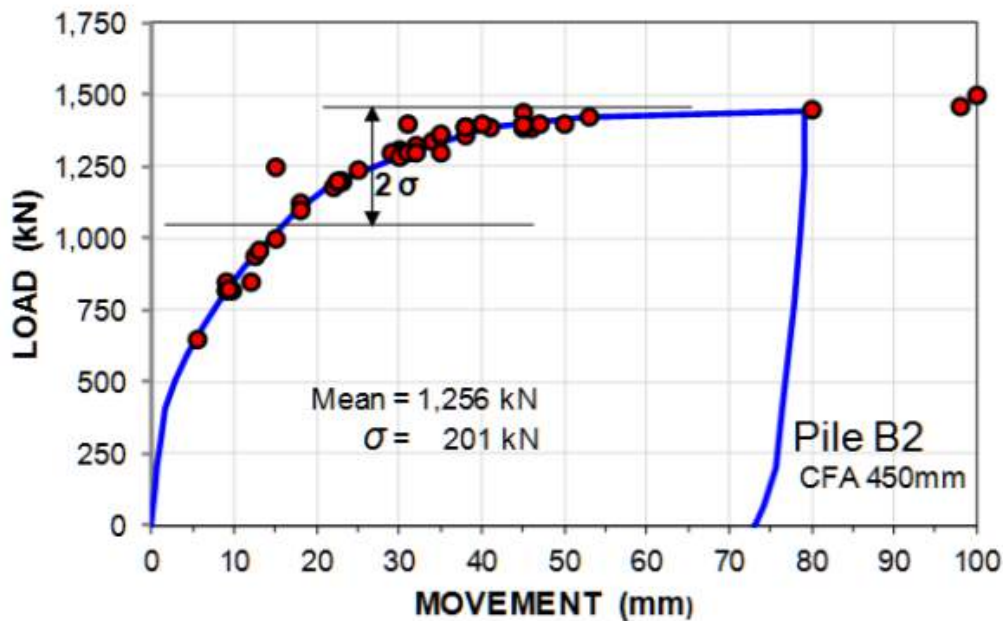


Figure 2.9: Capacities set from given load-movement curves submitted via survey (B. Fellenius, 2017a)

There are several different pile loading test techniques, but it is the static loading test (Static Maintained Load) that is treated in this thesis. Conducting a Maintained Load Test (MLT), a load is applied to the pile head during a set of loading steps, and the resulting pile movement is monitored. Following load steps are only applied when the minimum specified time period has elapsed and the rates of induced settlement are below the specified criteria. Normal practice is to load the pile up to design verification load (DVL), then to unload back to zero loading. Following load cycles can be applied, taking the loading to specified values above the DVL depending on the requirements and aims of the test. Another common procedure is to simply apply the loading steps until soil failure and then initiate cyclic loads. The MLT method is normally the most suitable in determining the load/settlement performance of a pile under working loads and at 1.5 times working load conditions (Federation of Piling Specialists, 2006)

The design of long piles, 50 m and longer, is mainly based on loading tests performed on considerably shorter piles, along with a few tests made during the 1960s and 1970s on longer piles (B. H. Fellenius, 1972) (Eriksson et al., 2004) (Jendeby, 1986). For example, 1968 to 1972, two 50 m long piles was tested in Gothenburg Sweden (B. H. Fellenius, 1972). By testing longer piles, it can be further investigated if and how the design techniques developed during the 1960s and 1970s can be applied to longer piles. It should be mentioned though that static loading tests on piles is generally uncommon in Sweden.

2.6 Axial pile performance- t - z curves

The principals of load- movement response makes use of axial pile shear transition vs. local pile deflection. This is used to model the relationship between mobilized soil- pile-shear- transfer and pile deflection (t - z curve). There are numerous different methods for interpret these kind of axial load transfer and pile displacement curves (API, 2007). The most commonly approach is by modeling the mobilization of shaft friction modeled as a set of springs distributed along the pile shaft, and the axial elastic stiffness of the pile (Karlsrud, 2014). Figure 2.10 illustrates a principal sketch of the system (Karlsrud et al., 1990). The recommended and most commonly applied t - z - curves are from the American Petroleum Institute (API).

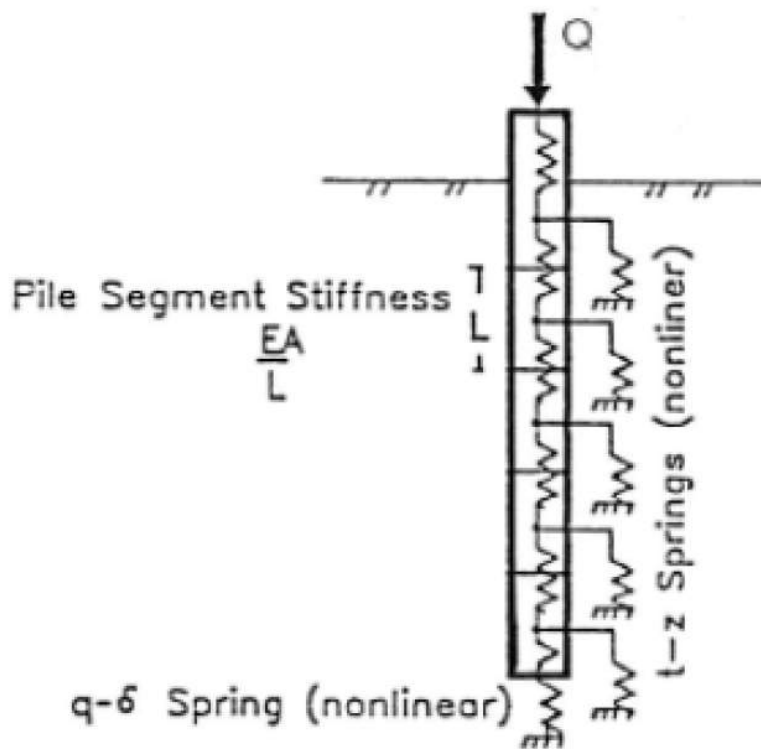


Figure 2.10: Illustration of a principal spring model from (Karlsrud et al., 1990)

Figure 2.11 presents a proposed $t-z$ curve from API. It includes a non-linear response to a peak value, followed by a reduction to a residual value. Values for the residual adhesion shear, t_{max} (earlier mentioned as τ_s) should be carefully considered between a value of 0.7-0.9 times τ_m , similar to what is stated in Chapter 2.1.

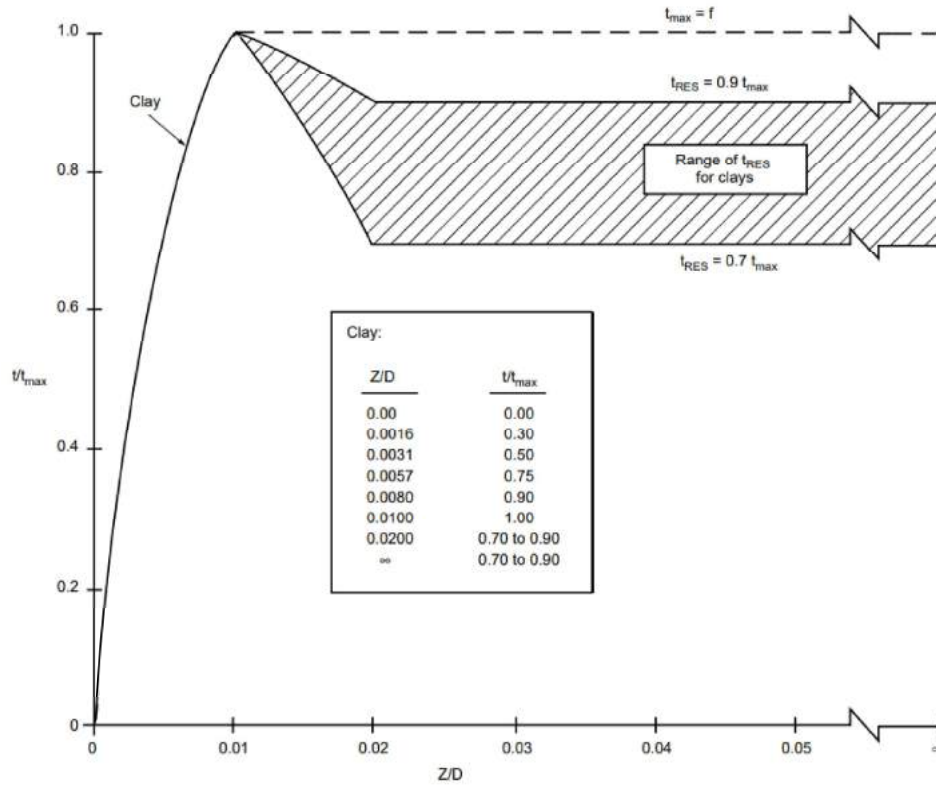


Figure 2.11: Example of a typical axial loaded pile $t-z$ curve. (API, 2007).

Where:

z = Local pile deflection [mm]

D = Pile diameter (side length in this case) [mm]

t = Mobilized soil pile adhesion [kPa]

t_{max} = Maximum soil pile adhesion [kPa]

Another approach to develop a $t-z$ curve has been made by Kjell Karlsrud in his doctoral thesis (Karlsrud, 2014). He suggests that the peak value in the x-axis (z_p/D) is in the range $z_p/D = 0.01-0.02$ for open piles and $z_p/D = 0.02-0.04$ for closed piles, rather than $z_p/D = 0.1$ as was suggested by API. He also emphasizes in his study that the post peak, residual strength, is mostly in range of a 10-20% reduction. Figure 2.12 shows proposed $t-z$ curves compared with (API, 2007).

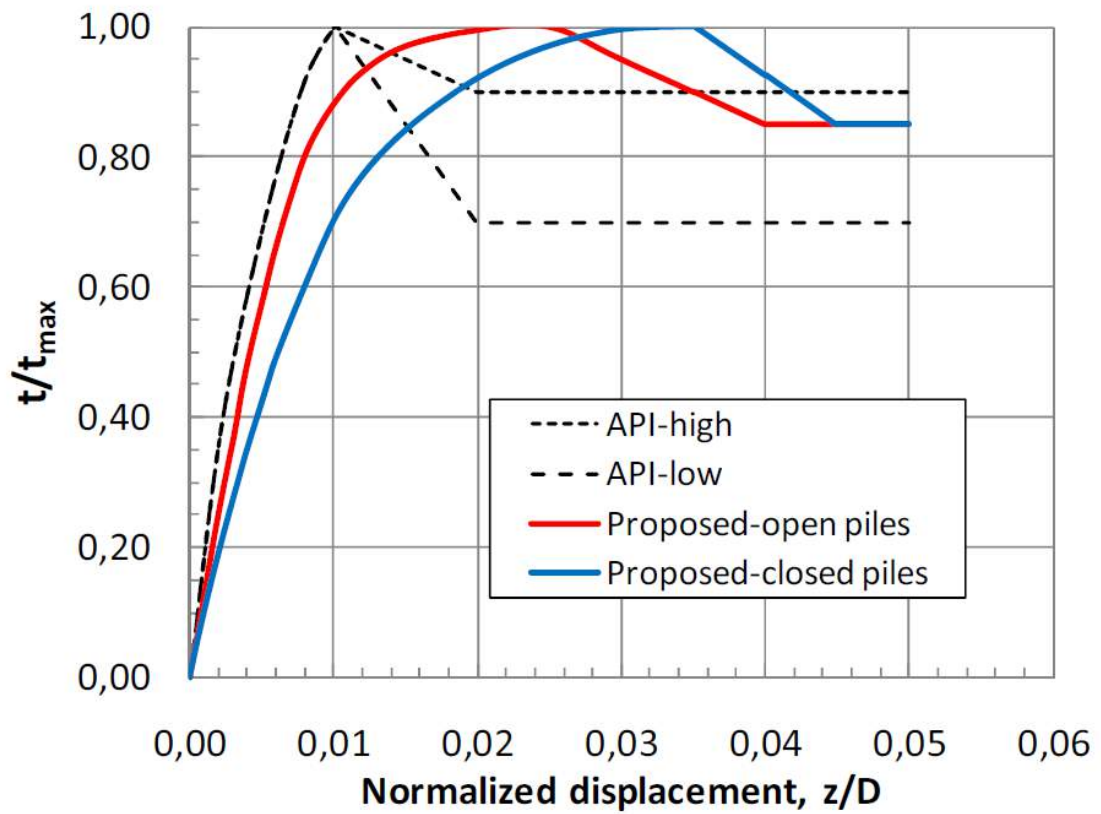


Figure 2.12: t - z curves proposed by (Karlsruh, 2014) compared with (API, 2007).

3

Methodology

3.1 Ultimate resistance calculations

The ultimate was calculated with α - and β - method according to literature, see chapter 2.4. Pile diameter, shape and length is specified in chapter 4

α method

The evaluation of shear strength was made in 2 steps:

- Over all trend from direct shear (DSS), CPT, Triax and CRS tests
- Adjust trend to DSS made by the contractor in the area.

It was assumed that shaft resistance is equal to ultimate resistance, hence toe resistance is negligible.

$$R = \int_{L_p} \alpha c_u \theta dz + N_s c_u A_s \quad (3.1)$$

$$R = \int_{L_p} \alpha c_u \theta dz \quad (3.2)$$

Shear strength was evaluated based on soil values from chapter 4. Plotted trend lines were adjusted with result from direct shear strength tests from borehole 16GT03 and 16GT07. Both of these tests indicate a higher shear strength with increased depth than the over all trend and it was therefore believed that the local soil is stiffer, hence it was adjusted.

Adjustment factor κ (see chapter 2.4.1), for diameter, shape and time, were selected accordingly, along with time dependant factor κ_t .

β method

$$R = \int_{L_p} \beta \sigma'_v \theta dz \quad (3.3)$$

The resistance calculated with the β -method is dependent on the effective stress of the soil surrounding the pile. The advantage of this method is that changes in effective stress due to future construction can be taken into account when designing the pile. As can be seen in chapter 2.1, the shear strength is directly dependent on the effective stress. Since the pile testing occurs during one day only, and no additional load is exposed to the surrounding soil, no additional effective stresses needs to be added, thus an empirical relation between the α - & β - methods can be obtained. This is further examined in chapter 5.1.2.

3.2 Static loading test

The Static loading test was carried out April 10 2018. This chapter includes and describes the test setup, implementation, instruments used, and interpretation of the test result.

3.2.1 Test setup

The test pile is surrounded with four 40 meter long concrete piles, called supporting piles, attached to two HEB800 Beams with dimensions 800 x 300 mm. These are welded on the surrounding piles and creates a cross over the middle test pile. See Figure 3.1, it illustrates the test setup in 2D plane.

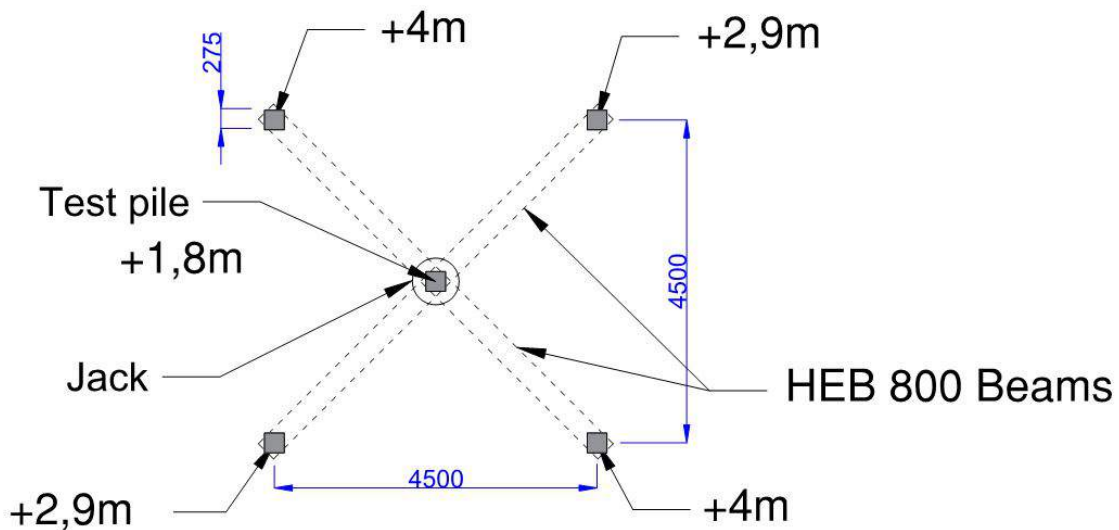


Figure 3.1: Test setup in 2D

During the test, the hydraulic jack seen in Chapter 3.2.2 applies pressure on the test pile which creates a drag force on the acting supporting piles as well as a pressure force on the test pile, see Figure 3.2. This will successively mobilize the pile as more load is applied. The diagonal length between the middle test pile and supporting piles is 3.2 m which is long enough to ensure that the uplift of supporting piles do not affect the soil adjacent to the test pile (Ottolini et al., 2014).

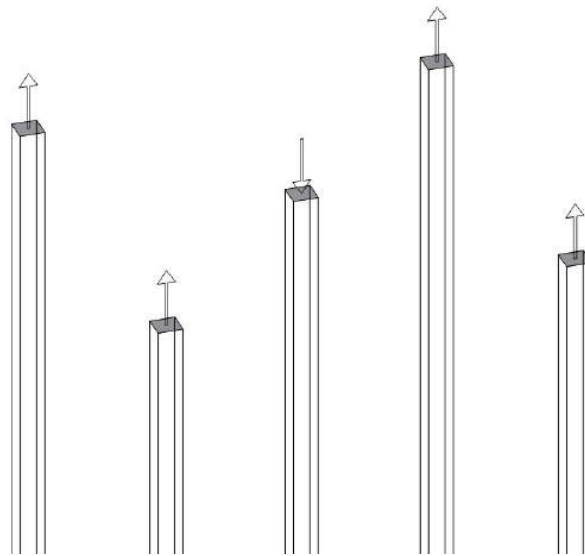


Figure 3.2: Test setup in 3D

Figure 3.3 shows footage of the test area during the static loading in April 2018. To stabilize the test setup and prevent bending of the supporting piles, an area of 5 x 5 meter was cast in 15 cm concrete, fixing the supporting piles in place. This do not apply the middle pile whereas the area closest to the test pile remains untouched to ensure that it is not effected by surrounding movement, see Figure 3.4. A wooden frame between surrounding soil and test pile creates gap, allowing passage for measuring cables between soil surface and protective half pipe steel frame, Chapter 3.2.2.



Figure 3.3: Footage from test setup, April 2018



Figure 3.4: Footage from the test setup, wooden frame protecting the test pile measuring instruments

3.2.2 Test instruments

The static loading test is carried out using a hydraulic jack and compressor. The procedure is monitored throughout the whole the test with continuous measurements of the pile head vertical movement, movements of the supporting structures, including surrounding piles and beams, and stresses in reinforcing bars. The vertical position of the pile head is correlated with a reference beam with constant height and measured with sprung-loaded displacement meters and a total station, this also gives information about any horizontal movements of the pile head. Supporting structures is measured with a total station, and the stress distribution in the test pile is monitored using vibrating strain gauges installed in its reinforcement bars.

Hydraulic Jack

A 320 metric ton calibrated hydraulic jack is placed between the pile head and the lower end of the steel cylinder welded underneath the lower support beam. Its properties is presented in Table 3.1. The jack is connected to a compressor equipped with a micro-processor based transmitter, and a dial indicator, to measure the pressure. The compressor was calibrated at two separate occasions by two different companies. The digital transmitter LEO 3 was in turn digitally logged to a computer.

Table 3.1: Properties for hydraulic jack

Unit	Value
Model	ZD 8403.300.8
Max load [t]	320
Max pressure [kN]	3206
Max pressure [bar]	700
Max piston length [mm]	300
Piston area [cm ²]	458
Jack weight [kg]	120.8

**Figure 3.5:** Hydraulic jack between the test pile and support beams

(a) Pressure gauge LEO 3 .



(b) Pressure gauge LEO 3, with dial indicator and compressor

Figure 3.6: Compressor with measuring equipment

Sprung-Loaded displacement meters

Mounted on the fixed wooden reference beams is three sprung-loaded displacement meters (DC LVDT from Monitran) to monitor the vertical displacement of the pile head. All three is digitally monitored with millimeter accuracy, and one is also equipped with a dial indicator which was read every third minute during the whole test and compared to the digital data.



Figure 3.7: Dial indicator for pile head movement

Total station

With the aid of a total station, the movements of both the test pile, and the supportive construction is monitored. Prisms is placed on the test pile head, and on the ends of the supportive beams. This allows both the vertical and possible horizontal movement of all elements involved to be tracked and logged.



(a) Prism on the lower support beam



(b) Prism on the upper support beam

Figure 3.8: Prisms for the total station

Vibrating strain gauges

The pile is provided with "Geokon Vibrating wire Rebar Strain Meters", called sister bars. These are strain gauges attached to the reinforcing bars and are designed to monitor stresses in the test pile. Figure 3.9 illustrates a close up of the sister bar, showing it welded and attached to a section of a structural concrete reinforcing bar. Bored and installed along its central core axis is a miniature vibrating wire strain gauge. As the steel is exposed to strain or compression, the vibrating frequency of the wire is picked up by an electromagnetic coil and sent to a readout unit console. The strain meter is also equipped with a thermostat to accommodate for expansions and contractions due to temperature changes

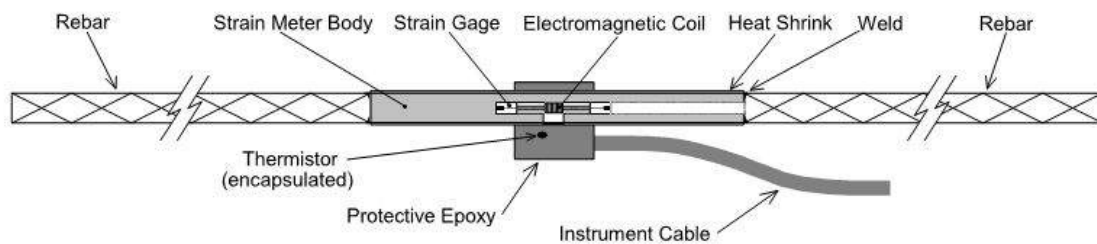
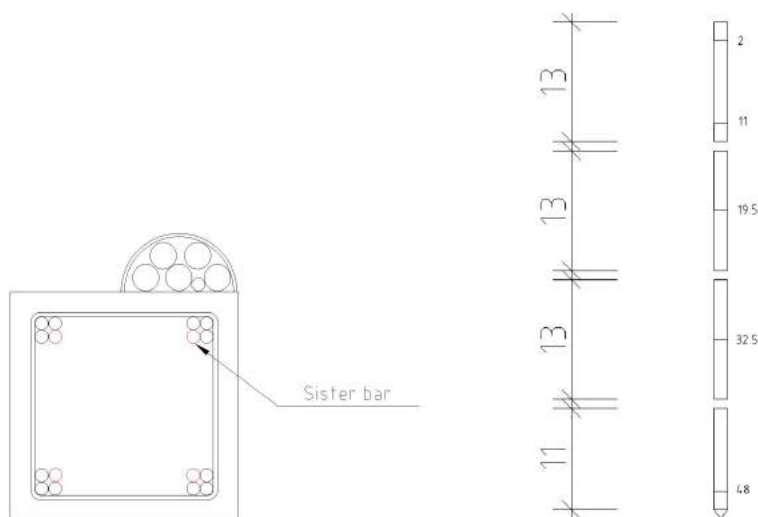


Figure 3.9: Geokon Vibrating wire Rebar Strain Meter, close up

The sister bars are installed at five levels, 2, 11, 19.5, 32.5 and 48 meters below pile head and are attached in each corner of the pile cross section, see figure 3.10.



(a) Cross-section of test pile with placement of sister bars.

(b) Elevation levels of sister bars

Figure 3.10: Strain meters placement in test pile

Digital data logging

Information from the embedded strain gauges, the sprung-loaded displacement meters, and the pressure gauge is collected via a Micro-1000 data logger (model 8032 from Geokon). The data is monitored digitally and compared with the analog readings during the whole test, and live plotted both in graphs and in Excel-sheets.



Figure 3.11: Computers for collection of test data

3.2.3 Assessment

The static loading test procedure will be performed in equal load steps of 130 kN, and an interval time of 15 minutes. During each step, the load will be held constant for 15 minutes or until:

- A pile head movement of 50 mm is reached.
- Excessive movement resulting in the jack unsuccessfully holding a constant pressure, i.e soil collapse.
- Maximum available jack load is reached.

The pile head vertical movement relative to the reference beam will be measured digitally every 15 seconds and manually every 3 minutes, along with indicated results from strain gauges digitally every 2 min. When a total movement of 50 mm is reach or if any of the other criteria stated above has occurred, the first part of the test ends. The hydraulic jack will then be turned off in order for it to stabilize in a steady state (τ_s), see Chapter 2.1. After stabilization, a cyclic loading procure begins with loading to failure once again, unloading to first time step and reloading to failure a thirist time. The cyclic loading and unloading intervals will be made in 2.5 minutes and 130kN each.

3.2.4 Strain and load interpretation

Theoretically, the assumption is made that the pile is vertically straight and that it will be axially loaded at the very center of its cross section. However, it is highly unlikely that these conditions were accurate. To compensate for a non homogeneous load distribution origin from certain unwanted pile placement and test loading procedure, the strain indications from each corner were interpolated to the center of the pile. The readout indicates temperature and "digits units", based on vibrating frequency every 2 minutes. These are converted to μ -strain [mm/m]. The following equation applies, this is the apparent strain of the sister bar before and after loading (Geokon, 2013):

$$\epsilon_{apparent} = (R_1 - R_0)C \quad (3.4)$$

Where:

R_0 is the initial reading units

R_1 is the reading units at the loading interval

C is a calibration factor, in this case 0.343, see manual (Geokon, 2013)

Due to thermal compression and expansions of materials, the actual strain is corrected considering temperature change:

$$\epsilon_{actual} = ((R_1 - R_0)C) + ((T_1 - T_0)K) \quad (3.5)$$

Where:

T_0 is the initial temperature

T_1 is the temperature at the loading interval

K is the thermal coefficient, see table 3.2, (Geokon, 2013)

Positive strain (ϵ) indicates tension and negative equals compression.

Table 3.2: Thermal coefficient K for Steel and Concrete

Material	K [ppm/°C]
Steel	12.2
Concrete	10

To convert the μ -strain to load, Equation 3.8 applies appropriate E-modulus, cross sectional area and strain in μ -strain:

$$F = A\sigma \quad (3.6)$$

$$\sigma = E\epsilon \quad (3.7)$$

$$F = E\epsilon A \quad (3.8)$$

Due to uncertainties in altered concrete E-modulus during compression, "E" in equation 3.8 is unknown, making a total of two unknown variables "E" and "F" on each pile level. Therefore, it is assumed that pressure forces at pile head during the test is equal to loads registered at sister bars mounted 2 meters bellow surface.

$$E = F/A\epsilon \quad (3.9)$$

This new modulus in Equation 3.9 allows for calculation to convert μ -strain to load in every sister bar along the test pile.

3.3 Prediction survey

The prediction event is organized for practising engineers to evaluate the theoretical pile head load- movement- curve for the test pile during the static loading test. The submitted predictions will be compiled together with corresponding result curve from test and will be the basis for analysis and discussion.

An invitation to participate was send out in February to engineers in Sweden, Norway, Denmark, Finland and Canada (Appendix includes invitation letter and soil properties). This includes contacting the Swedish, Norwegian, Danish and finish geotechnical society. Contact information were acquired through master thesis supervisors and via labor market interviews. The invitation contained information about the master thesis itself along with necessary test pile and assessment information to get an understanding and catch an interest of the project and it´s intent. It also included a question to forward the forum to geotechnical colleagues and friends to reach a wider range of participants. In order to participate, each entrant were to register their intent to participant by email, deadline March 16. Each participant that submitted intent were replied with extensive soil and pile parameter document and detailed test information. The deadline for final submission of the theoretical load- movement- curve were set to April 15. However, all submissions submitted before all result data is processed and ready to be shared will be accepted. Though it is stated in the invitation that the result will be shared in May, it will be sent out when ready.

All submitted predictions and participants will be kept confidential and only known by the authors of the thesis (Petttersson, Edvardsson).

3.4 t - z implementation

Load- movement response of the pile will be calculated using the API and Karlsruds approach on t - z curves from Chapter 2.6 and also applying pile compression. The method for pile compression is based on evaluating average stresses in the pile and the length of the pile segment of which is assumed to be affected by any compression. These calculations is based on stress formula $\sigma = F/A$ and Hookes law: $\sigma = E\epsilon$. The interpretations of stress and load distribution is stated in the analysis chapter along with further calculations and equations. A Young´s modulus for the concrete of 45 GPa and a maximum shear (t_{max}) measured from the test result will be used. The calculated load- movement curves will be compared and analyzed with test result.

4

Project properties and site description

4.1 Soil properties

Figure 4.2 shows the test area with bore holes and test pile location. Soil data is mainly collected from previously made geotechnical and hydrogeotechnical investigations from the project geotechnical field research (MUR) from Peab Anläggning. Appendix 3 "A.3 Soil tests" in the appendix contains compiled graphs with result from these tests with the following content:

- Shear strength
- Pre-consolidation pressure
- Water content
- Atterberg limits
- Density
- Sensitivity

Further can the evaluation of CPT probe BG11-4 and GP11-7 be found in the appendix, this material is collected from the "Regionens hus" project in Gothenburg. In addition, Peab have made two more tests on boreholes named 16GT03 and 16GT07 (both marked in Figure 4.2). These have been analyzed with direct shear test (DSS), triax and CRS. Raw data from these tests can be found in the Appendix 3.

Shear strength evaluation made in this thesis is based on DSS test result from 16GT03 and 16GT07 and shear strength compilation from figure 4.1.

4. Project properties and site description

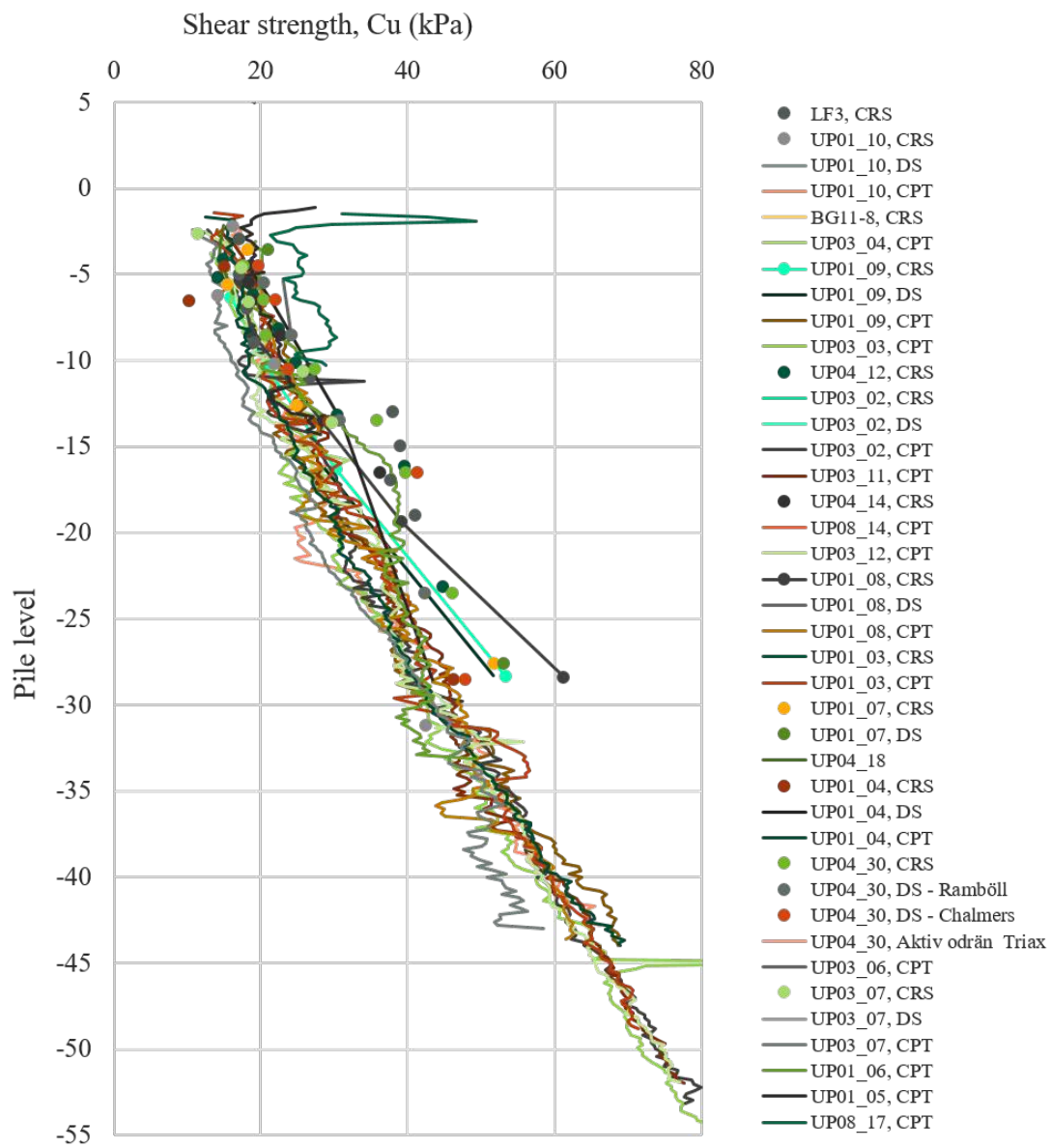


Figure 4.1: Shear strength compilation

Density and characteristics of testing pile soil**Table 4.1:** Compiled density from CPT probe test performed by Bohusgeo AB 2011-04-12, see appendix A.3

z [m]	Density [1000 kg/m ³]	Soil Type
0 to 2.1	1.9	Excavation Soil
2.1 to 5	1.64	Excavation Soil
5 to 7.5	1.64	Silty Clay
7.5 to 12.5	1.55	Clay
12.5 to 17.5	1.54	Clay
17.5 to 22.5	1.65	Clay
22.5 to 27.5	1.66	Silty Clay
32.5 to 37.5	1.63	Silty Clay
37.5 to 42.5	1.94	Silty Clay
47.5 to 50	1.66	Silty Clay

Hydraulic conductivity

The hydraulic conductivity of the clay is set to 10^{-9} m/s, based on conducted CRS- attempts.

Ground water level

The ground water level has been measured in well KP 02 (40 meters from the test pile) during a period of 20 months. The average depth to the water surface during this time was $z = 1.17$ m below ground level. The topology between the well and the test pile is flat.

4. Project properties and site description

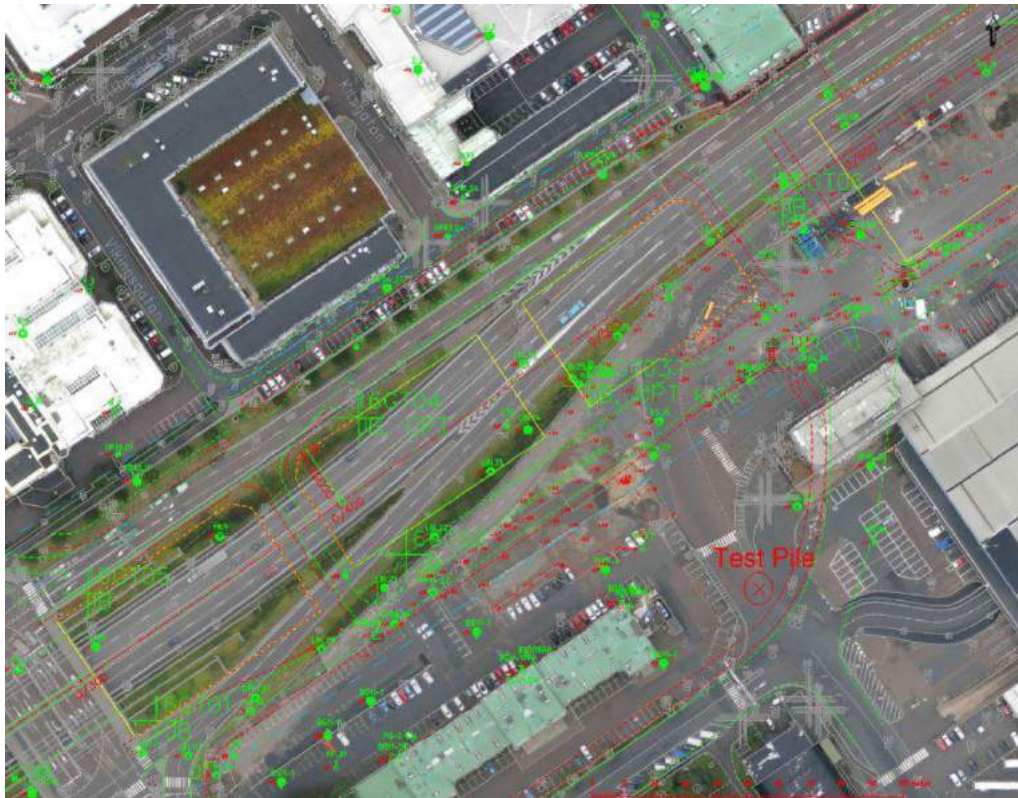


Figure 4.2: Map of test pile area



Figure 4.3: Project location in Gothenburg (Google Maps)

4.2 Pile properties

Installation date of the pile was September 7 2017. The test pile is a 50 meter long, 275 mm wide square reinforced concrete displacement pile. It consist of 4 elements, 13 meters each, connected with 3 joints. The pile along with the joints are designed to sustain construction load, meaning it is assumed that the failure will occur in the soil and not the pile or its components. Along the pile is a mounted 140 mm steel half-pipe, containing the cables from the measure devices along the pile, see Figure 4.4. The pile is vertically driven and assumed to be straight. Concrete and reinforcing bar properties is shown in Table 4.2 and 4.3.

Table 4.2: Pile properties, concrete

Length	50 m
Width	275 mm
Circumference	1.1 m
Pile type	SP3+
Concrete class	C60/75

Table 4.3: Pile properties, reinforcement bars

Type	B500B
Diameter	16 mm
Number of bars	12
E-modulus	200 GPa

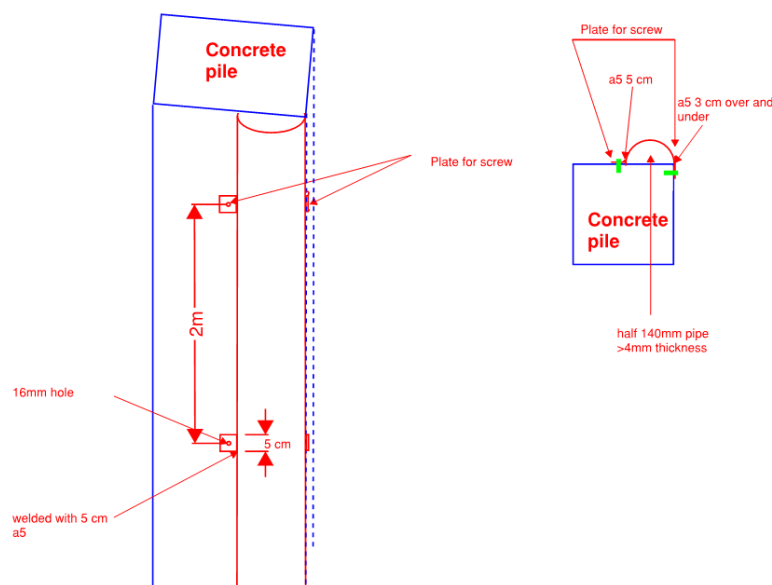


Figure 4.4: Profile of test pile

4. Project properties and site description

5

Results

5.1 Ultimate resistance evaluation

5.1.1 α - method

Figure 5.1 illustrates the evaluated trend line with DSS in borehole 16GT03 and 16GT07, and adjusted final C_u line.

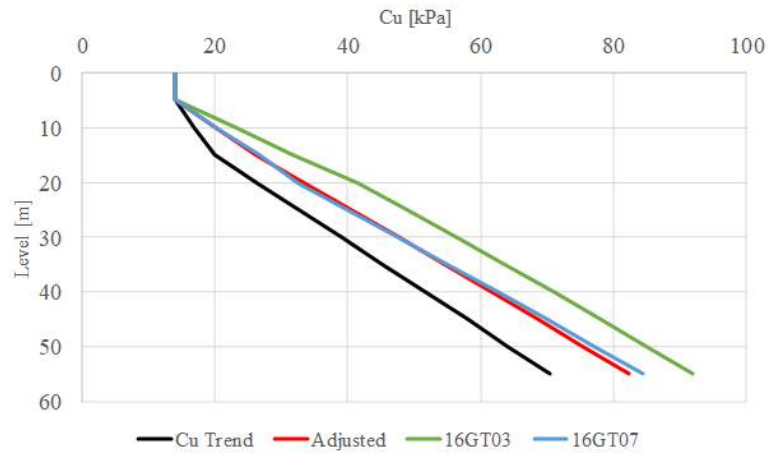


Figure 5.1: Shear strength evaluation. Black line is the over all trend. Green and blue is local DSS and red is the used, adjusted evaluation.

$$R = \int_{Lp} \alpha c_u \theta dz$$

c_u is adjusted with regard to loading time, the load increments is seen as short time, minute loading, hence it is adjusted with factor $\kappa_t=1$ according to Chapter 2.4.

Table 5.1: Adjusted α with factor κ depending on diameter, shape and time

κ_ϕ	0.9
κ_f	1
κ_T	1
$\alpha_{unadjusted}$	1
$\alpha_{adjusted}$	0.9

Table 5.2: Ultimate resistance result from α - method

Alpha	0.9
Circumferential area	1.1 m ²
Total Cu integral	2056 kPa
Ultimate resistance	2036 kN

Figure 5.2 presents the resistance effect in the pile from Chapter 2.4, based on a ultimate resistance of 2036kN.

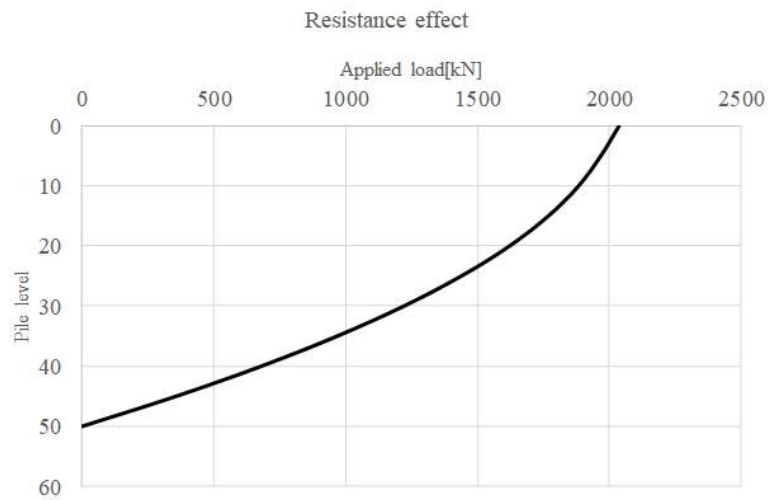


Figure 5.2: Resistance effect of the test pile based on ultimate resistance

5.1.2 β - method

$$R = \int_{L_p} \beta \sigma'_v \theta dz \tag{5.1}$$

The total stress of the pile soil is calculated with the soil density data compiled in Table 4.1. The ground water level is at $z = -1.17$ meters from pile head, and together with the total stress, the total vertical effective stress is calculated and presented in Table 5.3. The β - factor is determined from Figure 5.3. Silt and clay normally has a density of about 1700 kg/m³ (Larsson, 1989). As can be seen in Table 4.1 the site density of the clay and silty clay is about 1600 kg/m³, and therefore the β - value is obtained from where the *little less than normal relative density* line is intersecting the *50m pile length-* line.

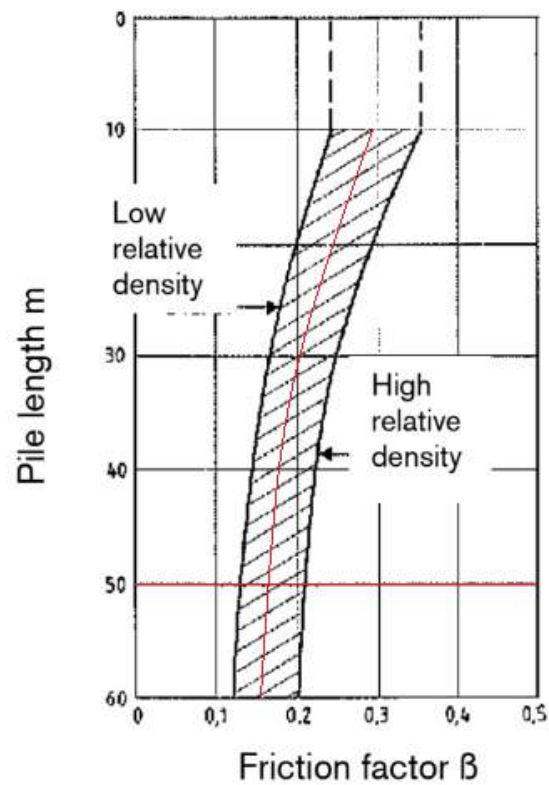


Figure 5.3: Evaluated graph for determining β (NGF, 2012).

Table 5.3: Ultimate resistance result with β from Norsk Peiliveiledning (NGF, 2012)

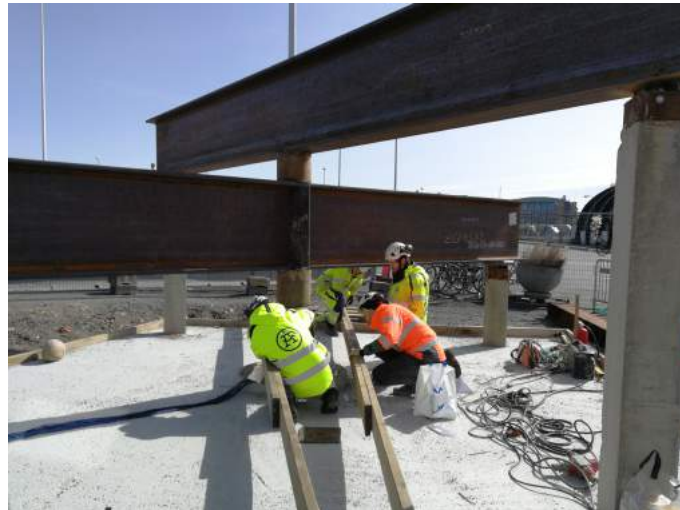
Beta	0.15
Circumferential area	1.1 [m ²]
Total σ'_v integral	8460 [kPa]
Ultimate resistance	1396 [kN]

5.2 Static loading test

The static loading test were preformed a sunny day in April 2018. The following part will present the result from this test. Figures 5.4, 5.5 and 5.7 presents footage from the test day.



(a) Jack installation

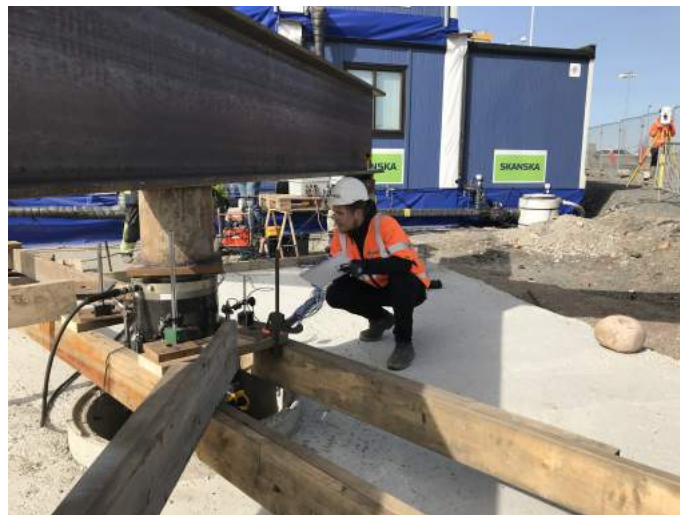


(b) Jack installation

Figure 5.4: Footage from the static loading test preformed April 10 2018



(a) Test setup



(b) Displacement reading



(c) Hydraulic jack

Figure 5.5: Footage from the static loading test performed April 10 2018



(a) Manual digital reading



(b) Total station measuring



(c) Crew

Figure 5.6: Footage from the static loading test performed April 10 2018



(a) Crew



(b) Authors

Figure 5.7: Footage from the static loading test performed April 10 2018

5.2.1 Load-movement response at pile head

A graph containing the full movement response of the pile head is presented in figure 5.8. The pile head movement is increasingly between 0.5 and 2.0 mm per load step, until the load of 1820 kN. At this load, during the first 6 minutes a creep of 2 mm was measured before the vertical movement were superior to the hydraulic jack capacity. This means that condition no 2 from the test assessment was fulfilled "Excessive movement resulting in the jack unsuccessfully holding a constant pressure, i.e soil collapse". Here, the compressor connected to the hydraulic jack operated at maximum capacity without the hydraulic jack being able to maintain 1820 kN. Pressure was not further added, and the pile crept until the rapid movement stalled, and the pile head stabilized at 1435 kN for 6 min after soil failure. This is the horizontal part of the graph at 160 min in figure 5.9. A total movement of 56 mm was reached (34 mm after soil failure). An additional 90 kN was added to a total of 1525 kN. This load was maintained for 3 min with a resulting movement during the whole load step of about 2.5 mm. Another 130 kN was attempted to add, but at 1640 kN of load 7 mm of movement was measured and the load was decreased once again to 1435 kN for 2 min.

Now a cyclic load pattern was initiated, and the load was first decreased with the same load step internals as before but during 2.5 min each, from 1300 kN to 130 kN. And then increased with 2.5 min intervals from 130 kN to 1560 kN. Each load step up to 1430 kN generated a movement of about 1-2 mm each, before reaching 1560 kN which generated a movement of 11 mm, and the whole test procedure was terminated.

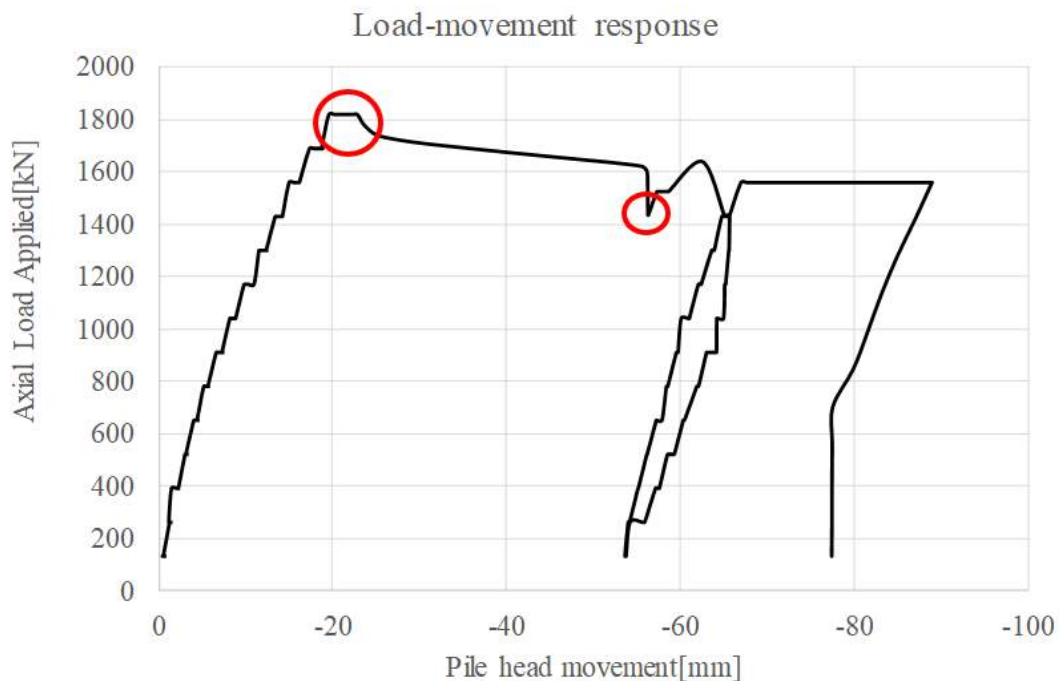


Figure 5.8: Load- movement response curve of the full test. Red circles indicates, from the left, peak shear (τ_m) and steady state (τ_s)

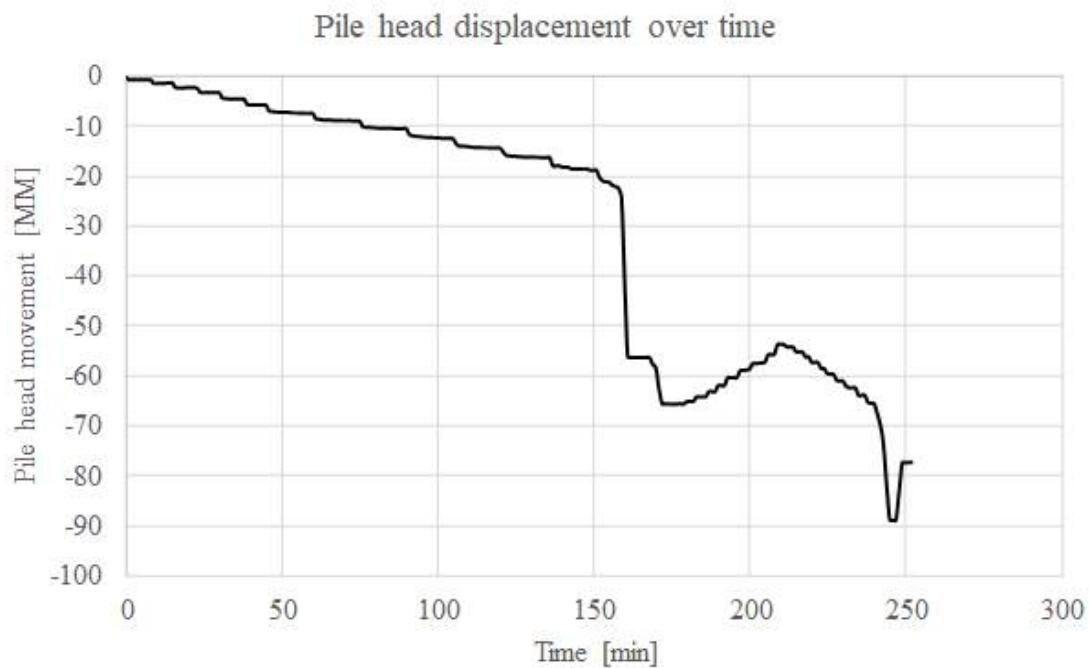


Figure 5.9: Pile head movement over time

5.2.2 Force distribution

The first two elements of the pile were pressed down without using a drop hammer. Element number 3 and 4 were hammered, see Table 5.4.

Table 5.4: Number of drop hammer impacts and associated force

Element	Hammer impacts	Force [kNm]
1	-	-
2	-	-
3	519	2
4	655	4

Using Equation 5.2, calculation of E- modulus at the shallow sister bars mounted two meters bellow surface indicates an average modulus of 15 GPa for every load applied, see Appendix 5 for full list of values. Applying this value to Equation 5.3 for every load interval on each strain gauge gives a load distribution for every applied load, see Figure 5.10.

$$E = F/A\epsilon \quad (5.2)$$

$$F = EA\epsilon \quad (5.3)$$

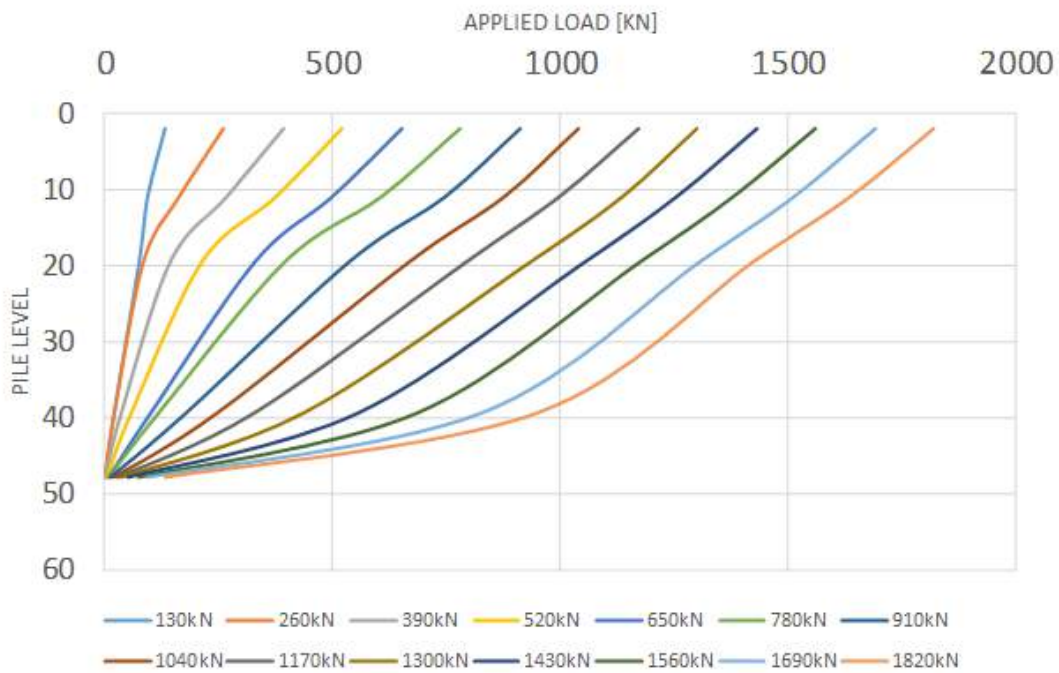


Figure 5.10: Force distribution at every applied load

5.3 Prediction event

A total of 23 predictions from 10 different countries were submitted with a load movement response curve, see Figure 6.2. 20 submissions also responded to the second part of the survey which included specifying pile capacity. All submissions were made by practising engineers knowledgeable in the field of geotechnical engineering.

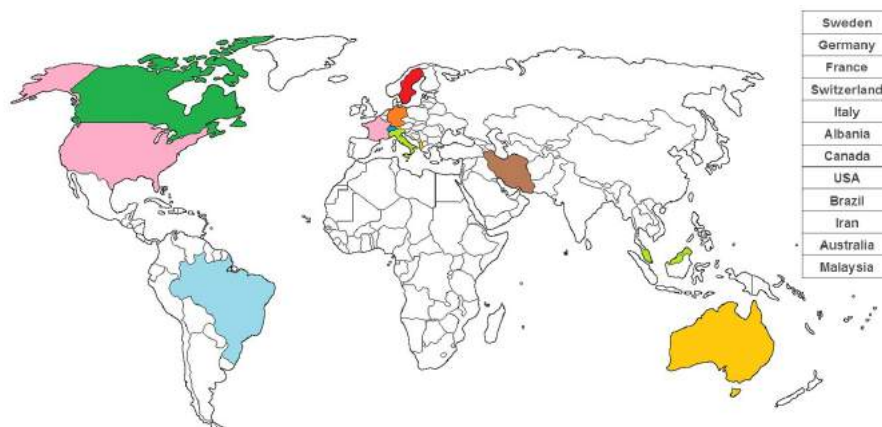


Figure 5.11: Countries participating in the prediction event

All submitted predicted load- movement responses are shown in Figure 5.12. Further analysis of the predicted responses is made in Chapter 6, including comparison with test result, and submitted *capacities*.

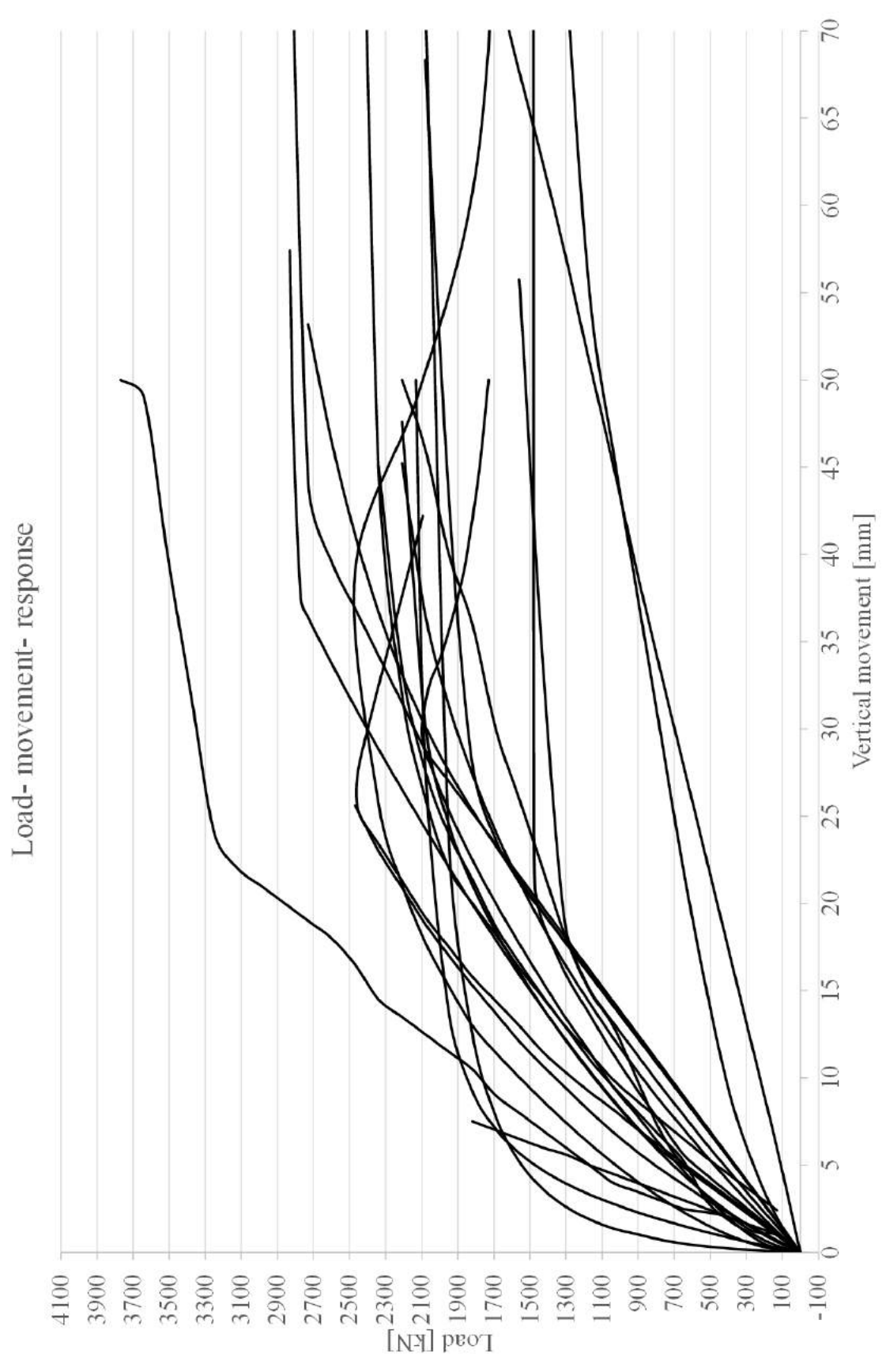


Figure 5.12: Predicted load- movement curves from the prediction survey

6

Analysis

6.1 Loading test observations and error sources

6.1.1 Overall impression of the loading test

The testing procedure went relatively fine without any severe unforeseen events. All measuring instruments except one sister bar continuously fed information to the computers, the hydraulic jack operated well, and no failures occurred in the supportive beams. However the metallic beam that was supposed to rest outside the cast concrete plate in order to provide a stable fix reference point for the sprung-loaded displacement meters, turned out too short. Instead a system of wooden planks were constructed. This resulted in a less steady reference point at times since winds gusts made the planks wobble. However, the dial indicator were easy to read anyway. Also one of the two welders were unable to attend this day, and the welding work took longer than planned. Due to this, the decision was taken to half the time of all loading steps up to 1040 kN.

The test crew was well prepared through the whole procedure. The load, loading time, and movements were continuously monitored, and when failure occurred the cyclic loading procedure went as planned.

6.1.2 Correction with regard to uneven pressure at pile head

After installing the test pile it was measured with spirit level that the pile head surface, and most likely the rest of the pile, was not at perfect level with the ground. When installing the whole pressing device, the surfaces of the hydraulic jack and the pile head needed to be corrected for full contact. This to get a homogeneous and centric load on the pile head surface, and further down the pile. To achieve this, small metal plates were placed on top of the hydraulic jack to create an inclination in order to be level with the lower supportive beam. The result of this can be seen in Figure 6.1.



Figure 6.1: Skewing of surface between hydraulic jack and supportive beam

6.1.3 Impact of surrounding support piles

The four supporting piles makes up a symmetric unloading system and resulting, during maximum hydraulic jack test load, in a drag of about 450 kN in each support pile. During the later phase of the loading, cracks were visible in the concrete slab in connection with one of the supportive piles. With a distance of about 3.2 m from the center test pile to each supportive pile, the uplifting force from these is assumed not to affect the immediate soil conditions of the test pile.



Figure 6.2: Cracks in the concrete slab, spreading out from one of the supportive piles

6.2 Rate of settlement and post peak response

After soil failure the pile were allowed to stabilize by decreasing jack load until the rapid pile head movement stalled, it did so at 1435 kN. As can be seen in Figure 6.3 the rate of creep during the 6 min of post peak stabilization is less than 0.1 mm. 6 minutes is a short period of time in this context, Jorge Yannie concluded in his doctoral thesis (Yannie, 2016) that pile creep rate changes over longer time periods. However in the same doctoral thesis, and according to The Swedish pile commission report (Eriksson et al., 2004), and API (API, 2007) to name a few, it is concluded that the long term ultimate resistance is around 70 - 80% of the short term ultimate resistance. 1435 kN makes for 79% of failure load. With that in mind, it can be said that 1435 kN is in the long term ultimate resistance range.

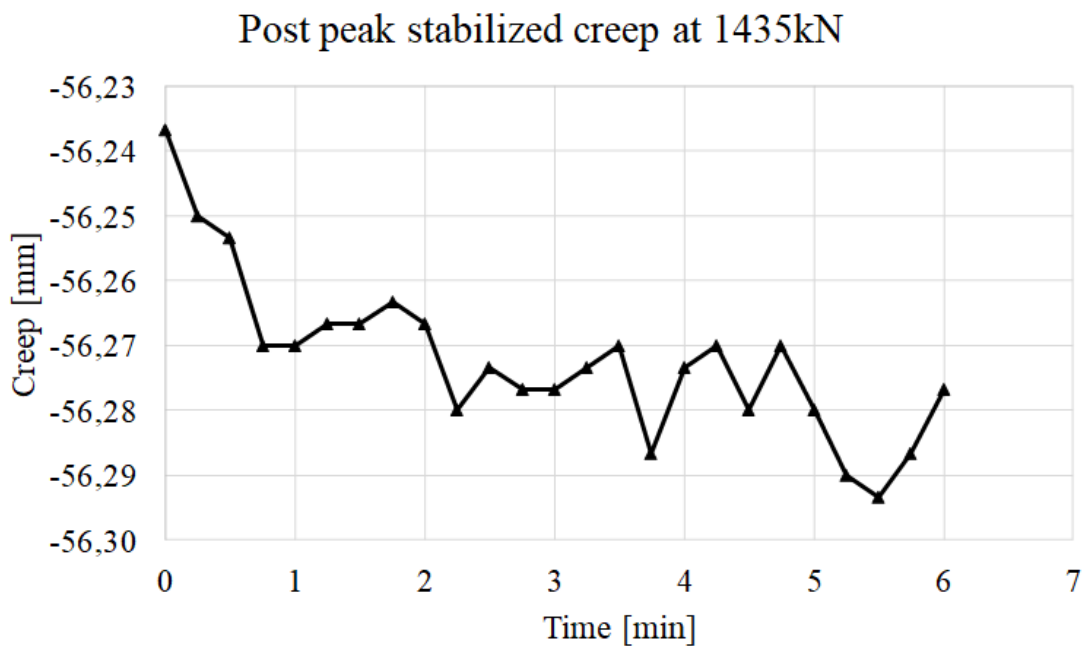


Figure 6.3: Pile head creep after re-stabilization at 1435 kN

The rate of vertical settlement during the static loading test can be derived from settlement factors, instantaneous settlements and creep, see Figures 6.4 and 6.5. Together they make for a total pile head settlement.

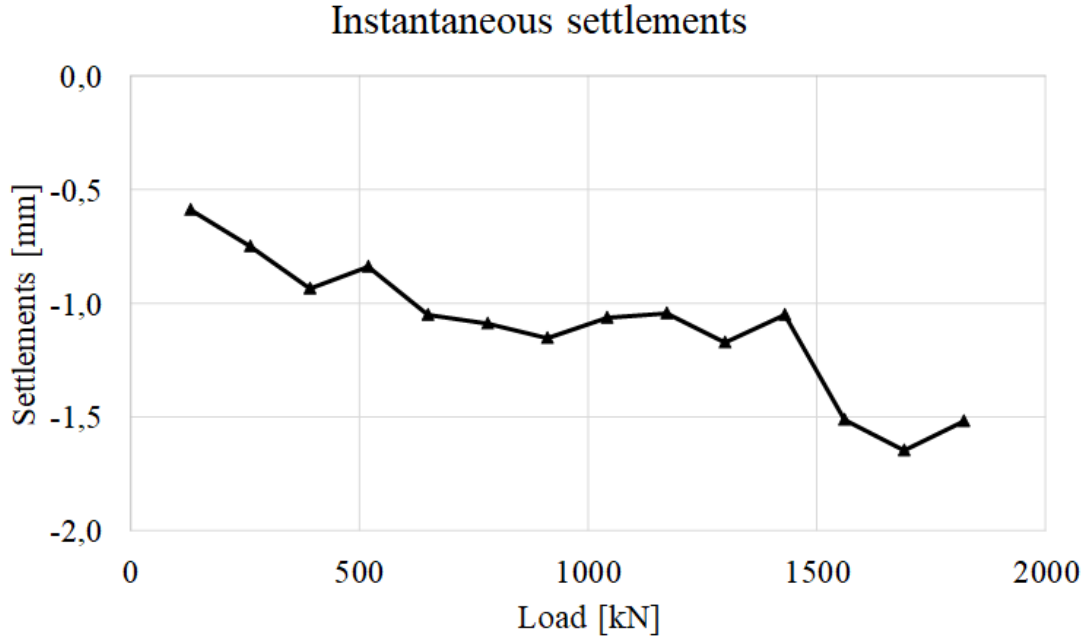


Figure 6.4: Instantaneous vertical settlements with increased load

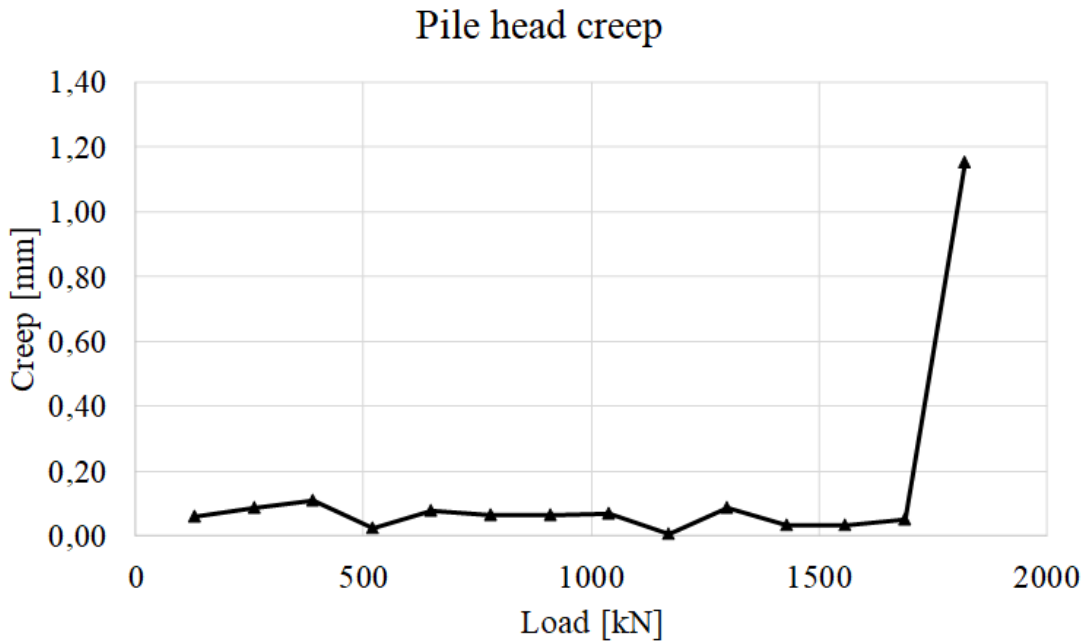


Figure 6.5: Pile head creep during the last 3 minutes of each loading step

Instantaneous movement, or direct settlements, Figure 6.4 is independent of the load interval time, assuming that the increment itself is instant or very quick. The result show an increase in direct settlements until 600 kN applied load. From there, it is an almost constant at approximately 1.1 mm/load increment except from minor differences. At about 1400 kN applied load, the rate of settlement increases once again to approximately 1.6-1.7 mm/load increment. The point of interest is at 1400 kN where the test later on re stabilize post peak. It insinuates that for this specific test, the magnitude of instantaneous movement relates to the post peak, long term capacity.

Pile head creep is the vertical movements that occur during the loading intervals, between each new applied load. It is time dependent but do not make for a major short term settlement factor compared the direct settlements. The values in figure Figure 6.5 corresponds creep settlements during the last 3 minutes in each load interval up to soil collapse. The result shows a constant creep rate in every load step with minor differences. Unlike the result with instantaneous settlement, the is no real conspicuous point of interest where the creep rate increases or decreases, except from 1820kN where soil failure occur and the pile sinks. However, this might be because of the relatively short creep time.

6.3 Theoretical and empirical load movement response and Capacity

6.3.1 Predicted responses with empirical result

Over all, comparing predicted load movement curves with actual test result shows a wide range of over- and underestimated stiffness and movements. Most participants predicts a stiffer response and assumes a larger movement before reaching the peak load. Some predictions are close in terms of soil failure load, but miss predicts the pile head movement, whereas others have accurate predictions in movement and curve similarities but are off in maximum load. Note that the test result (red line) in Figure 6.6 is simplified after the point of soil collapse to better resemble predictions based on the excel template.

The reasons why the predictions not only differs from the test result, but also from each others are many. The first aspect is through the participant point of view. The participants were not asked to describe the methods used for producing the predictions, but many participants did state their methods in the submission template. Due to the anonymous participation, the methods will not be revealed, but the fact that different methods were used is one important contributor to the variety of the results. Another reason to the scattered results is different interpretations and use of provided pile, and perhaps even more, soil data. As can be seen in the soil- data- part of the appendix, the participants were provided with a wide range of different soil tests providing basis for different methods and interpretations. This, combined with different personal engineering experiences and cultural backgrounds contributes to a wide range of predictions.

The second aspect is concerning the actual test. As stated in Chapter 4.2, one of the sides of the test pile is largely covered by a metal half-pipe tube. This was stated in the pile information provided with the test. The surface of this is less rough than the concrete pile, and it is likely that participants have not included this in their predictions. The inclination of the pile was not stated in the provided test information. A skew pile along with a smooth side results in torque, and uneven exposure of shear stress to the surrounding soil yields other test values than a *naked* straight test pile would. Also the time interval of each loading step was told to be 15 min in the test information. Due to delays during the assembly of the test rig, the load steps up to 1040 kN was halved to 7.5 min each. The load- movement- response- curves provided by the test participants is time independent and the creep between the on-loading were only about 1 mm per load step, but along with previous stated uncertainties these add up to a appreciable margin of error.

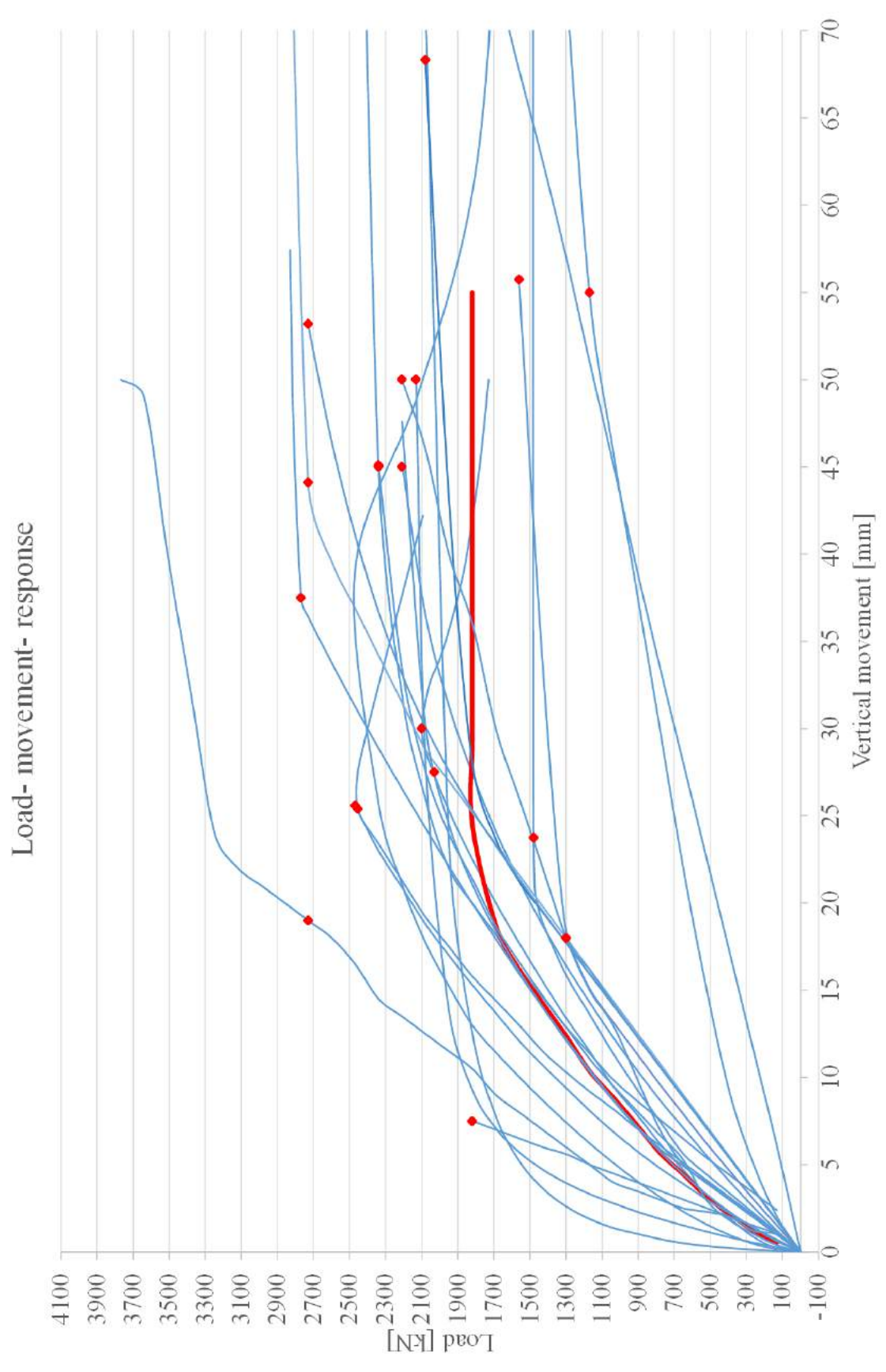


Figure 6.6: Pile head movement compared to prediction survey

6.3.2 t - z response of pile head movement

A load- movement- response is also developed with two t - z - curves, one proposed by Kjell Karlsrud (Karlsrud, 2014), and one by API (American Petroleum Institute), see Chapter 2.6.

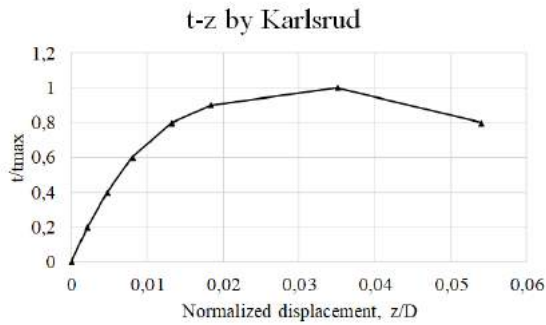


Figure 6.7: t - z - curve proposed by (Karlsrud, 2014).

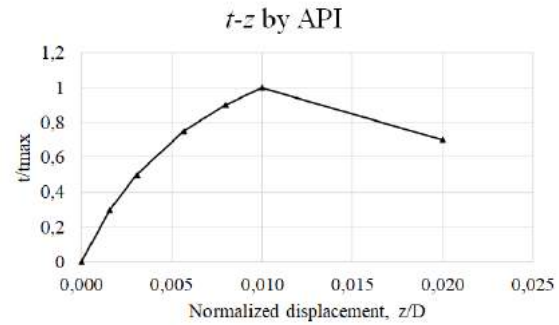


Figure 6.8: t - z - curve proposed by (API, 2007).

For the Karlsrud t - z curve, the load rate t/t_{max} is divided into seven *loading steps* including one post-peak load, and the normalized displacement z/D is evaluated in figure 6.7. For the API t - z curve, six load steps were already proposed with corresponding z/D values (API, 2007), see Figure 6.8. With the given pile diameter D of 275 mm, the pile head deflection z is determined and is presented in Figure 6.9 for both approaches.

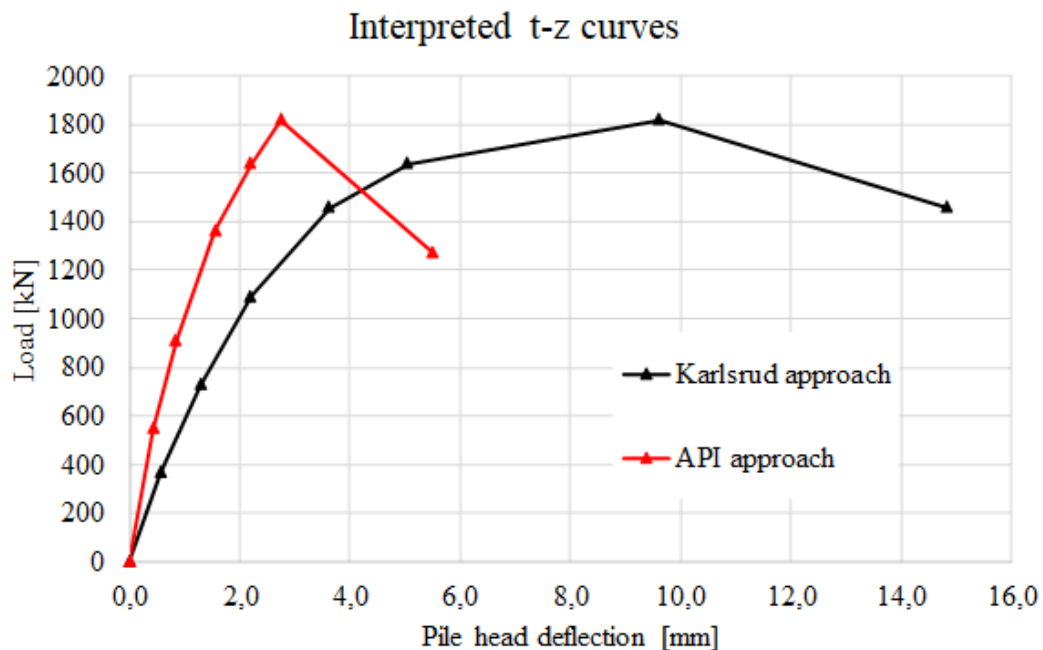


Figure 6.9: Evaluated load- movement- response based on t - z - analysis with the API and Karlsrud approach, excluding pile compression.

Both calculations is based on a peak shear stress (τ_{max}) of 1820 kN from the loading test result. Apart from the differences in displacement at peak load, the two methods both indicate different soil behavior. The soil shar stiffness in the API approach is almost linear throughout the whole test, whereas Karlsrunds approach slowly reduces it until the point of soil failure.

Along with the load- movement- response from Figure 6.9, compression of the pile at each loading step for both $t-z$ - curves, is also evaluated in order to compare the $t-z$ - analysis with the loading test result with respect to total pile head vertical movement. Pile compression is directly linked to strain and length of the pile segment affected by stress. This is calculated with Equations 6.1 and 6.2:

$$\epsilon = \sigma_a/E \quad (6.1)$$

$$Compression = L_{aff} \epsilon \quad (6.2)$$

Where:

ϵ = Strain

σ_a = Average stress of the pile segment affected by stress

L_{aff} = Length of the pile segment affected by stress

The load at each load step yields stresses on a certain pile segment from pile head. The length of this segment is the length where the sum of the soil shear strength at this depth is equal to the applied load. These lengths are calculated by first adjusting the α - method result to the loading test result by multiplying the evaluated shear strength with a factor of 1820/2036 at all depths down to 50 m, see Table 6.1. The adjusted shear resistance is plotted as load transfer between pile and soil, and used to determine both the pile length affected by stress, and the average stress of this pile segment. Figures 6.10 and 6.11 presents the pile length affected by stresse (L_{aff}) for every load step by both approaches. Figures 6.12 and 6.13 provides an example of how the average stress of the affected pile segment is calculated.

$$0 = q - \int_{L_{aff}} \alpha c_u \theta dz \quad (6.3)$$

Where:

q = Applied load

6. Analysis

Table 6.1: Evaluated α shear strength values over depth, adjusted for loading test result of 1820 kN

Level	Shear strength c_u	Shear strength alpha	Shear strength adjusted
0	0.00	0.00	0.00
5	70.00	69.30	61.94
10	85.19	84.34	75.39
15	115.62	114.47	102.31
20	149.02	147.53	131.87
25	184.84	182.99	163.57
30	220.15	217.95	194.81
35	255.46	252.91	226.06
40	290.77	287.86	257.30
45	325.63	322.37	288.15
50	360.04	356.44	318.60
	2056.73	2036.16	1820.00

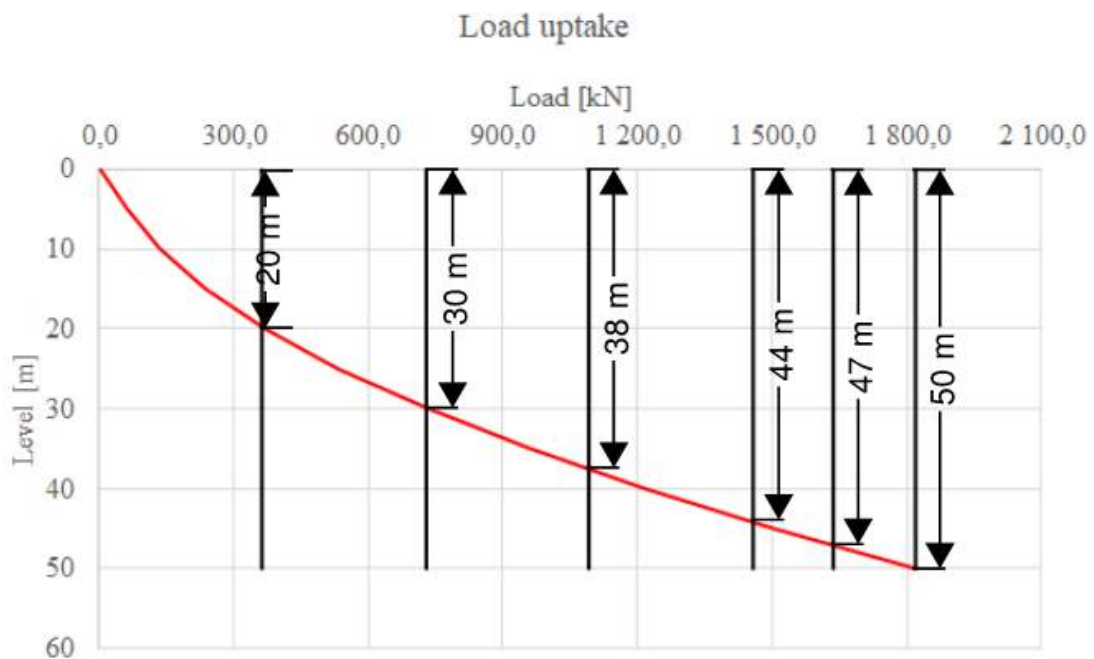


Figure 6.10: [Pile length affected by stress at every loading step, API approach.]

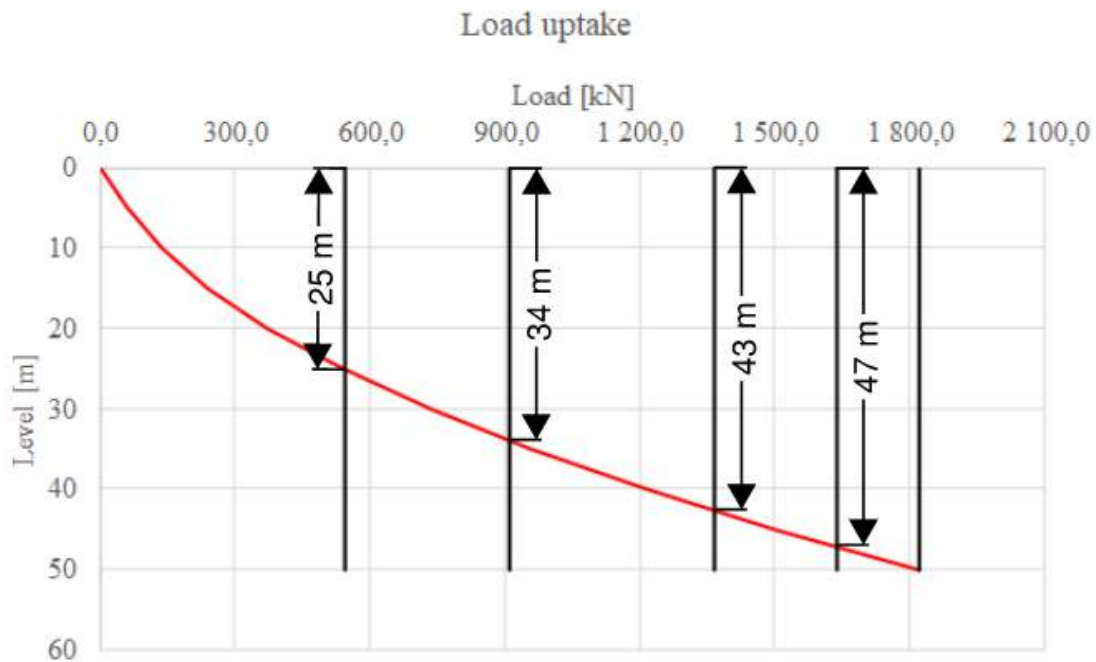


Figure 6.11: Pile length affected by stress at every loading step, Karlsrud approach.

The average stress of the affected pile length is evaluated using the load distribution from the applied load, similar to resistance effect, and dividing it with cross sectional area A_p . An example of the calculation for load step two for the Karlsrud approach, 728 kN, can be seen in Figures 6.12 and 6.13. The evaluation for every step is found in Appendix 5. Applying a pre-calculated Young's modulus of 45 GPa for the pile, Equation 6.2 is used to calculate pile compression for each loading step and approach, see Tables 6.2 and 6.3.

Approach: Karlsrud		Load: 728kN			Sigma average/5
Level	Resistance Alpha-method	Load [kN]	Sigma [kPa]	m	
0	0	730	9652		
5	62	668	8833	9243	
10	137	593	7836	8335	
15	240	490	6483	7160	
20	372	358	4739	5611	
25	535	195	2576	3658	
30	730	0	0	1288	
35	956	Average		5882	
40	1213				
45	1502				
50	1820				

Figure 6.12: Evaluation of average stress

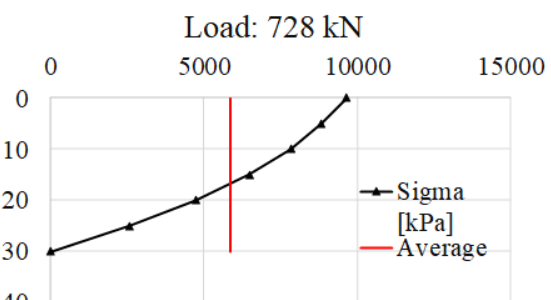


Figure 6.13: Stress distribution for applied load 728 kN. Segment length 30m.

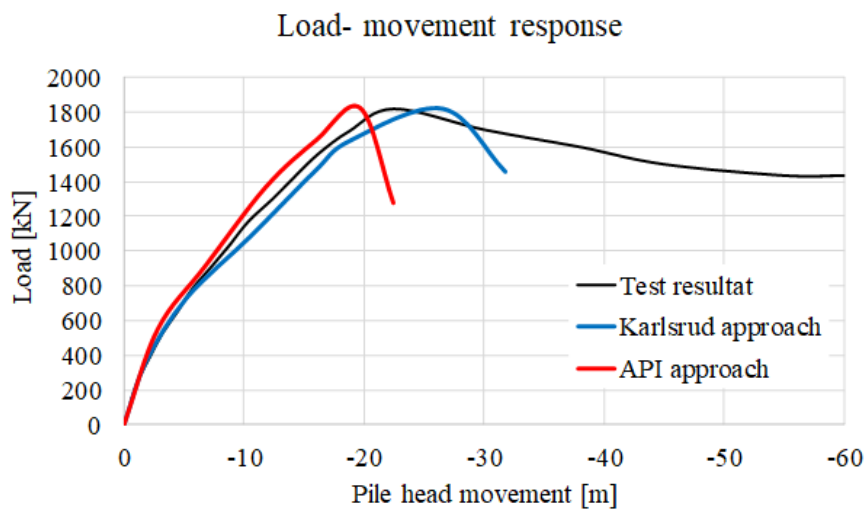
Table 6.2: Pile compression at loading steps of the Karlsruds approach

Karlsrud approach				
Load [kN]	Stress [kPa]	E[Gpa]	L [m]	Compression [mm]
0	0	45	0	0.0
364	2848	45	20	1.3
728	5882	45	30	3.9
1092	10031	45	38	8,5
1456	12515	45	44	12,2
1638	13265	45	47	13.9
1820	15266	45	50	17.0
1456	19253	45	-	17.0

Table 6.3: Pile compression at loading steps of the API approach

API approach				
Load [kN]	Stress [kPa]	E [Gpa]	L [m]	Compression [mm]
0	0	45	0	0.0
546	4225	45	25	2.3
910	7818	45	34	5.9
1365	10716	45	43	10.2
1638	13265	45	47	13.9
1820	15266	45	50	17.0
1274	15266	45	-	17.0

Combining with the evaluated load- movement- response based on the t - z - analysis, results in a final pile head movement that is presented and compared with the actual loading test result in Figure 6.14.

**Figure 6.14:** Load- movement- response from t - z analysis along with loading test result.

6.3.3 Ultimate resistance compilation

What defines pile "capacity" was unspoken in the event information and each participant has made their own interpretation of the term. Looking at the curves in figure 6.6, the result insinuates that most participants indicate pile capacity equal to, or very close to maximum load before soil failure. Figure 6.15 compiles each prediction and compares them to maximum load during the test (1820kN) and the short time ultimate resistance using α - method and long term ultimate capacity using the β - method.

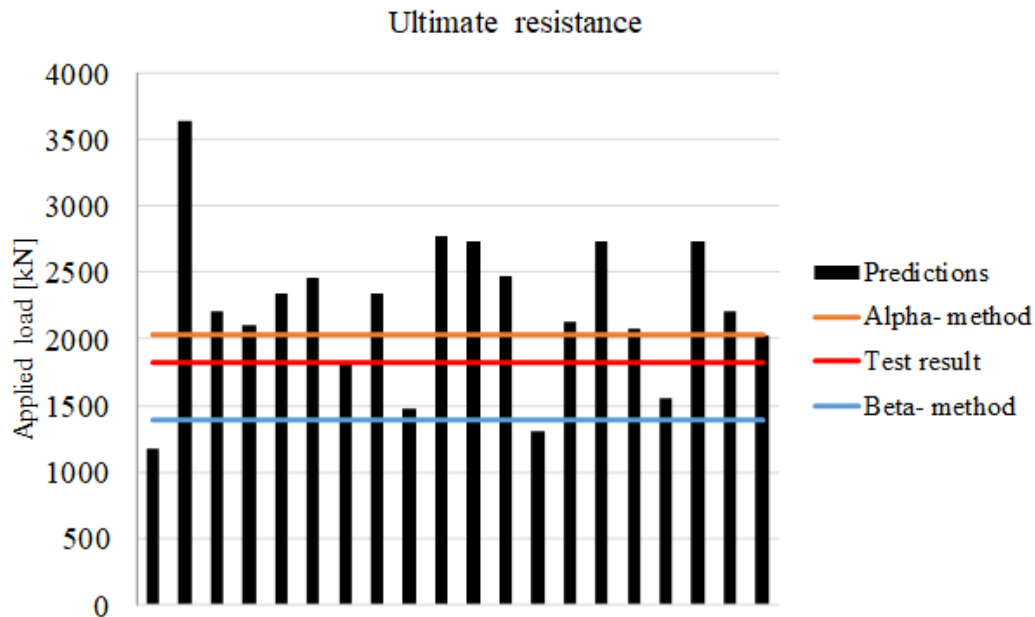


Figure 6.15: Compiled ultimate resistances of the test pile from predictions, compared with the static loading test, and the α - and β - methods

Only a few predictions underestimate the failure load (or capacity), the majority overestimates, including the alpha method which is normally used in "Gothenburg clay". Note that this is our interpretation of the alpha method, it is fair to assume that several other predictors has used it as well with different outcome. Apart from every "incorrect" interpretation, one individual has assumed the correct soil failure load in this test. However, soil strength in clay is very time dependant, faster loading equals higher stiffens and vice verse. It is important to understand that the result of ultimate capacity shown in Figure 6.15 illustrates a result acquired during this specific loading time. Decreased loading time would give less creep in between loading intervals and less vertical movement over all, which insinuates that more load could be applied before reaching soil failure.

One important aspect regarding pile capacity is the real meaning of the term. It has been stated in the report that each participant has made their own interpretation and most has stated the capacity as the load of which soil failure occurs, or very close to occurring. Figure 6.16 illustrates assessed movement corresponding to predicted pile capacity. The test result indicates a settlement of 22 mm before soil failure and is used as reference.

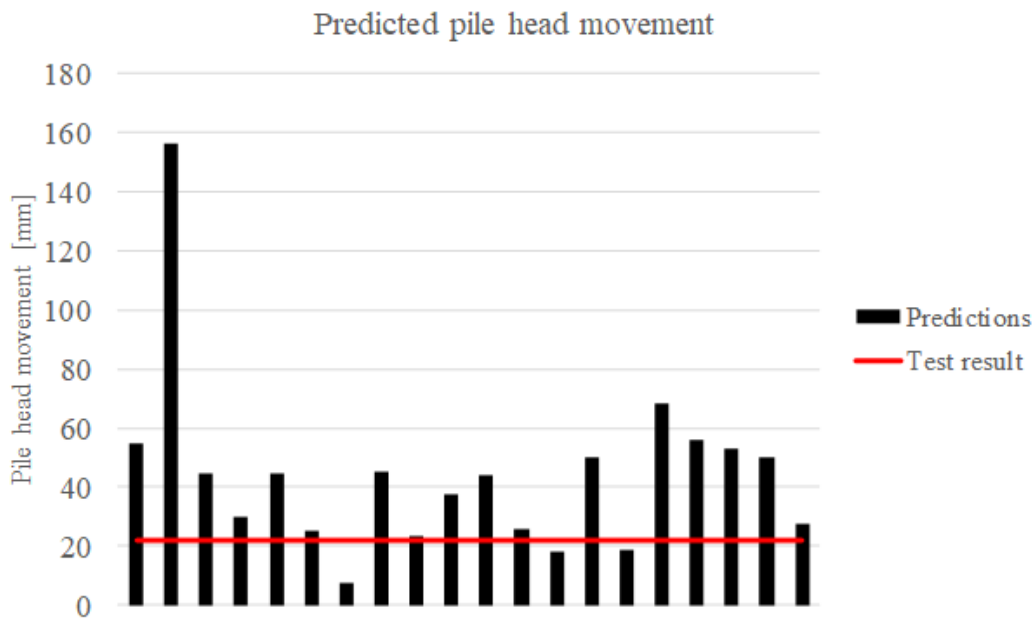


Figure 6.16: Assessed movement at predicted pile capacity

Theoretical pile capacity, or ultimate resistance often refers to maximum load applied before soil collapse, practical pile capacity is necessarily not the same thing. Depending on construction plan and restrictions, maximum allowed settlements varies. Strict settlement regulations for short or long term settlement can be a determining factor and can therefore be seen as the capacity. It should of course be noted that participants might have misunderstood what was asked for and simply replied with ultimate resistance. However, some submissions have been followed with assumptions of allowed short term settlements, and others have stated that "capacity is dependant of settlements regulations" and left this part of the submission form blank. Either way, it is not surprising that the results show a large spread of predicted movements. The literature study explains how vertical settlements of pile head is dependent of pile compression and shear of adjacent soil. The many uncertainties in these calculations makes for a complicated and challenging task. Stiffness of the pile changes with load increment, changing the strain rate of the concrete. Movements of adjacent soil differs horizontally according to chapter 2.1.1, "load transfer between pile and soil", and effects of the protective half pipe is unknown.

6.3.4 Force distribution and resistance effect

The result shows varying μ -strains at each level with sister bars. Figures 6.17 and 6.18 illustrates measured strains over increased load at 2, 11, 19, 39 and 48 meters depth. Note there is only 3 registered working strain gauges at 39.5 meter. Over all, it shows an increased variation with increased load, especially at shallower levels. This indicates a non-centred axial load which in turn means there is a rotational force (torque), moment, in the pile. Exactly how much this torque affect the result in terms of elasticity modulus, resistance or settlements is unknown and has to be further evaluated. But, since force calculation indicate similar E-modulus regardless of load, see Appendix, the varying μ -strains and its effect is assumed to be small enough to be seen as negligible.

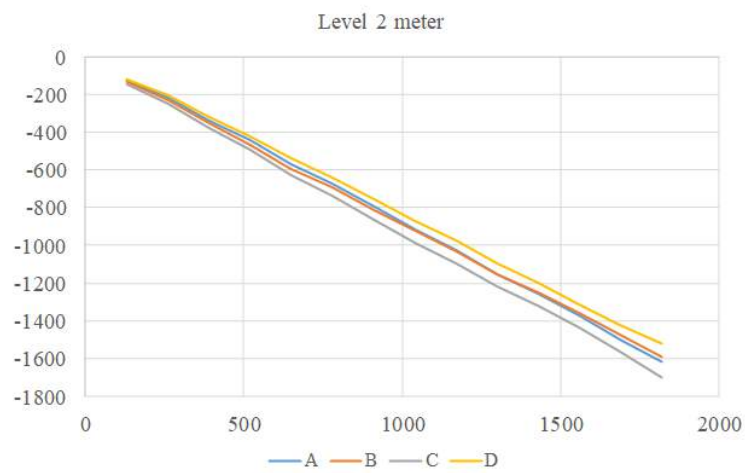
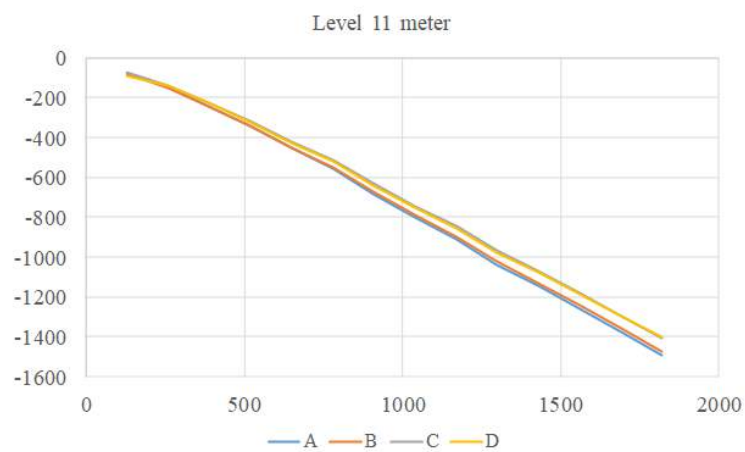
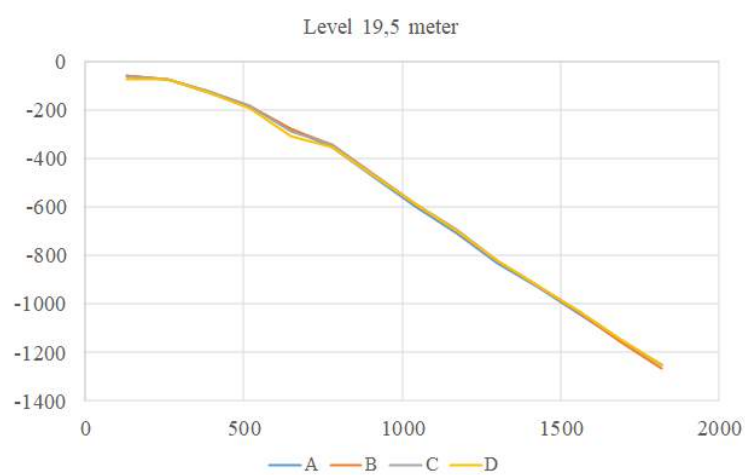
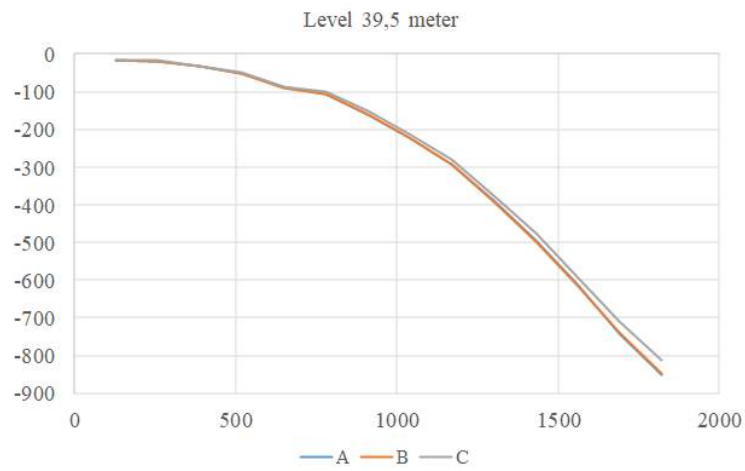
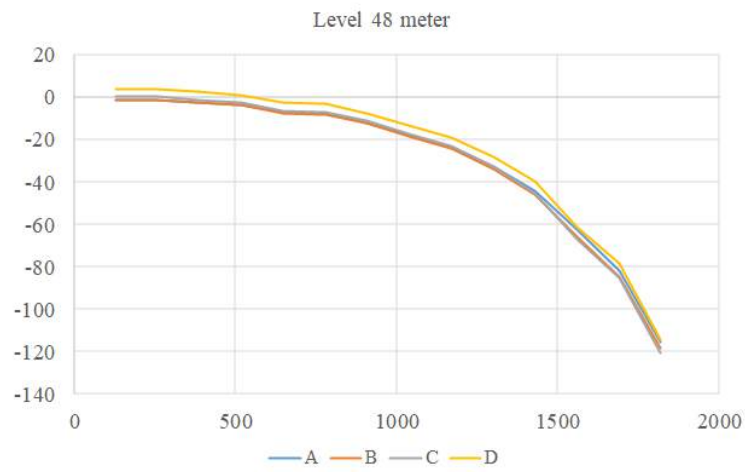
(a) μ -strains at 2 meters(b) μ -strains at 11 meters(c) μ -strains at 19.5 meters

Figure 6.17: μ -strains registered from every sister bar mounted on level -2, -11 and -19.5m from ground surface.



(a) μ -strains at 39.5 meters



(b) μ -strains at 48 meters

Figure 6.18: μ -strains registered from every sister bar mounted on level -39.5 and -48m from ground surface.

Resistance effect is calculated according to Chapter 2.1.2, integrating from pile toe to pile head, assuming zero toe resistance.

$$R = R_{toe} + \int_L^{L_p} f_m dA$$

It is based on a pre-calculated alpha and evaluated shear strength used when calculating geotechnical bearing capacity. To better see how the resistance effect compares to the force distribution in the pile, they are plotted together in Figure 6.19.

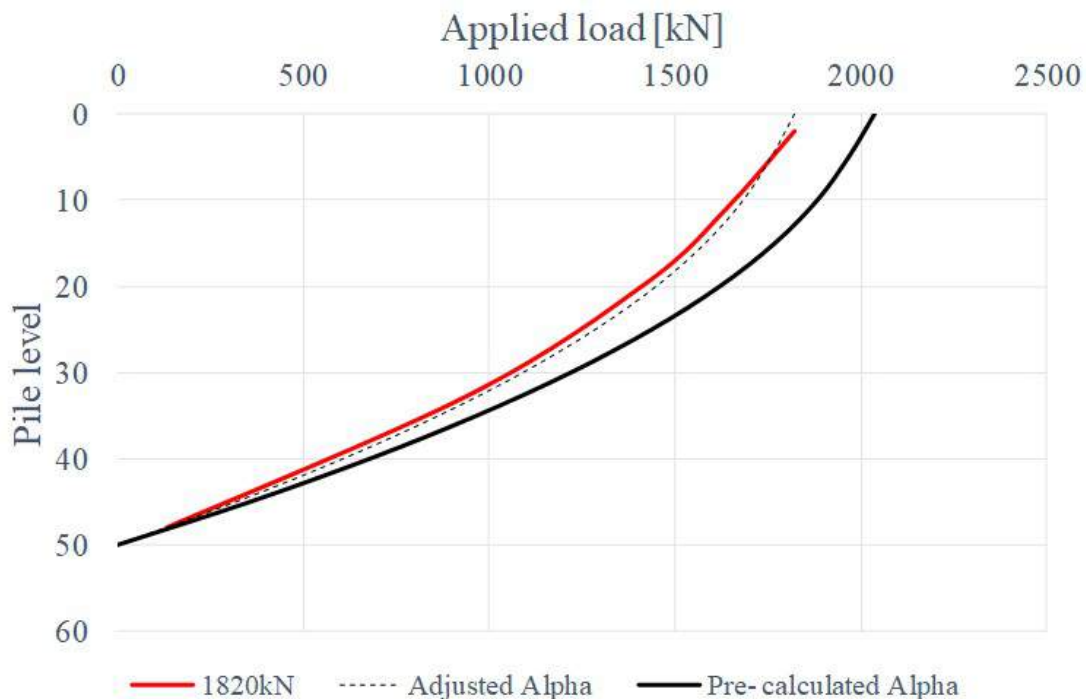


Figure 6.19: Adjusted and pre-calculated alpha together with force distribution from the loading test result

The illustration presents the load distribution of resistance effect using pre-calculated soil parameters and force distribution corresponding to the test result. The figure indicates a much stiffer pile response in its lower parts than what is assumed in the resistance effect. An interesting aspect is that 65% of the applied load is transferred and taken up by the lower 18 meters of the pile, and more than 50% by the last 10 meters. The theoretical resistance effect shows a well distributed load with smooth increase in stiffness behavior, when in reality, the stiffness behavior after 30-35 meter is considerably greater. They are however similar at shallower levels, the dotted line illustrates the resistance effect with an adjustment factor to match the ultimate resistance of 1820 kN. The behavior and appearance of the curves the first 20-25 meters indicates that current calculation methods are derived from emery of test of shorter piles.

6.3.5 Ultimate resistance (α - method) and shear strength

To calculate the pile ultimate resistance or "Capacity", the two most used methods in Sweden, the α and β -method is used.

The result from the α - method shows an ultimate resistance of 2036kN, compared to 1820kN which is the result from the static loading test. Considering the calculation steps included in the method, it is straight forward and easy to follow. An alpha value of 0.9 seem accurate following instructions from the Swedish pile commission report. However, the adjustment factor κ_t can be discussed. It is stated in the commission report that the the factor κ_t should be treated with regard to load duration in terms of "minute", "day", "month" or "long time" loading, see Table 6.4. The static loading test was ongoing for several hours, but each loading increment was only active for minutes at the time, and there is no "hour" duration for adjustment purposes. It is unclear how to determine from what point of the static loading test should be counted when defining κ_t . If assuming that the characteristic long time capacity of the pile is somewhere between 70%-80% of the maximum ultimate resistance (1820kN) from looking at the test result and at Jorge Yannie's doctoral thesis (Yannie, 2016), and also considering all load increments from the test above those 70% - 80% as some kind of variable load. Then, the total loading time above characteristic long term capacity is more than 1 hour, and so, it can be argued that it is not a "minute" load. Even though it is not a "day" load it might be closer to a short time material setup rather than a passing car. With that in mind, considering the static loading test as some kind of "hour" load. κ_t is put to 0.95. Applying this new adjustment factor to shear strength C_u results in an ultimate resistance of 1934.2 kN.

Table 6.4: Loading time adjustment factor κ_t , (Eriksson et al., 2004)

Duration	Example of load types	κ_t
"Minute"	Soil testing machines, wind loads, by- passing cars etc.	1.0
"Day"	Short time material setup etc.	0.9
"Month"	material stocking, high tides etc.	0.8
"Long time"	Dead load, stocking etc.	0.7

With or without the adjusted time factor κ_t , the from α - method gives an acceptable result in terms of ultimate resistance. Also, comparing it with participants in the prediction event indicates that our interpretation of the soil parameters are good. Because the result is very much dependant on a good soil interpretation, reducing the α value has minor effect compared to misinterpreting shear strength.

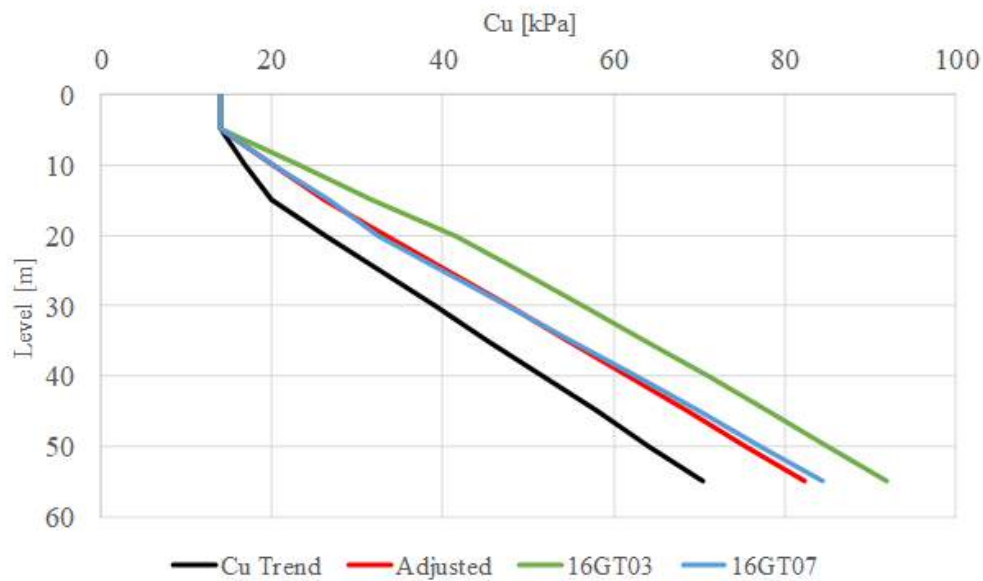


Figure 6.20: Shear strength evaluation

Comparing the static loading test with evaluated ultimate resistance, it shows an overestimated c_u . If evaluating the test result with the interpreted shear strengths in Figure 6.20, it can be said that the shear trend (black line) in the local area is underestimated but in fact to a degree accurate. This might be true comparing with borehole 16GT03. 16GT07 is however not at all far away from giving a very good answer, better than the trend. It can also be argued that an underestimated c_u is better than an overestimated, in favor of the trend. On the other hand, underestimated shear strength evaluations often entails more expensive geotechnical solutions. Considering that every geotechnical case is, or can be different in parameter data, adjusting the trend with good preformed soil tests from the local area is a economical favorable application.

It should be noted that when the α - method was developed, the α - factor was mainly derived from unadjusted shear vane attempts. The Swedish pile commission report 100 (Eriksson et al., 2004) also refers to this when the α - method is used. Today it is known that unadjusted shear vane attempts often overestimates results of the top soil layers, and underestimates the lower. Since our shear evaluation mainly is based on CRS, triax, and DSS attempts, this is noted as a source of error in the α - calculations. With this said, the evaluated ultimate resistance from the α - method corresponds well with the loading test result.

Using force distribution from Figure 6.19 and back calculating force uptake between each level of sister bar, and dividing it with pile circumference, the shear strength used at these levels were calculated. Figure 6.21 shows back calculated c_u at each level of strain gauges at different loads, and compares it to trend line and evaluated c_u .

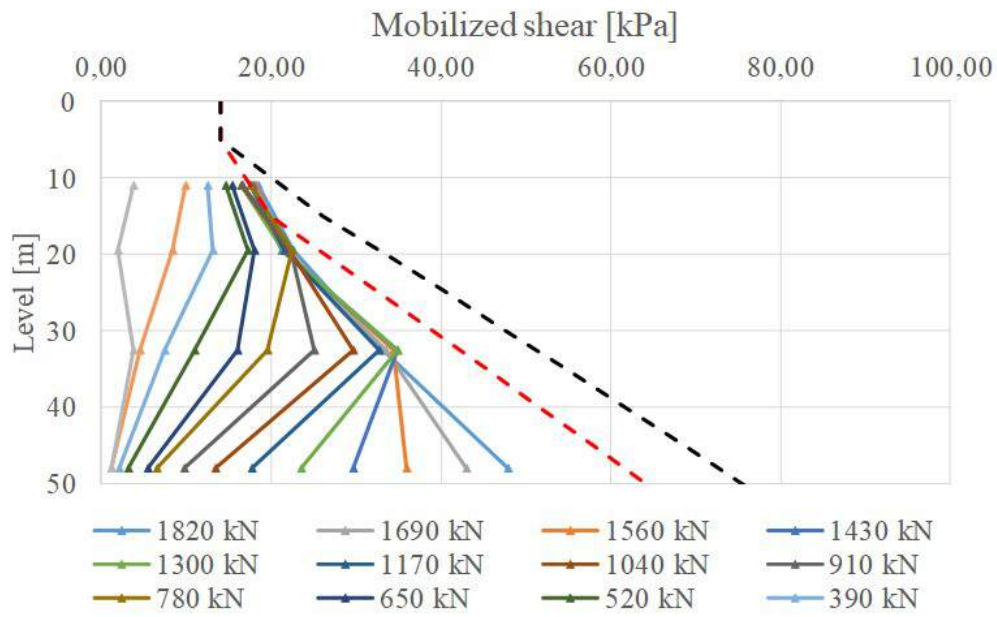


Figure 6.21: Back calculated mobilized shear strength with c_u trend lines and used, adjusted c_u .

Before further evaluating this result, the literature study illustrated how adjacent soil is affected at different elevation levels of the pile, see Figure 6.22. According to the literature, the position at the stress strain relationship curve for surrounding soil differs. It shows local "Soil collapses" or progressive soil failure, meaning that the position on the curve is beyond peak values for soils at shallower levels whereas deeper clay layers are still not mobilized. The result in Figure 6.21 shows that mobilized resistance increases with increased load, even at high loads. In order for the response to correspond to literature, resistance would somewhat decrease at a certain point of load. When this do not happen, it is difficult to determine the post peak resistance. It can be due to fast loading, resulting instead of mobilizing the load correctly along the pile, the majority of the load is consumed instantly by the deeper clay levels when the stiffness is significantly higher. This behavior can be a result of a very stiff pile, the phenomenon in Figure 6.22 is partly dependent on pile deformation, and an absence of, or a very small pile deformation can be a contributing factor to this result. However, the behavior of the graphs in Figure 6.22 clearly illustrated how the deeper levels of the surrounding soil continuously increase in mobilized shear, and even though the final mobilization is lower than expected, the behavior is very similar. The reason for the low resulted shear could be a layer of softer material with different structure and strength.

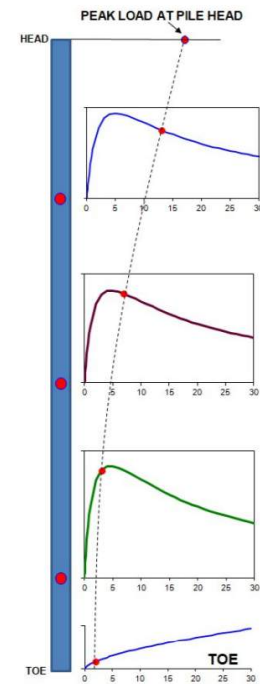


Figure 6.22: Force distribution, and load-movement relationship along a floating pile. *Fellenius 2018, Development of t-z curves*

Nothing on any evaluated soil test (Appendix 3) indicates that this would be the case, however, since no tests have been performed specifically on the testing spot of the pile (they rarely are) this can not be precluded. An influencing factor to this result can also be a form of high local overburden pore pressure ground, in which case the buoyancy effect can lower the effective stresses. If the effect can be so very significant is hard to say and yet to be evaluated. It should be emphasized that it might not even be possible to translate load distribution in the pile to surrounding shear strength, meaning that in reality, the shear strength in the soil is different from what the result in Figure 6.22 shows.

6.3.6 Ultimate resistance (β - method)

The calculated ultimate resistance from the β - method 1396 kN is about 77% of the load during soil failure at the static loading test. The β - value 0.15 was evaluated with the Norsk Peileveiledning- report.

Other suggestions of the β - value can be found. In Meyerhof's report from 1976, it is stated that for soft to medium stiffness clays, β tend to decrease with pile length from typically 0.3–0.5 at depths less than approximately 15 m to 0.1–0.25 at a depth of 60 m (Meyerhof, 1976).

Using the test result at soil failure of 1820 kN to evaluate the *true* β - value, a value of 0.1977 is obtained, see Table 6.5. This is quite higher than both Meyerhof's suggestion of range for a 50 m long pile, and Norsk Peileveiledning. However the test result presents a ultimate resistance for a *shorter* amount of time, the test lasted for a few hours only, and the β - method calculates a long term ultimate resistance. As discussed in the α - part of the analysis, the long term ultimate resistance is 70- 80% of the short term. Since the ultimate resistance using the β from Norsk Peileveiledning is 77% of the short term (pile test result), it is likely that this value is correct for the long term ultimate resistance.

Considering that the effective stress is directly dependent on the density of the soil and the β variable is independent of soil properties excluding the relative density, it is fair to assume that β equals 0.15 and $\beta = 0.17*\alpha$ is applicable in the Gothenburg region for piles with length of 50 m or longer (in Figure 5.3 β is vertical between 50 and 60 m).

Table 6.5: β calculated from test result

Total σ'_v integral	8460 [kPa]
Circumferential area	1.1 [m^2]
Test load at soil failure	1840 [kN]
Beta	0.1977

7

Conclusion

α & β methods

The initial α was set to 0.9, only corrected for the pile circumference. This resulted in a ultimate resistance of 2036 kN which is 11% higher than test result, second best prediction in the prediction event. However the loading time coefficient κ_T was initially set to 1 (minute load). Since the critical part of the load test lasted about one hour, κ_T was set to 0.95 in the analysis. This resulted in an ultimate resistance of 1934 kN, 6% higher than test result. The short duration of the loading test provides a higher ultimate resistance than the long term case, and when applying a κ_T of 0.7 (long term), the ultimate resistance is instead 1367 kN. This is 95% of the 1435 kN of post-peak stabilization load measured.

The β - method is used for long term ultimate capacity, and using a β - value of 0.15 a ultimate resistance of 1396 kN was obtained. This is 77% of the test result, but 97% of the post-peak stabilization load.

The long term results from the α - and β - method fits well within the 70- 80% long term interval based on the test result, and the results also correlates well with the post-peak stabilization load. Also, the long term results differs only 2% between the two methods. Based on this one loading test, the α - and β - method is valid on piles with lengths of 50 m. Furthermore, based on this test the post-peak stabilization load can be seen as the long term ultimate resistance.

t - z - analysis

Provided the pile compression part of the pile displacement analysis, the API and the Karlsrud approach gives good representations of pile head movement and soil stiffness behavior when compared to the load- movement curve of the loading test. The calculated pile head displacement at peak load for the API approach is 19.7 mm, and for the Karlsrud approach, 26.6 mm. This corresponds to 22.5 mm from the loading test result. The pile compression contribution to the pile displacement is 85% for the API and 64% for Karlsrud approach, which emphasizes the importance to include this in a t - z - analysis.

Prediction event

The submitted predictions from the event shows a wide variety of both pile behaviour and ultimate resistance. Out of 23 predictions one presented the correct ultimate resistance, and five presented correct load- movement stiffness. Most participants interprets the term *ultimate resistance* as the load before soil failure. Since the predictions was submitted from across the globe, engineering experience from the participants local conditions affects the results in term of interpretation and gut. However it can be concluded that there is a variety of methods and programs to analyze the pile behaviour and ultimate resistance with varying results. These may in their turn be more accurate in their local conditions where they are mainly used.

Further analysis

Based on the vast amount of raw data collected from the loading test further analysis can be made. Four times per minute the strain was logged in five levels of the test pile, in all four rebars. These measurements shows that the strain is not equal between the rebars in each level of the pile. This data can be used to analyze of the torque along the pile in order to further evaluate the bending and the young's modulus of the pile. The strain load relation indicates a modulus of about 15 GPa which is lower than expected. This can be examined further.

Future pile loading tests

Loading tests is an important tool to evaluate and develop current design methods. Results from this particular test gives better insight on the validity of current methods for longer piles than earlier empirical data for shorter piles. Further loading tests on similar piles in the same soil conditions is necessary to further justify the results from this one test. The same pile is set to be tested again in a year with the same procedure when and if the surrounding soil has re-consolidated. When designing a new loading test, additional instrumentation is recommended. An inclinometer would provide useful information about the inclination of the pile. This would enable a better understanding of the different strains in the cross sections at different heights of the pile. Also, a pore pressure meter next to the pile would be preferable. The effective stress evaluated for the β - method relied alone on density evaluation and ground water level. A long term test is perhaps too impractical, but a *longer* test with similar conditions would further verify the long term ultimate resistance result from this one test.

References

- Alén, C. (2009). Pile Foundations – Short Handbook. , 1–33.
- API. (2007). Recommended practice for planning, designing and constructing fixed offshore platforms–working stress design..
- Bowles, J. E. (1997). *Foundation Analysis and Design Fifth Edition* (Vol. 20) (No. 3). doi: 10.1016/0013-7952(84)90010-3
- Bradshaw, A. S., Haffke, S., & Baxter, C. D. (2012). Load transfer curves from a large-diameter pipe pile in silty soil. In *Full-scale testing and foundation design: Honoring bengt h. fellenius* (pp. 590–601).
- Briaud, J. (2013). *Introduction to geotechnical engineering: unsaturated and saturated soils, hoboken*. John Wiley & Sons, Inc.
- Burland, J. (1973). Shaft friction of piles in clay—a simple fundamental approach. *Publication of: Ground Engineering/UK/*, 6(3).
- Byggnorm, S. (1983). Statens planverks författningssamling. *Stockholm: LiberTryck*.
- Chandler, R. (1968). The shaft friction of piles in cohesive soils in terms of effective stress. *Civil Eng & Public Works Review/UK/*, 60(708).
- Eriksson, P., Jendeby, L., Olsson, T., & Svensson, T. (2004). Commission on Pile Research.
- Federation of Piling Specialists. (2006). Handbook on Pile Load Testing. *Handbook*(February), 47.
- Fellenius, B. (2016). Report on the b.e.s.t. prediction survey.
- Fellenius, B. (2017a). *Basics of foundation design*. Lulu. com.
- Fellenius, B. (2017b). Summary and comments on my prediction to the 3rd cfpb.
- Fellenius, B. (2018). Discussion of “development of axial pile load transfer curves based on instrumented load tests” by céilia bohn, alexandre lopes dos santos, and roger frank. *Journal of Geotechnical and Geoenvironmental Engineering*, 144(4), 07018005.
- Fellenius, B. H. (1972). Down-drag on piles in clay due to negative skin friction. *Canadian Geotechnical Journal*, 9(4), 323–337.
- Geokon. (2013). Installation manual Models 4911A/4911.
- Jendeby, L. (1986). Friction piled foundations in soft clay. a study of load transfer and settlements. *D. thesis, Chalmers Univ. of Technology*.
- Karlsruud, K. (2014). Ultimate shaft friction and load-displacement response of axially loaded piles in clay based on instrumented pile tests. *Journal of Geotechnical and Geoenvironmental Engineering*, 140(12), 04014074.
- Karlsruud, K., Nadim, F., et al. (1990). Axial capacity of offshore piles in clay. In *Offshore technology conference*.

- Larsson, R. (1989). *Jords egenskaper*. Statens geotekniska institut.
- Mayerhof, G. (1976). Bearing capacity and settlement of pile foundations. *Journal of Geotechnical and Geoenvironmental Engineering*, 102(ASCE# 11962).
- NGF. (2012). *Peleviledningen*.
- Olsson, C., & Holm, G. (1993). *Pålgrundläggning*. AB Svensk Byggtjänst.
- Ottolini, M., Dijkstra, J., & van Tol, F. (2014). Immediate and long-term installation effects adjacent to an open-ended pile in a layered clay. *Canadian Geotechnical Journal*, 52(7), 982–991.
- Poulos, S. J. (1971). *The stress-strain curves of soils*. Geotechnical Engineers Incorporated.
- Skov, R., & Denver, H. (1988). Time-dependence of bearing capacity of piles. In *Proc. third international conference on the application of stress-wave theory to piles. ottawa* (pp. 25–27).
- Smith, G. N. (1982). *Elements of soil mechanics for civil and mining engineers* (No. Monograph).
- Tomlinson, M. (1970). Some effects of pile driving on skin friction. In *Conf. on behaviour. of piles, inst, civ. engrs., london* (pp. 107–114).
- Torstensson, B.-A. (1973). *Kohesionspålar i lös lera: en fältstudie i modellskala*.
- Wrana, B. (2015). Pile load capacity–calculation methods. *Studia Geotechnica et Mechanica*, 37(4), 83–93.
- Yannie, J. (2016). *On the long-term behaviour of tension loaded piles in natural soft soils* (Unpublished doctoral dissertation). Chalmers University of Technology.

A

Appendices

- Appendix 1.** Prediction event invitation
- Appendix 2.** Test site location
- Appendix 3.** Soil tests
- Appendix 4.** Shear strength evaluation
- Appendix 5.** Stress distribution evaluation

A.1 Prediction event invitation

This e-mail was sent to potential participants of the prediction event in mars 2018.

Prediction event invitation

Invitation to predict a pile head load- movement response due to static test loading at Construction site E45 in Gothenburg city. The event is made as a part of a Master thesis in geotechnical engineering at Chalmers University of Technology in association with PEAB anläggning.



(a) Installation

(b) Measuring equipment

Figure 1: Installation of test pile, September 2017

Fredrik Edvardsson Johannes Pettersson

Department of Civil and Environmental Engineering
Chalmers University of Technology
Gothenburg, Sweden
2018-02-08

Registration

In order to participate in the Prediction event, please register your intent to submit by informing Johannes Petterson at:

< jopetter@student.chalmers.se >

All submitted predictions and participants will be kept confidential and only known by the authors of the thesis (Petterson, Edvardsson). When the registration is submitted the participants will receive all necessary information on geometry, soil, pile and methodology as well as a template for submission of prediction. Please submit the registration before March 16. Deadline for submitting the prediction is set to April 15, and the results will be sent to the participants before May 31.

For more information or questions, please contact:

Johannes Petterson; 0768085525; jopetter@student.chalmers.se

Fredrik Edvardsson; 0761616100; freedv@student.chalmers.se

Introduction

This prediction event project is made as a part of a Master thesis in geotechnical engineering at Chalmers University of Technology. It intends to provide the opportunity for other engineers to try their ability to predict a load- movement response on a single cohesion pile at static load, and to show on the complexity of foreseeing this type of geotechnical problem. The provided results from the participants will be anonymous, and the compilation of these along with the test result will be shared with all participants and in the Master thesis itself.

The test pile is installed at an ongoing project at E45, Lilla Bommen-Marieholm in central Gteborg, where the main road is to be submerged 6 meters below ground level. The construction is scheduled to be completed in 2021 and it will then include a 400 meter long tunnel to enable for future housing and office areas at ground level. The soil profile at the site consists of a more than a 90 metre deep layer of marine glacial and post-glacial clay. In order to support the forthcoming tunnel, roads, and buildings, a total of about 3,000, floating piles will be driven to about 65 m embedment. A static loading test will be carried out on a pile located outside the immediate construction area. The pile is instrumented with strain gauges attached to the reinforcing bars at five depths.

The prediction event consist of evaluating the theoretical pile head load-movement curve of this research pile based of geotechnical data of the surrounding soil and pile properties. The static load test itself is preformed by the entrepreneur, but the prediction event with its compilation and analyzation of submitted results is part of the independent master thesis by Johannes Petterson and Fredrik Edvardsson only.

Pile Details

The test pile is a 50 meter long, 275 mm diameter square reinforced concrete displacement pile. It consists of 4 elements 13 meter each, connected with 3 joints. The pile along with the joints are dimensioned to sustain construction load. Along the pile is mounted 140 mm half-pipe, containing the cables from the measure devices along the pile, see figure 2.

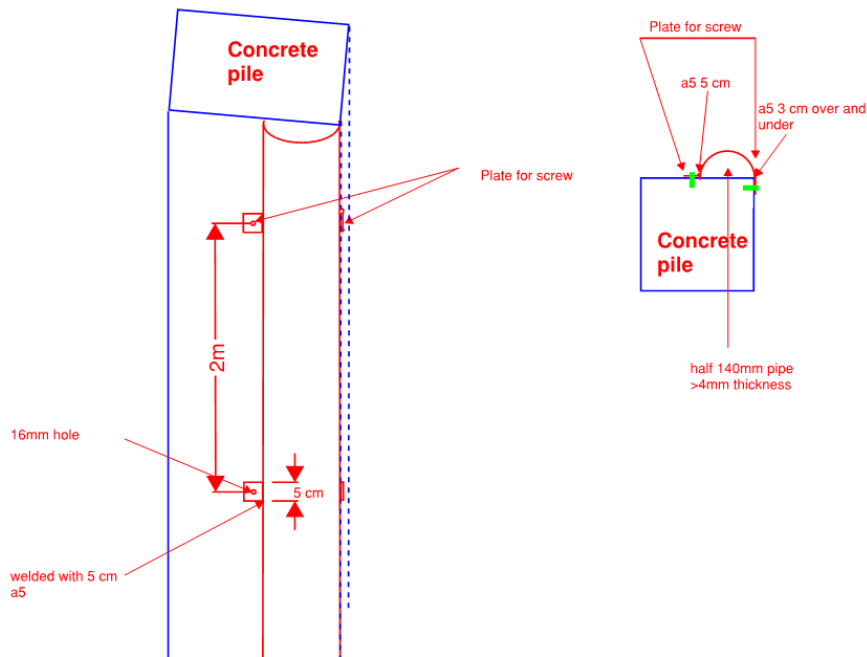


Figure 2: Profile of the pile

Equipment

The measuring equipment consists of rebar strainmeters or "Sister bars". These Strain gauges are attached to the reinforcing bars at five elevation levels, see figure 3, the first one at -2 meters from pile head. They are designed to measure concrete strains due to imposed loads. During the static load test these instruments will indicate deformations in the bars which will be used to measure force distribution along the pile. The hydraulic jack will be calibrated before test start and the force indicated by the jack is compared with the first strain gauge. Pile head movement will be measured during the whole test and correlated with reference points close to the pile.

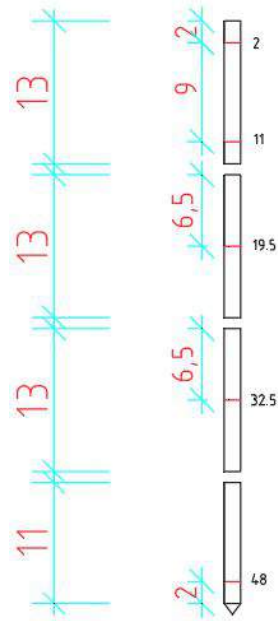


Figure 3: Test pile close up

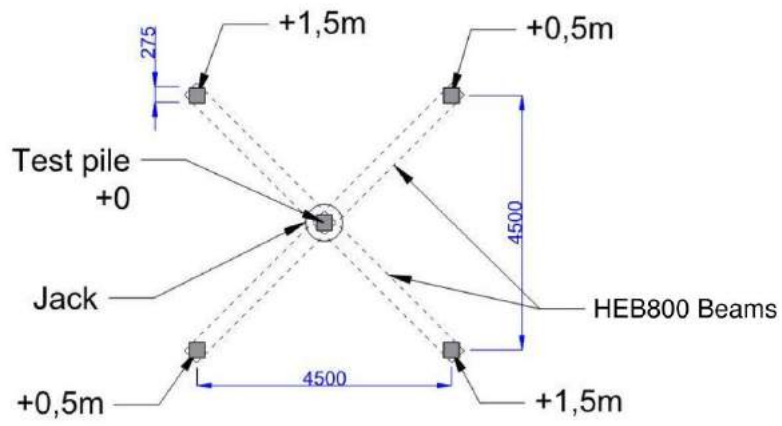
Test implementation

The static load test procedure will be performed with several load intervals, consisting of series of equal load increments with an interval of 30 minutes. During this time, the load will be held constant until:

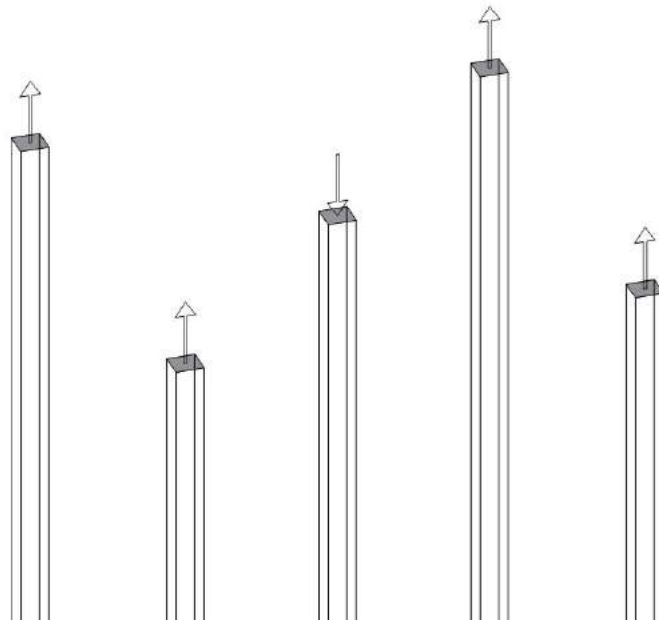
- A pile head movement of 50 mm is reached.
- Excessive movement resulting in the jack unsuccessfully holding a constant pressure.
- Maximum available jack load is reached.

Upon when any of the above situations occur, the prediction event procedure is over.

Figure 4a illustrates the test setup in 2D plane. The test pile is surrounded with four support piles. Two HEB800 Beams with dimensions 800 x 300 mm are welded on the supporting piles and creates a cross over the middle test pile. The hydraulic jack applies pressure on the test pile which creates a drag force on the acting supporting piles as well as a pressure force on the test pile, see figure 4b.



(a) Test setup in 2D plane. Four supporting piles surrounding the test pile



(b) 3D view of acting forces on piles

A.2 Test site location

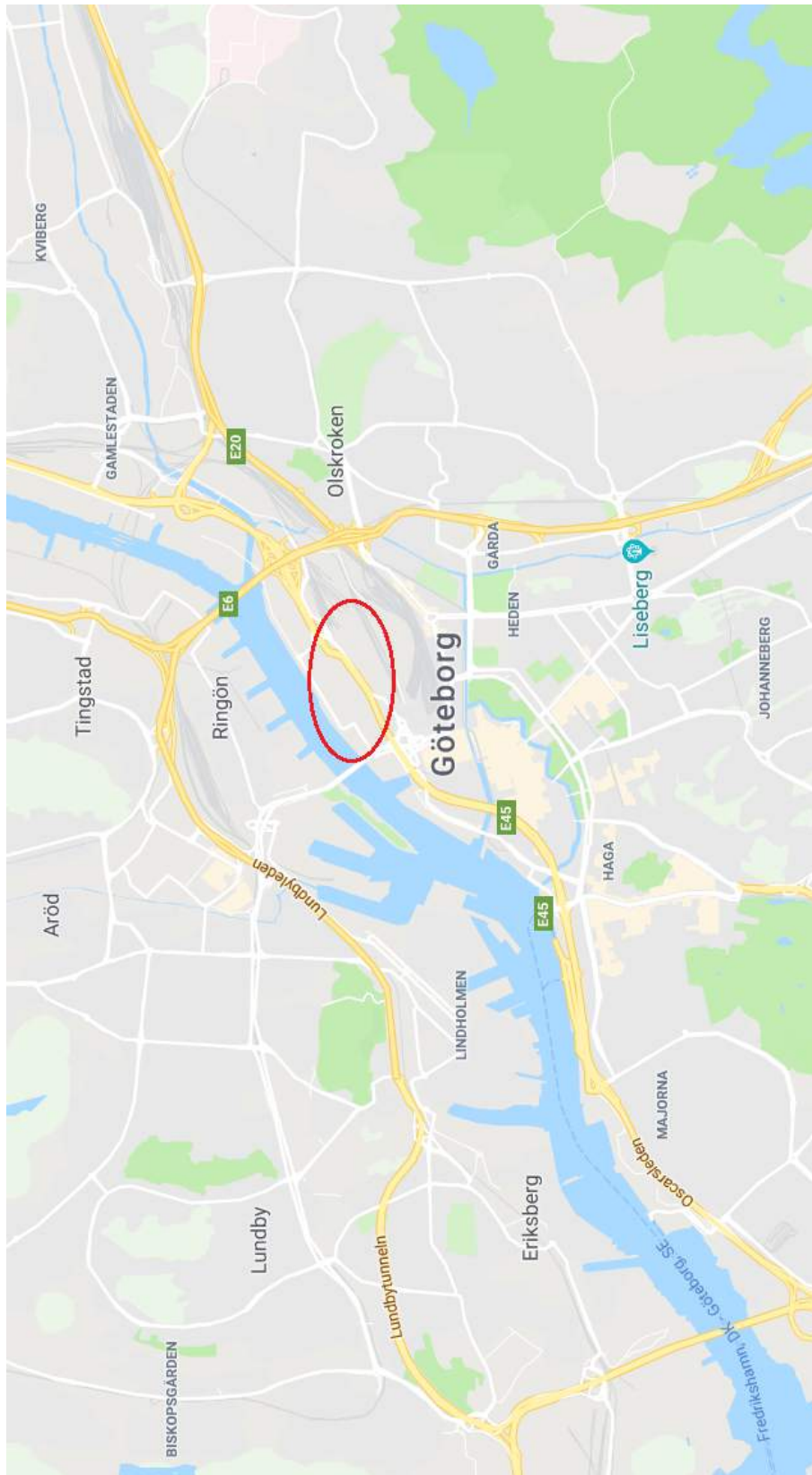


Figure A.1: Map of performed tests and test pile location

A.3 Soil tests

These soil tests were sent to the participants of the prediction event. Direct shear test (DSS) or "Direkt skjuv" in Swedish made 2016 were used to evaluate shear strength (figure A.16 - A.23).

CPT-sondering

Projekt Nytt Regionens Hus		Plats Göteborg																																																																																																																															
Projektnummer U11004		Borrhål BG11-4																																																																																																																															
Borrföretag Bohusgeo AB		Sonderingsdatum 2011-04-12																																																																																																																															
Förboeringsdjup 5.00 m	Geometri Normal																																																																																																																																
Startdjup 5.00 m	Vätska i filter Glycerol																																																																																																																																
Stoppdjup 90.90 m	Fältgeotekniker Jan Axelsson																																																																																																																																
Grundvattenyta 1.10 m	Utrustning Geotech																																																																																																																																
Referens my	<input checked="" type="checkbox"/> Portryck registrerat vid sondering																																																																																																																																
Kalibreringsdata Sond nr 4260 Inre friktion O_i 0.0 kPa Datum 2011-01-24 Inre friktion O_i 0.0 kPa Areafaktor a 0.834 Cross talk c_1 0.000 Areafaktor b 0.000 Cross talk c_2 0.000		Nollvärden <table border="1"> <thead> <tr> <th></th> <th>Portryck (kPa)</th> <th>Friktion (kPa)</th> <th>Spetstryck (MPa)</th> </tr> </thead> <tbody> <tr> <td>Före</td> <td>280.20</td> <td>121.90</td> <td>6.88</td> </tr> <tr> <td>Efter</td> <td>280.70</td> <td>122.00</td> <td>6.89</td> </tr> <tr> <td>Diff</td> <td>0.50</td> <td>0.10</td> <td>0.01</td> </tr> </tbody> </table>			Portryck (kPa)	Friktion (kPa)	Spetstryck (MPa)	Före	280.20	121.90	6.88	Efter	280.70	122.00	6.89	Diff	0.50	0.10	0.01																																																																																																														
	Portryck (kPa)	Friktion (kPa)	Spetstryck (MPa)																																																																																																																														
Före	280.20	121.90	6.88																																																																																																																														
Efter	280.70	122.00	6.89																																																																																																																														
Diff	0.50	0.10	0.01																																																																																																																														
Skalfaktorer <table border="1"> <thead> <tr> <th>Portryck Område Faktor</th> <th>Friktion Område Faktor</th> <th>Spetstryck Område Faktor</th> </tr> </thead> <tbody> <tr> <td>2.00 3310</td> <td>0.50 3845</td> <td>50 1368</td> </tr> </tbody> </table>		Portryck Område Faktor	Friktion Område Faktor	Spetstryck Område Faktor	2.00 3310	0.50 3845	50 1368	Korrigerig Portryck (ingen) Friktion (ingen) Spetstryck (ingen) Bedömd sonderingsklass CPT2																																																																																																																									
Portryck Område Faktor	Friktion Område Faktor	Spetstryck Område Faktor																																																																																																																															
2.00 3310	0.50 3845	50 1368																																																																																																																															
<input type="checkbox"/> Använd skalfaktorer vid beräkning																																																																																																																																	
Portrycksobservationer <table border="1"> <thead> <tr> <th>Djup (m)</th> <th>Portryck (kPa)</th> </tr> </thead> <tbody> <tr><td>1.10</td><td>0.00</td></tr> <tr><td>7.10</td><td>60.00</td></tr> <tr><td>19.00</td><td>181.00</td></tr> <tr><td>31.40</td><td>295.00</td></tr> <tr><td>43.00</td><td>423.00</td></tr> <tr><td>55.00</td><td>528.00</td></tr> <tr><td>67.20</td><td>666.00</td></tr> </tbody> </table>		Djup (m)	Portryck (kPa)	1.10	0.00	7.10	60.00	19.00	181.00	31.40	295.00	43.00	423.00	55.00	528.00	67.20	666.00	Skiktgränser <table border="1"> <thead> <tr> <th>Djup (m)</th> </tr> </thead> <tbody> <tr><td></td></tr> </tbody> </table>	Djup (m)		Klassificering <table border="1"> <thead> <tr> <th colspan="2">Djup (m)</th> <th>Densitet (ton/m³)</th> <th rowspan="2">Flytgräns</th> <th rowspan="2">Jordart</th> </tr> <tr> <th>Från</th> <th>Till</th> <th></th> </tr> </thead> <tbody> <tr><td>0.00</td><td>1.00</td><td>1.90</td><td></td><td>Exc</td></tr> <tr><td>1.00</td><td>3.10</td><td>1.74</td><td></td><td>Exc</td></tr> <tr><td>3.10</td><td>5.00</td><td>1.60</td><td></td><td>Exc</td></tr> <tr><td>5.00</td><td>7.50</td><td>1.64</td><td>0.61</td><td>siLe sk</td></tr> <tr><td>7.50</td><td>12.50</td><td>1.55</td><td>0.66</td><td>Le</td></tr> <tr><td>12.50</td><td>17.50</td><td>1.54</td><td>0.68</td><td>Le (sk) _si_</td></tr> <tr><td>17.50</td><td>22.50</td><td>1.65</td><td>0.63</td><td>Le (sk)</td></tr> <tr><td>22.50</td><td>27.50</td><td>1.66</td><td>0.66</td><td>siLe (sk)</td></tr> <tr><td>27.50</td><td>32.50</td><td>1.62</td><td>0.70</td><td>siLe (sk)</td></tr> <tr><td>32.50</td><td>37.50</td><td>1.63</td><td>0.78</td><td>siLe (sk)</td></tr> <tr><td>37.50</td><td>42.50</td><td>1.67</td><td>0.74</td><td>siLe</td></tr> <tr><td>42.50</td><td>47.50</td><td>1.66</td><td>0.72</td><td>siLe</td></tr> <tr><td>47.50</td><td>52.50</td><td>1.66</td><td>0.72</td><td>siLe</td></tr> <tr><td>52.50</td><td>57.50</td><td>1.70</td><td>0.71</td><td>siLe</td></tr> <tr><td>57.50</td><td>62.50</td><td>1.70</td><td>0.69</td><td>siLe</td></tr> <tr><td>62.50</td><td>67.50</td><td>1.71</td><td>0.67</td><td>siLe (sk)</td></tr> <tr><td>67.50</td><td>72.50</td><td>1.73</td><td>0.67</td><td>siLe</td></tr> <tr><td>72.50</td><td>77.50</td><td>1.76</td><td>0.62</td><td>siLe</td></tr> <tr><td>77.50</td><td>82.50</td><td>1.78</td><td>0.59</td><td>siLe</td></tr> <tr><td>82.50</td><td>87.50</td><td>1.85</td><td>0.54</td><td>siLe</td></tr> </tbody> </table>	Djup (m)		Densitet (ton/m ³)	Flytgräns	Jordart	Från	Till		0.00	1.00	1.90		Exc	1.00	3.10	1.74		Exc	3.10	5.00	1.60		Exc	5.00	7.50	1.64	0.61	siLe sk	7.50	12.50	1.55	0.66	Le	12.50	17.50	1.54	0.68	Le (sk) _si_	17.50	22.50	1.65	0.63	Le (sk)	22.50	27.50	1.66	0.66	siLe (sk)	27.50	32.50	1.62	0.70	siLe (sk)	32.50	37.50	1.63	0.78	siLe (sk)	37.50	42.50	1.67	0.74	siLe	42.50	47.50	1.66	0.72	siLe	47.50	52.50	1.66	0.72	siLe	52.50	57.50	1.70	0.71	siLe	57.50	62.50	1.70	0.69	siLe	62.50	67.50	1.71	0.67	siLe (sk)	67.50	72.50	1.73	0.67	siLe	72.50	77.50	1.76	0.62	siLe	77.50	82.50	1.78	0.59	siLe	82.50	87.50	1.85	0.54	siLe
Djup (m)	Portryck (kPa)																																																																																																																																
1.10	0.00																																																																																																																																
7.10	60.00																																																																																																																																
19.00	181.00																																																																																																																																
31.40	295.00																																																																																																																																
43.00	423.00																																																																																																																																
55.00	528.00																																																																																																																																
67.20	666.00																																																																																																																																
Djup (m)																																																																																																																																	
Djup (m)		Densitet (ton/m ³)	Flytgräns	Jordart																																																																																																																													
Från	Till																																																																																																																																
0.00	1.00	1.90		Exc																																																																																																																													
1.00	3.10	1.74		Exc																																																																																																																													
3.10	5.00	1.60		Exc																																																																																																																													
5.00	7.50	1.64	0.61	siLe sk																																																																																																																													
7.50	12.50	1.55	0.66	Le																																																																																																																													
12.50	17.50	1.54	0.68	Le (sk) _si_																																																																																																																													
17.50	22.50	1.65	0.63	Le (sk)																																																																																																																													
22.50	27.50	1.66	0.66	siLe (sk)																																																																																																																													
27.50	32.50	1.62	0.70	siLe (sk)																																																																																																																													
32.50	37.50	1.63	0.78	siLe (sk)																																																																																																																													
37.50	42.50	1.67	0.74	siLe																																																																																																																													
42.50	47.50	1.66	0.72	siLe																																																																																																																													
47.50	52.50	1.66	0.72	siLe																																																																																																																													
52.50	57.50	1.70	0.71	siLe																																																																																																																													
57.50	62.50	1.70	0.69	siLe																																																																																																																													
62.50	67.50	1.71	0.67	siLe (sk)																																																																																																																													
67.50	72.50	1.73	0.67	siLe																																																																																																																													
72.50	77.50	1.76	0.62	siLe																																																																																																																													
77.50	82.50	1.78	0.59	siLe																																																																																																																													
82.50	87.50	1.85	0.54	siLe																																																																																																																													
Anmärkning: CPT-sondering utvärderad enligt SGI Info 15, revidering 2007 Parametrar för utvärdering har tagits från skruv i denna punkt och kolprovtagning från punkt 8																																																																																																																																	

Bohusgeo AB

Datum: 2012-04-03

Figure A.4: CPT result

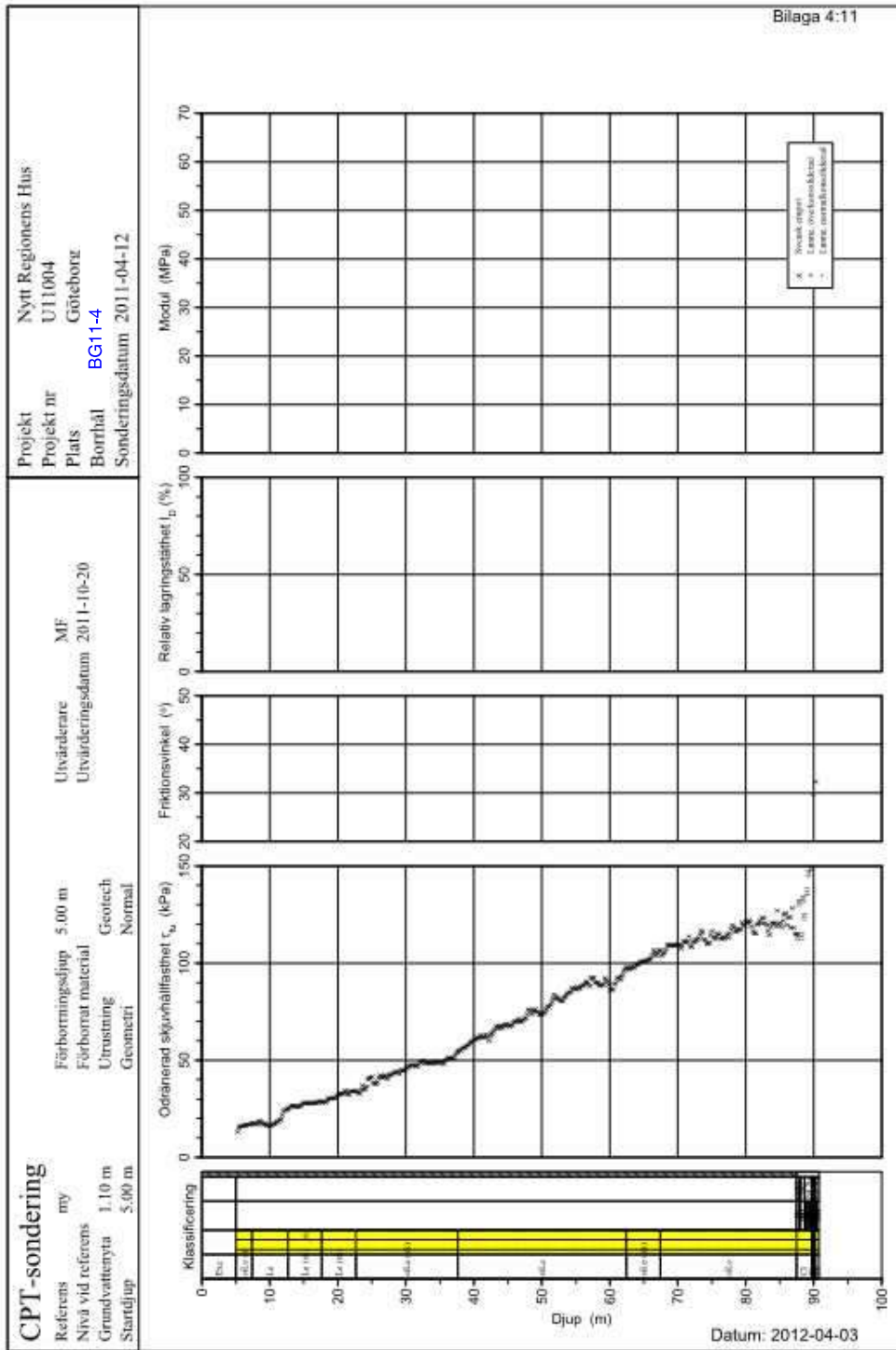


Figure A.5: CPT result

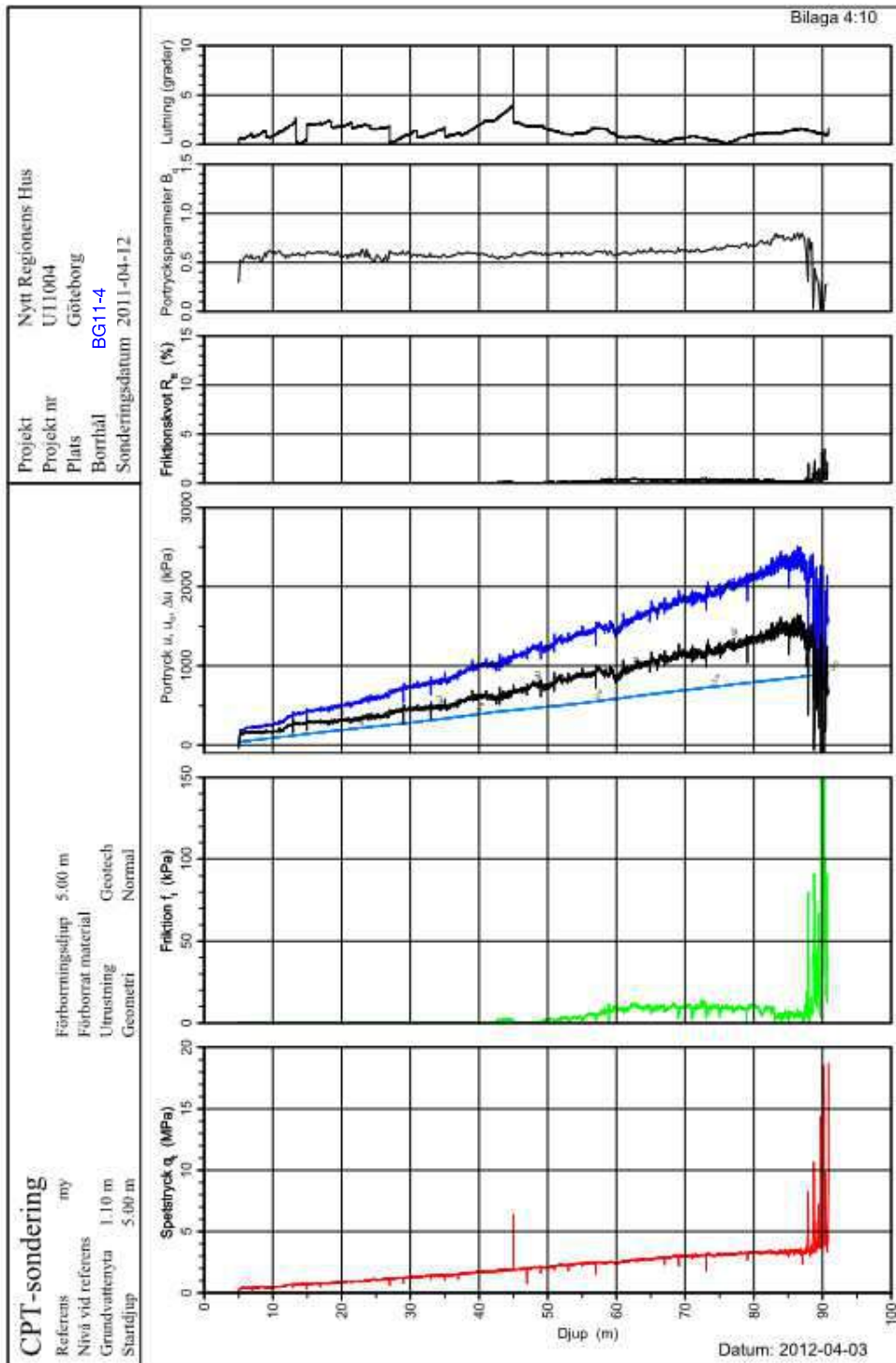
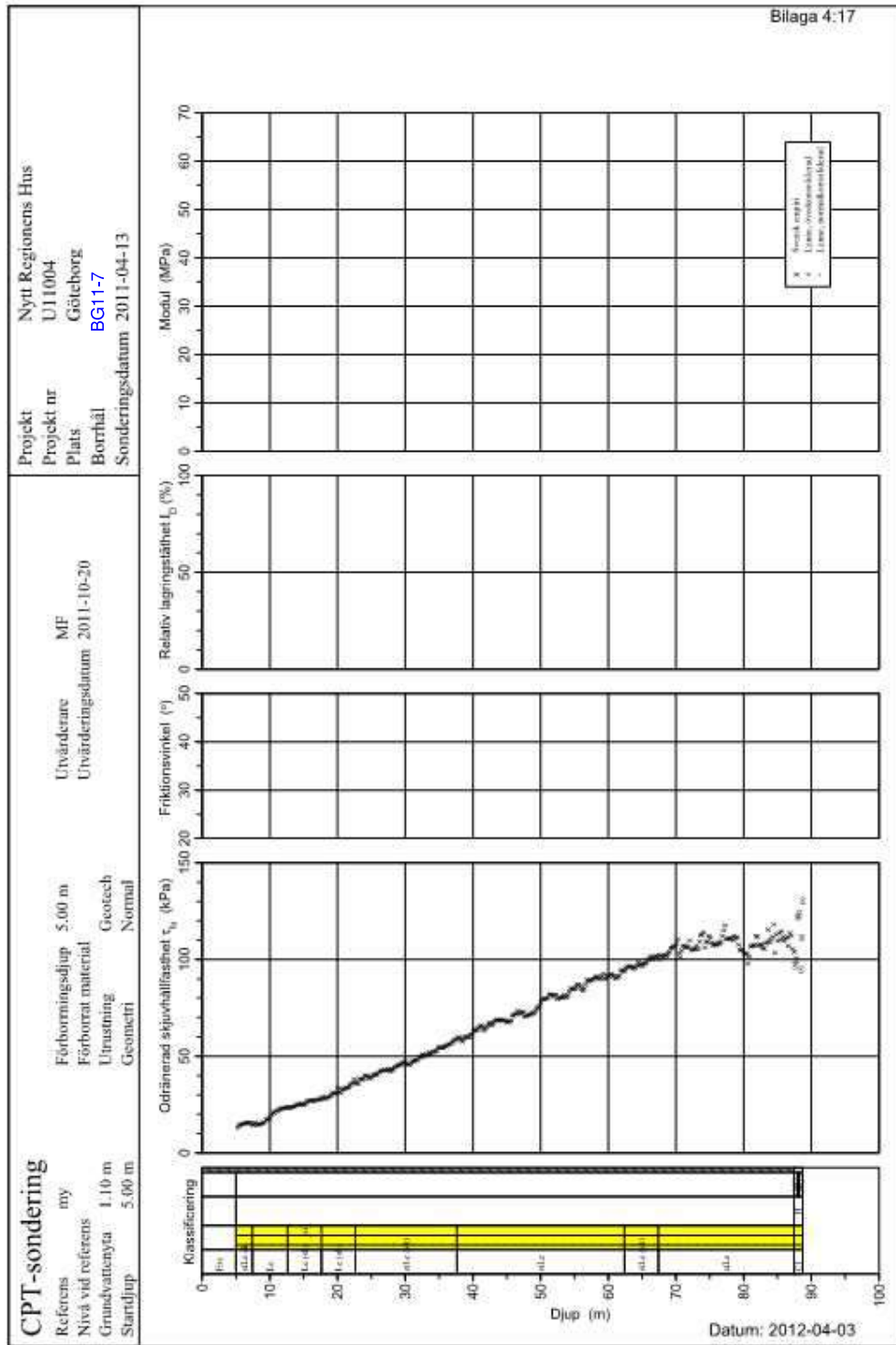


Figure A.6: CPT result

CPT-sondering

Projekt	Nytt Regionens Hus	Plats	Göteborg
Projektnummer	U11004	Borrhål	BG11-7
Borrforetag	Bohusgeo AB	Sonderingsdatum	2011-04-13
Förborrningsdjup	5.00 m	Geometri	Normal
Startdjup	5.00 m	Vätska i filter	Glycerol
Stoppdjup	88.82 m	Fältgeotekniker	Jan Axelsson
Grundvattenyta	1.10 m	Utrustning	Geotech
Referens	my	<input checked="" type="checkbox"/> Portryck registrerat vid sondering	
Kalibreringsdata		Nollvärden	
Sond nr	4260	Inre friktion O_c	0.0 kPa
Datum	2011-01-24	Inre friktion O_f	0.0 kPa
Areafaktor a	0.834	Cross talk e_1	0.000
Areafaktor b	0.000	Cross talk e_2	0.000
Skalfaktorer		Korrigerings	
Portryck	Friktion	Spetstryck	
Område Faktor	Område Faktor	Område Faktor	
2.00 3310	0.50 3845	50 1368	
<input type="checkbox"/> Använd skalfaktorer vid beräkning		Portryck (ingen)	
		Friktion (ingen)	
		Spetstryck (ingen)	
		Bedömd sonderingsklass CPT1	
Portrycksobservationer		Skiktgränser	Klassificering
Djup (m)	Portryck (kPa)	Djup (m)	Djup (m)
1.10	0.00		Från Till Densitet (ton/m ³) Flytgräns Jordart
7.10	60.00		0.00 2.10 1.90 Exc
19.00	181.00		2.10 5.00 1.64 Exc
31.40	295.00		5.00 7.50 1.64 0.61 siLe sk
43.00	423.00		7.50 12.50 1.55 0.66 Le
55.00	528.00		12.50 17.50 1.54 0.68 Le (sk) _si_
67.20	666.00		17.50 22.50 1.65 0.63 Le (sk)
			22.50 27.50 1.66 0.66 siLe (sk)
			27.50 32.50 1.62 0.70 siLe (sk)
			32.50 37.50 1.63 0.78 siLe (sk)
			37.50 42.50 1.67 0.74 siLe
			42.50 47.50 1.66 0.72 siLe
			47.50 52.50 1.66 0.72 siLe
			52.50 57.50 1.70 0.71 siLe
			57.50 62.50 1.70 0.69 siLe
			62.50 67.50 1.71 0.67 siLe (sk)
			67.50 72.50 1.73 0.67 siLe
			72.50 77.50 1.76 0.62 siLe
			77.50 82.50 1.78 0.59 siLe
			82.50 87.50 1.85 0.54 siLe
Anmärkning: CPT-sondering utvärderad enligt SGI Info 15, revidering 2007			
Parametrar för utvärdering har tagits från skruv i denna punkt och kolvprovtagning från punkt 8			

Figure A.7: CPT result



Bohusgeo AB

Figure A.8: CPT result

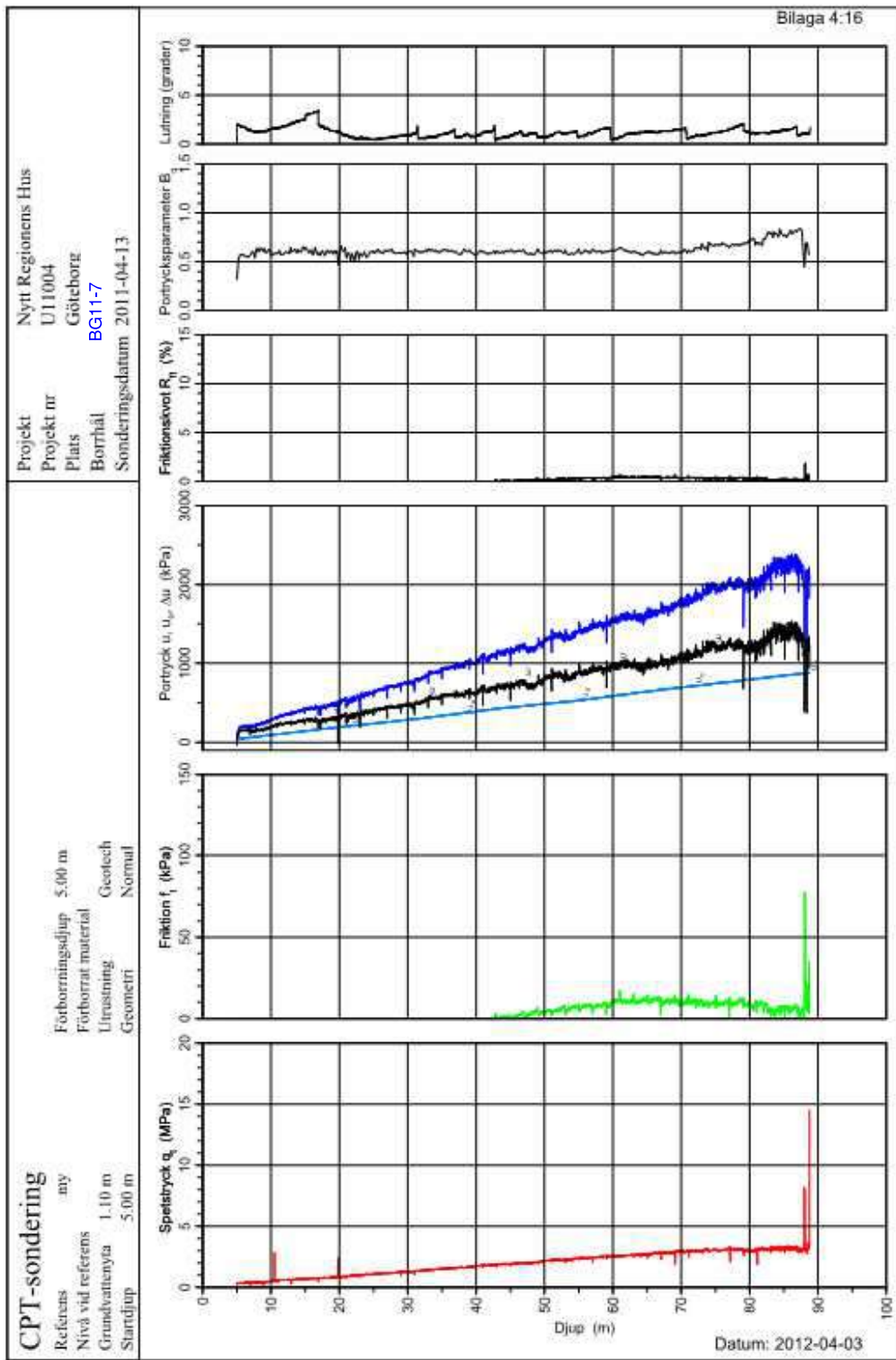


Figure A.9: CPT result

 CRS TEST 2016 PM LABTEK AB Madångsvägen 11 43932 ONSALA Tel. 0704674666	Datum:	2016-03-10	Borrhål:	16GT03	W_N före test = 66%
	Utfört av:	Peter Hedborg	Djup:	40m	δ före test = 1,61t/m ³
	Beställare	PEAB	Tub:	5059	
	Projekt	E45 Lilla Bommen	Jordart enligt okulärbesiktning:	Grå sulfidmelerad LERA	
	Er ref:	Michael B Svensson			

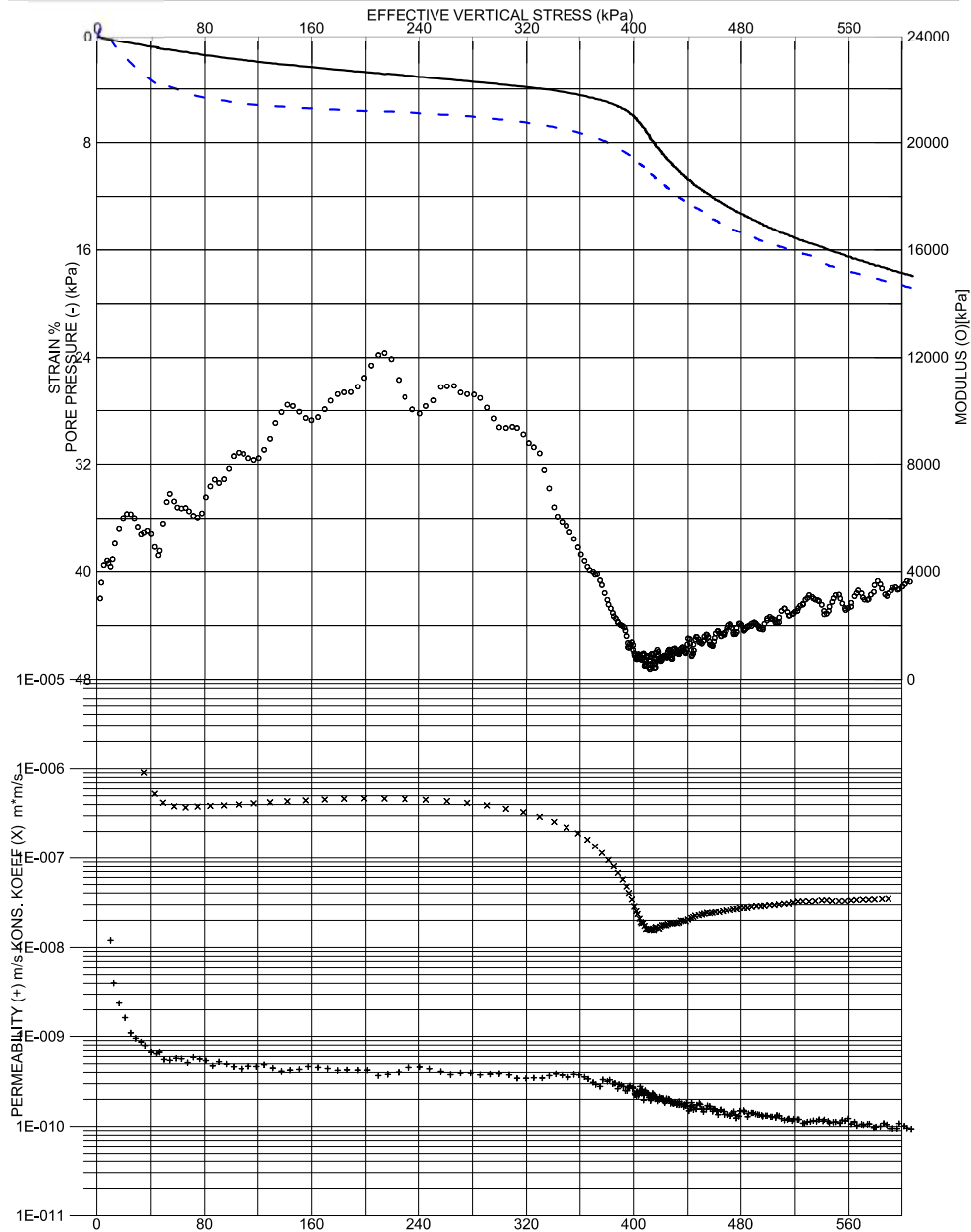


Figure A.10: CRS test

 CRS TEST 2016 PM LABTEK AB Madångsvägen 11 43932 ONSALA Tel. 0704674666	Datum:	2016-03-10	Borrhål:	16GT03	W_N före test = 58%
	Utfört av:	Peter Hedborg	Djup:	55m	δ före test = 1,65t/m ³
	Beställare	PEAB	Tub:	10-0778	
	Projekt	E45 Lilla Bommen	Jordart enligt okularbesiktning:	Grå svagt melerad LERA	
	Er ref:	Michael B Svensson			

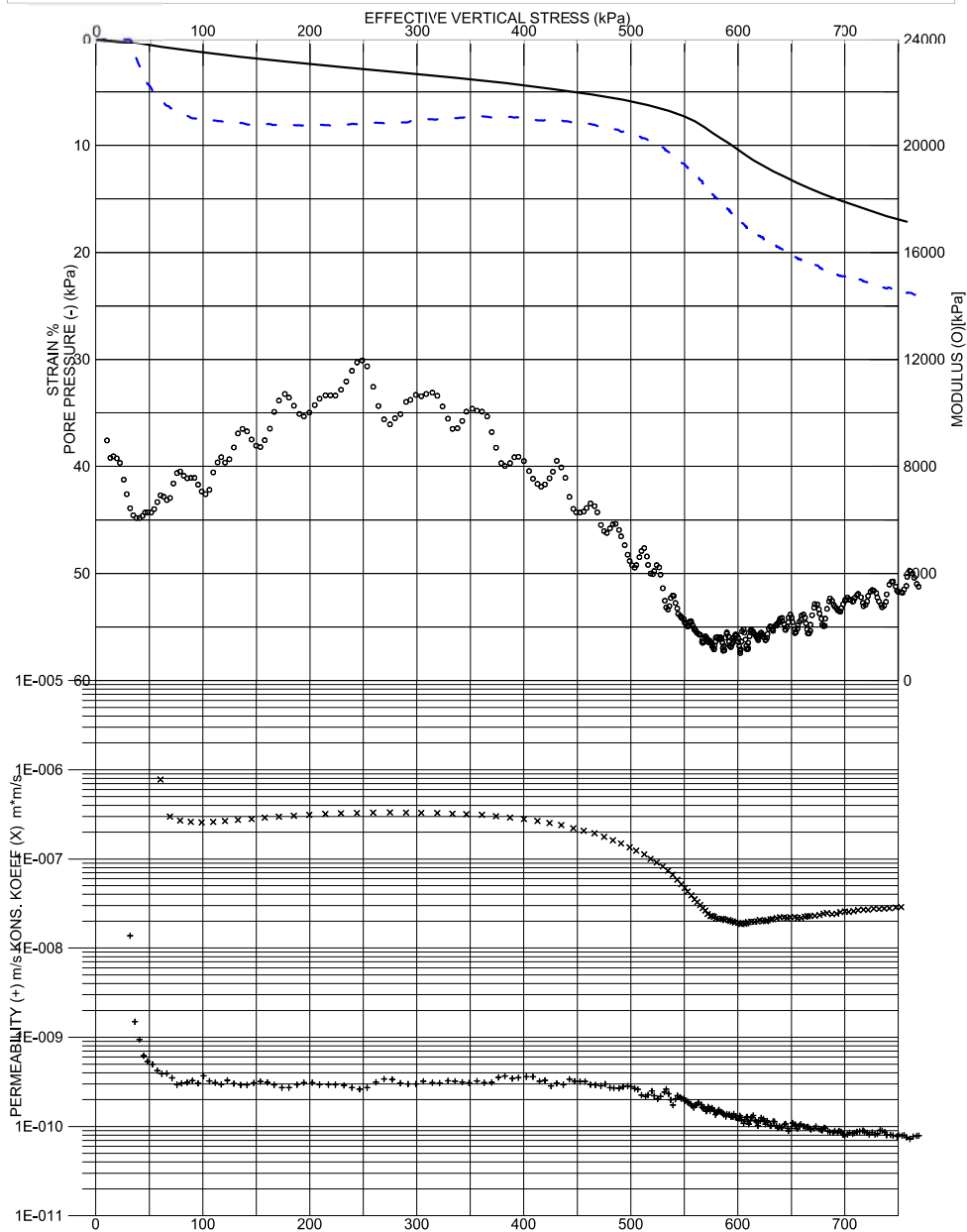


Figure A.11: CRS test

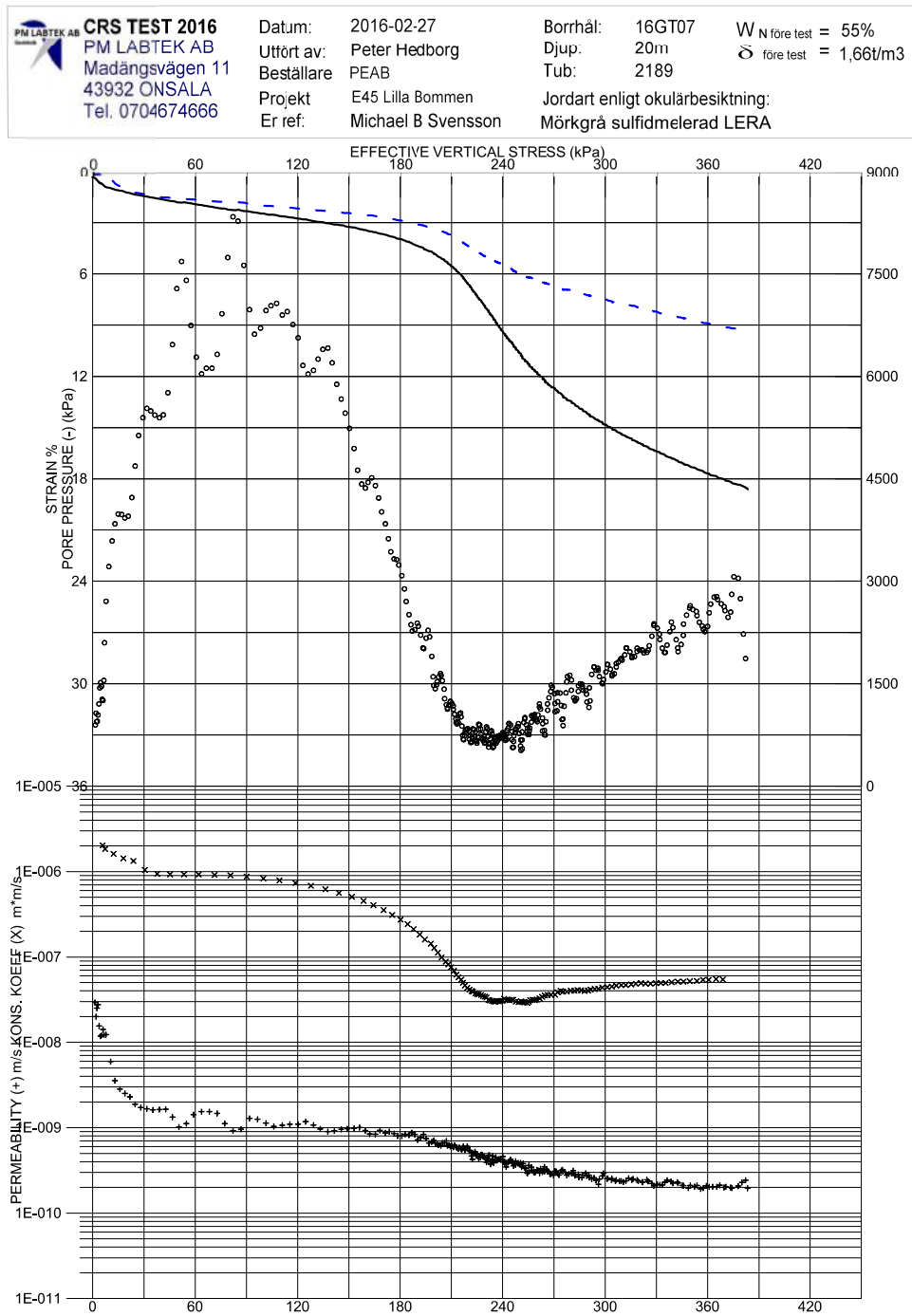


Figure A.12: CRS test

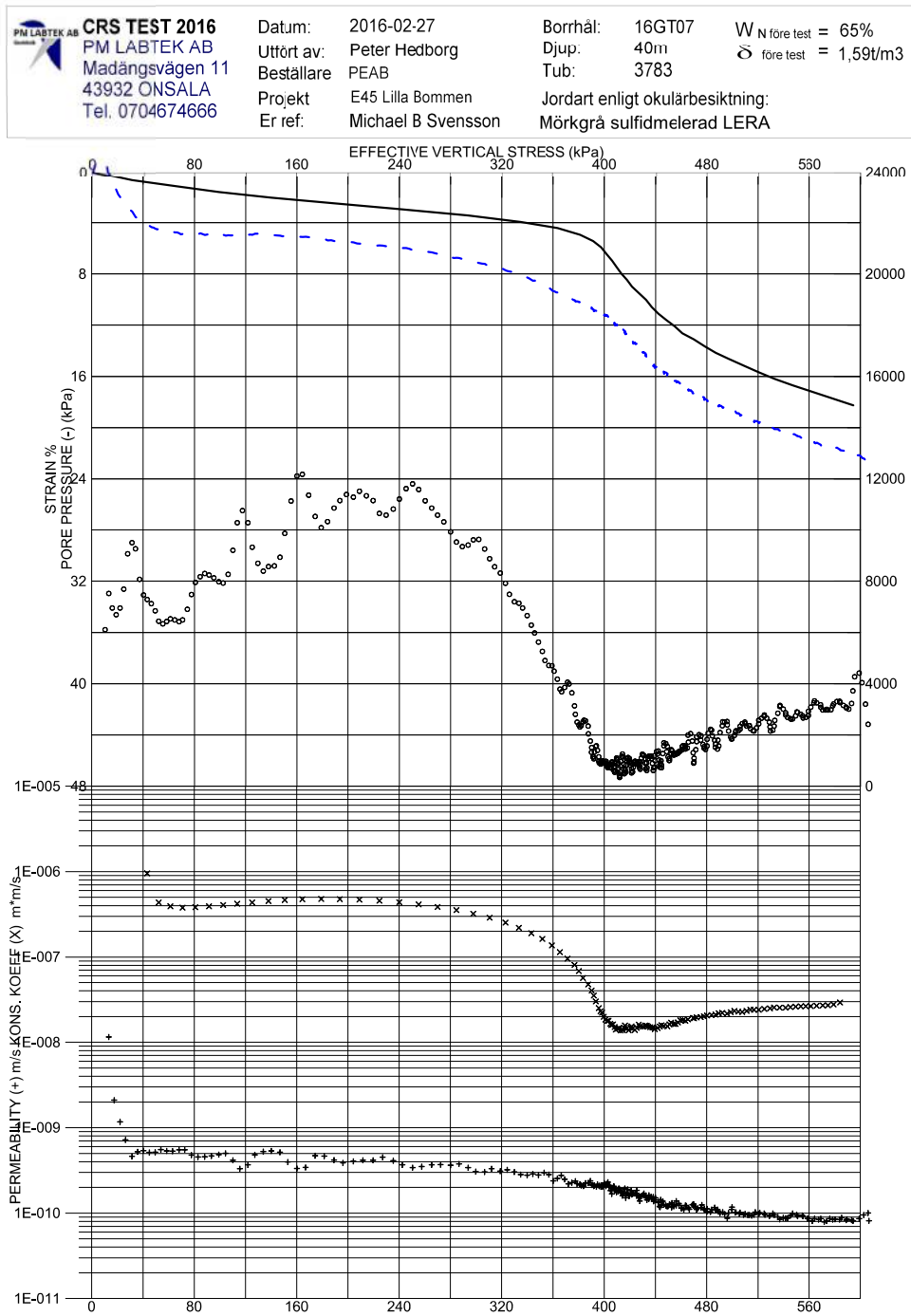


Figure A.13: CRS test

 CRS TEST 2016 PM LABTEK AB Madångsvägen 11 43932 ONSALA Tel. 0704674666	Datum:	2016-02-27	Borrhål:	16GT07	W_N före test = 57%
	Utfört av:	Peter Hedborg	Djup:	55m	δ före test = 1,65t/m ³
	Beställare	PEAB	Tub:	1360	
	Projekt	E45 Lilla Bommen	Jordart enligt okulärbesiktning:		
	Er ref:	Michael B Svensson	Grå sulfidmelerad LERA		

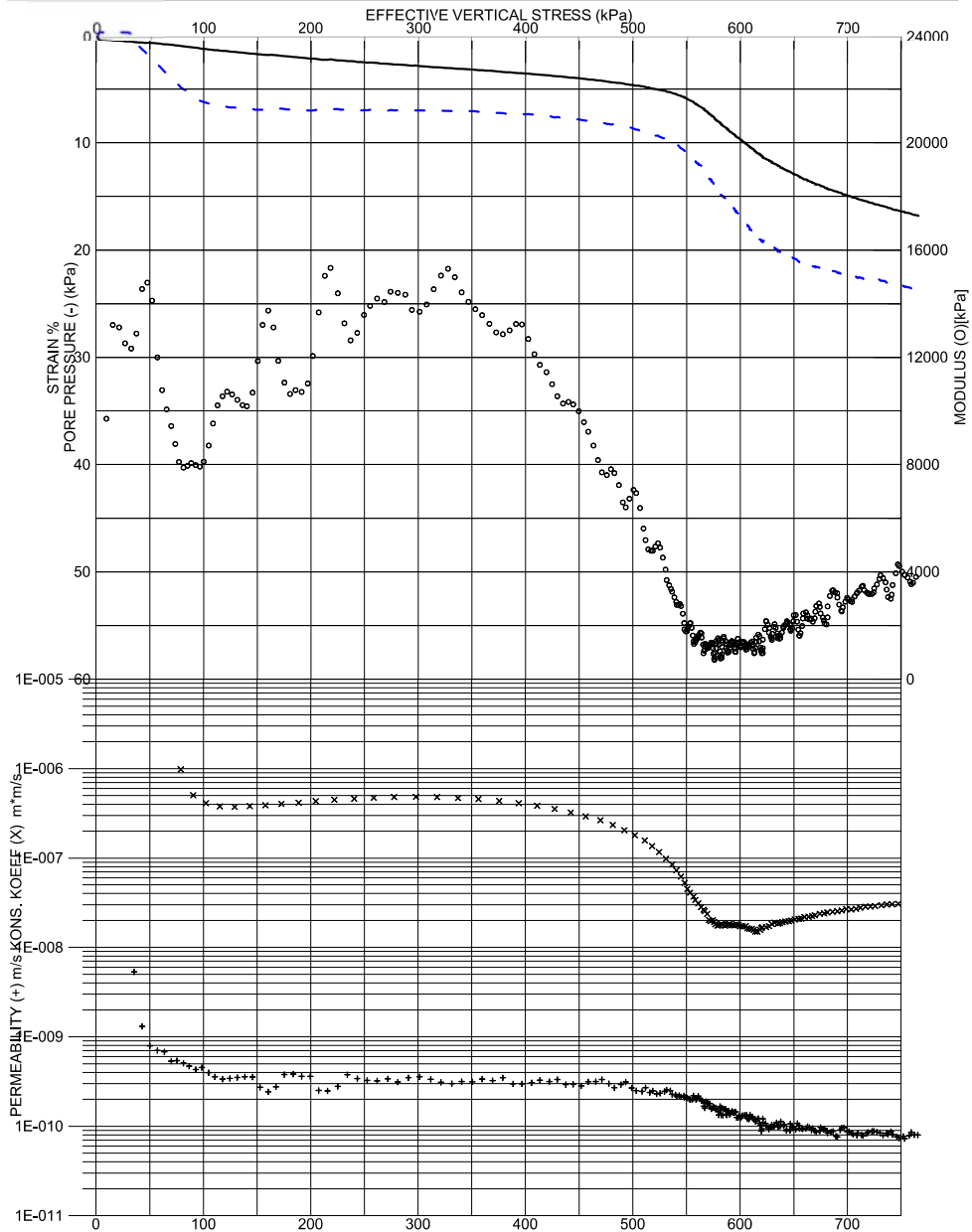


Figure A.14: CRS test

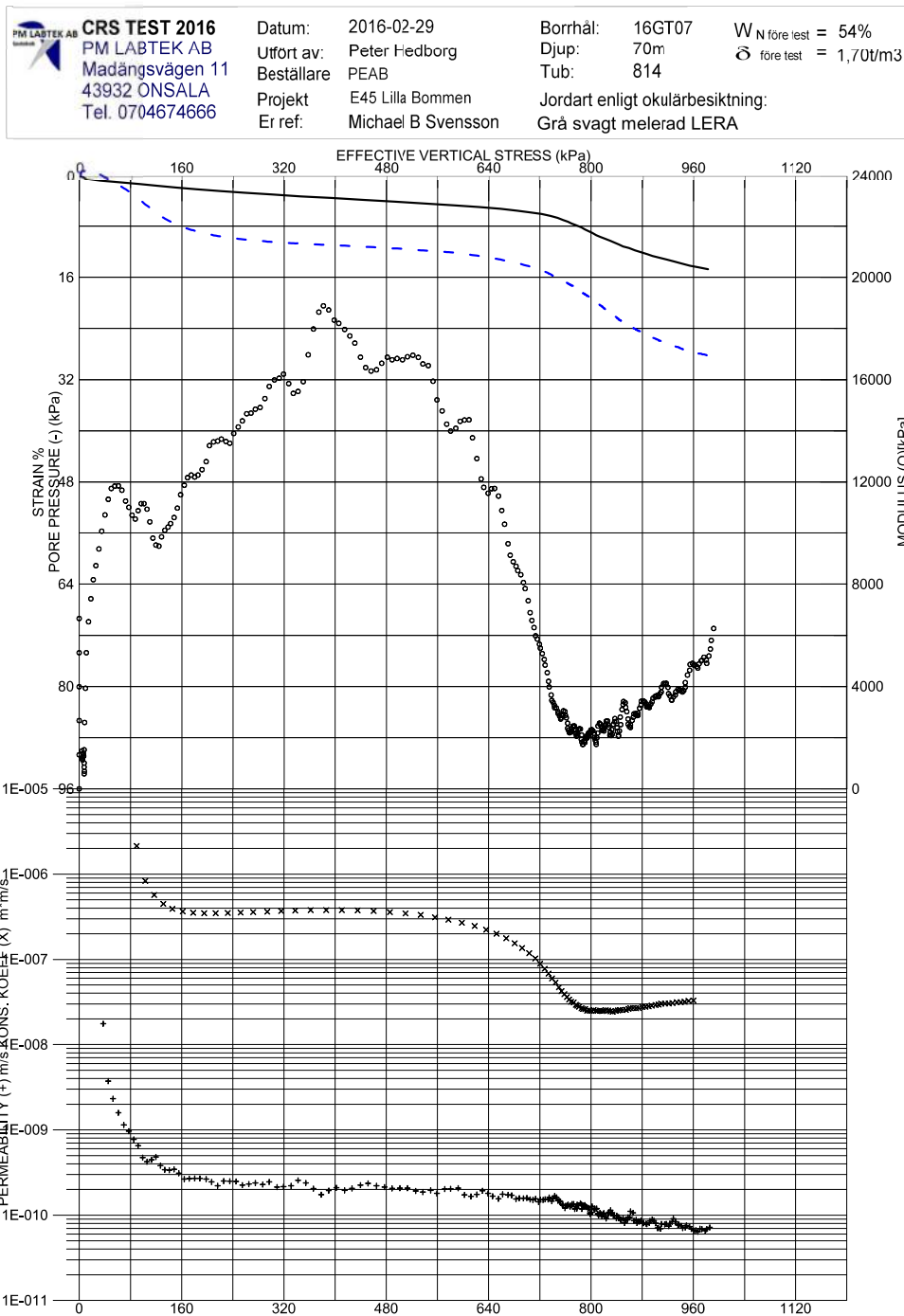


Figure A.15: CRS test



Projekt	E45 Lilla Bommen	Belastningshastighet	0,10mm/h
Datum	2016-03-12	Försöksmetod	odränerat
Borrhål	16GT03	Konsolideringsspänning	157(157)kPa
Beställare	PEAB	Vattenkvot före	85%
Uppdragsnr.		Skrymdensitet	1,47
Provtub	2800	Höjd	15,5mm
Djup:	20m	Diameter	50,0 mm
Utfört av	Peter Hedborg	Konsolideringstöjning	3,02%

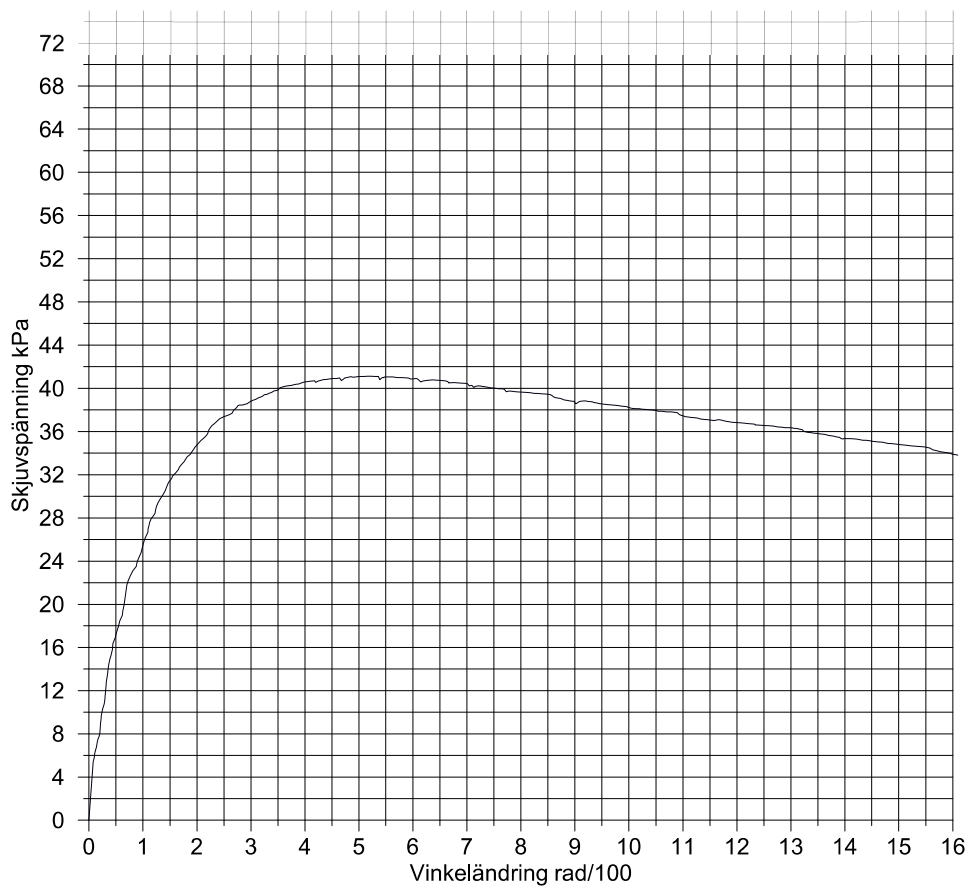


Figure A.16: Shear test



Projekt	E45 Lilla Bommen	Belastningshastighet	0,10mm/h
Datum	2016-03-10	Försöksmetod	odränerat
Borrhål	16GT03	Konsolideringsspänning	238(238)kPa
Beställare	PEAB	Vattenkvot före	65%
Uppdragsnr.		Skrymdensitet	1,60
Provtub	5059	Höjd	15,5mm
Djup:	40m	Diameter	50,0 mm
Utfört av	Peter Hedborg	Konsolideringstöjning	3,88%

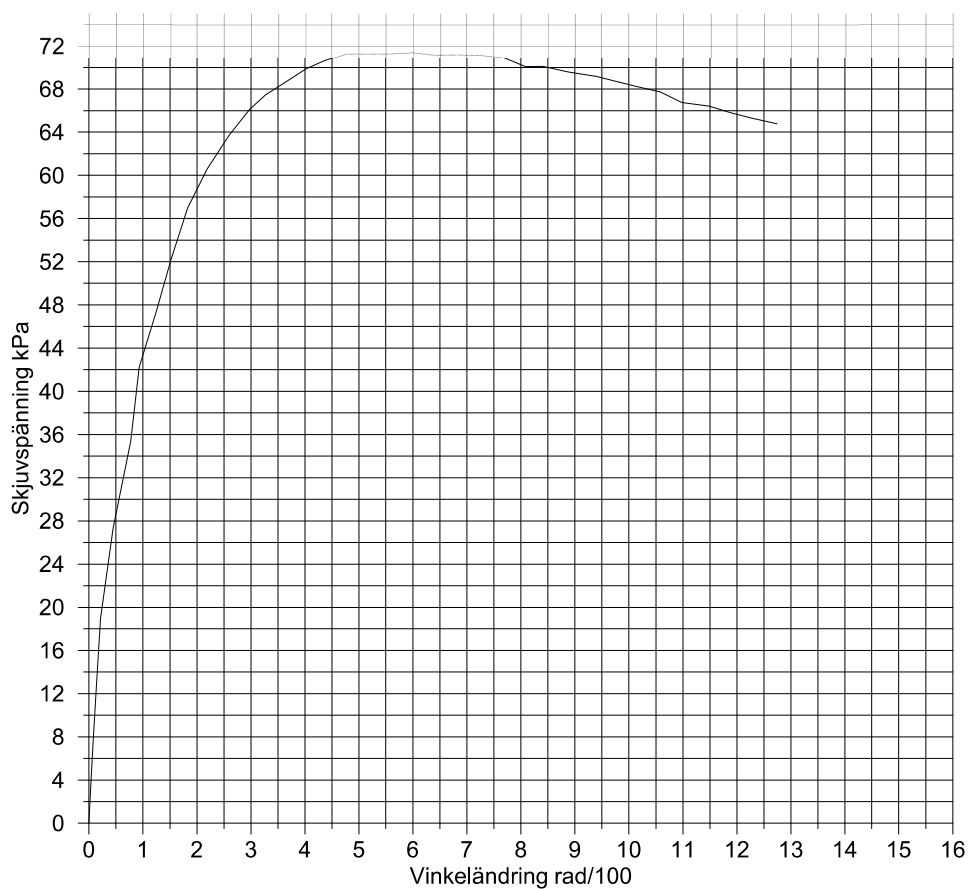


Figure A.17: Shear test



Projekt	E45 Lilla Bommen	Belastningshastighet	0,10mm/h
Datum	2016-03-10	Försöksmetod	odränerat
Borrhål	16GT03	Konsolideringsspänning	382(383)kPa
Beställare	PEAB	Vattenkvot före	60%
Uppdragsnr.		Skrymdensitet	1,66
Provtub	10-0778	Höjd	15,7mm
Djup:	55m	Diameter	50,0 mm
Utfört av	Peter Hedborg	Konsolideringstöjning	2,65%

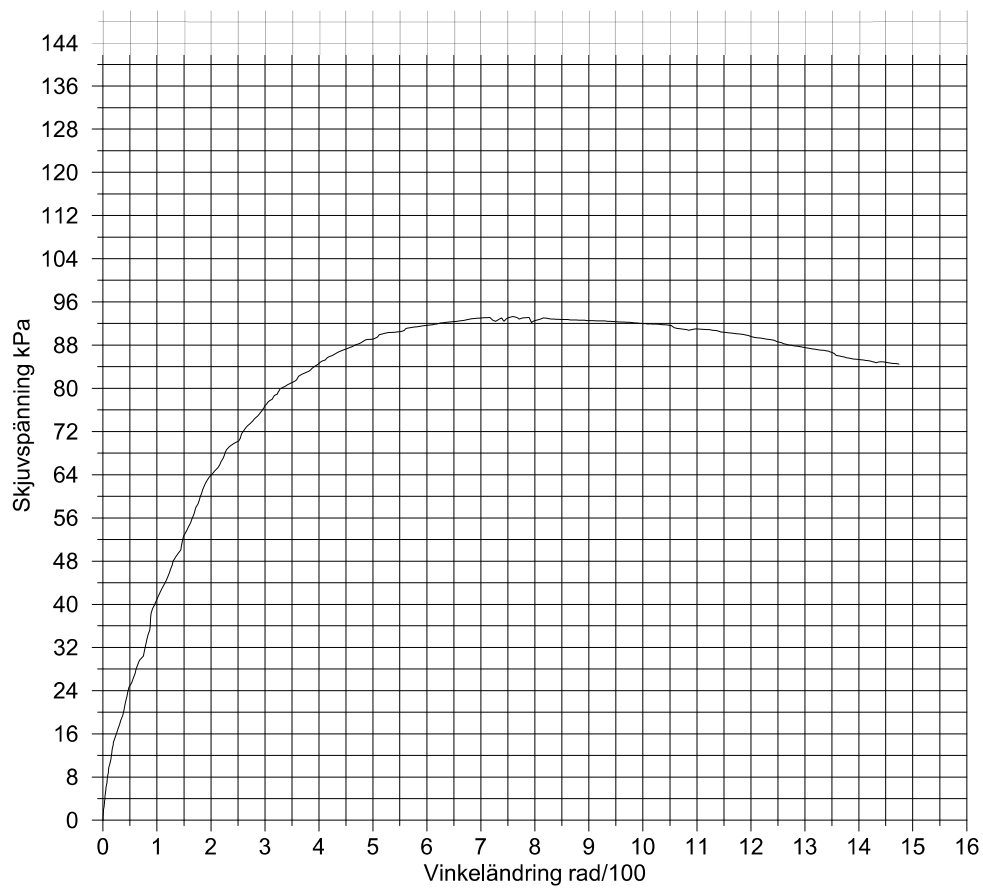


Figure A.18: Shear test



Projekt	E45 Lilla Bommen	Belastningshastighet	0,10mm/h
Datum	2016-03-12	Försöksmetod	odränerat
Borrhål	16GT03	Konsolideringsspänning	452(452)kPa
Beställare	PEAB	Vattenkvot före	51%
Uppdragsnr.		Skrymdensitet	1,74
Provtub	115	Höjd	15,3mm
Djup:	70m	Diameter	50,0 mm
Utfört av	Peter Hedborg	Konsolideringstöjning	3,42%

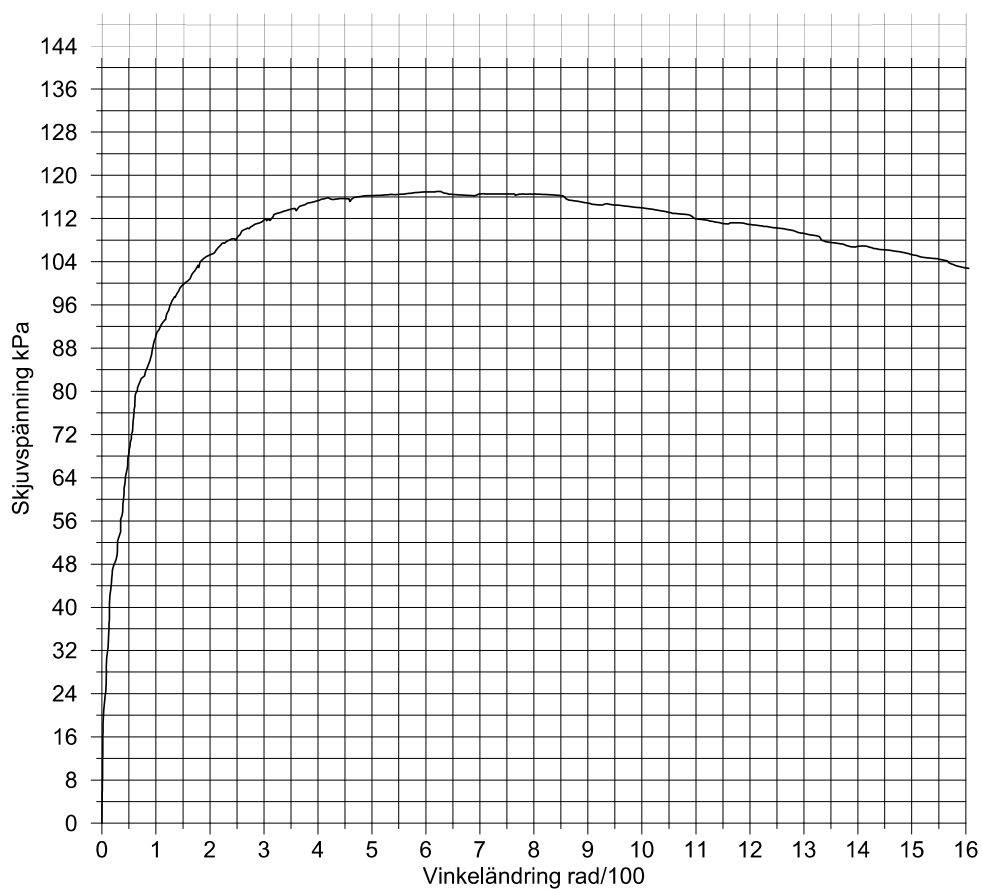


Figure A.19: Shear test



Projekt	E45 Lilla Bommen	Belastningshastighet	0,10mm/h
Datum	2016-02-29	Försöksmetod	odränerat
Borrhål	16GT07	Konsolideringsspänning	157(157)kPa
Beställare	PEAB	Vattenkvot före	63%
Uppdragsnr.		Skrymdensitet	1,61
Provtub	2189	Höjd	15,1mm
Djup:	20m	Diameter	50,0 mm
Utfört av	Peter Hedborg	Konsolideringstöjning	4,12%

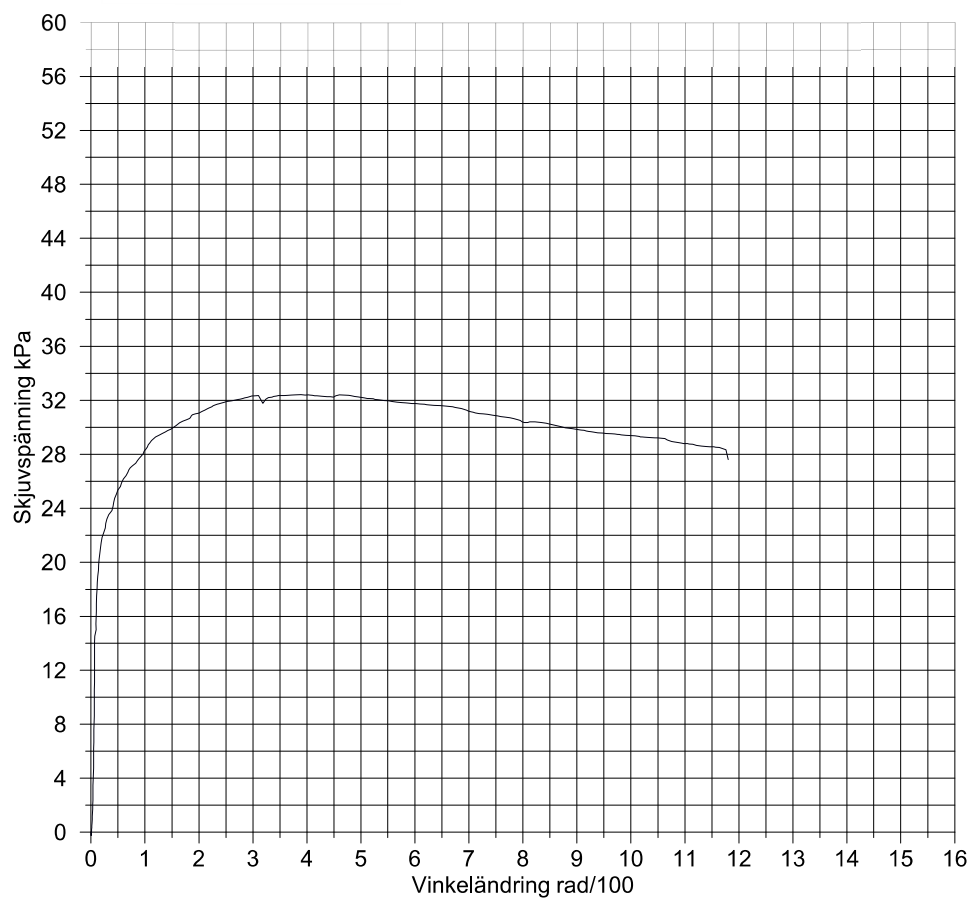


Figure A.20: Shear test



Projekt	E45 Lilla Bommen	Belastningshastighet	0,10mm/h
Datum	2016-02-27	Försöksmetod	odränerat
Borrhål	16GT07	Konsolideringsspänning	289(289)kPa
Beställare	PEAB	Vattenkvot före	69%
Uppdragsnr.		Skrymdensitet	1,59
Provtub	3783	Höjd	15,9mm
Djup:	40m	Diameter	50,0 mm
Utfört av	Peter Hedborg	Konsolideringstöjning	2,79%

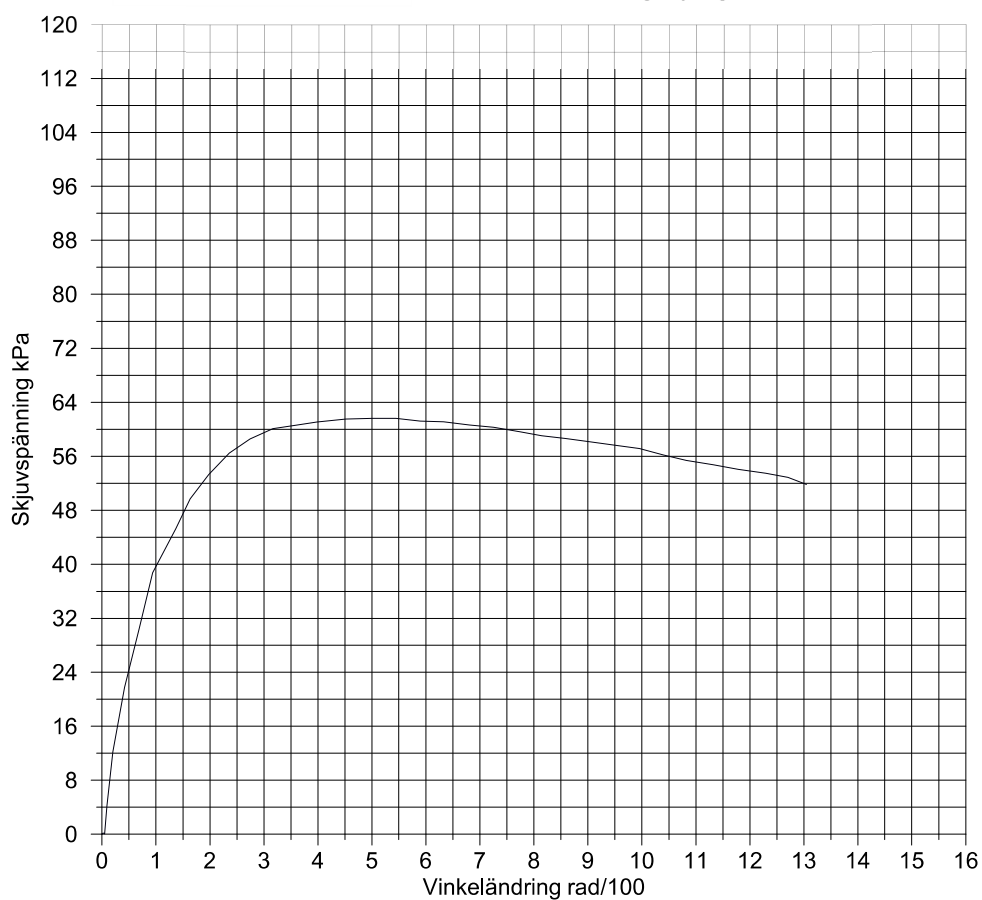


Figure A.21: Shear test



Projekt	E45 Lilla Bommen	Belastningshastighet	0,10mm/h
Datum	2016-02-27	Försöksmetod	odränerat
Borrhål	16GT07	Konsolideringsspänning	383(383)kPa
Beställare	PEAB	Vattenkvot före	62%
Uppdragsnr.		Skrymdensitet	1,65
Provtub	1360	Höjd	16,2mm
Djup:	55m	Diameter	50,0 mm
Utfört av	Peter Hedborg	Konsolideringstöjning	2,59%

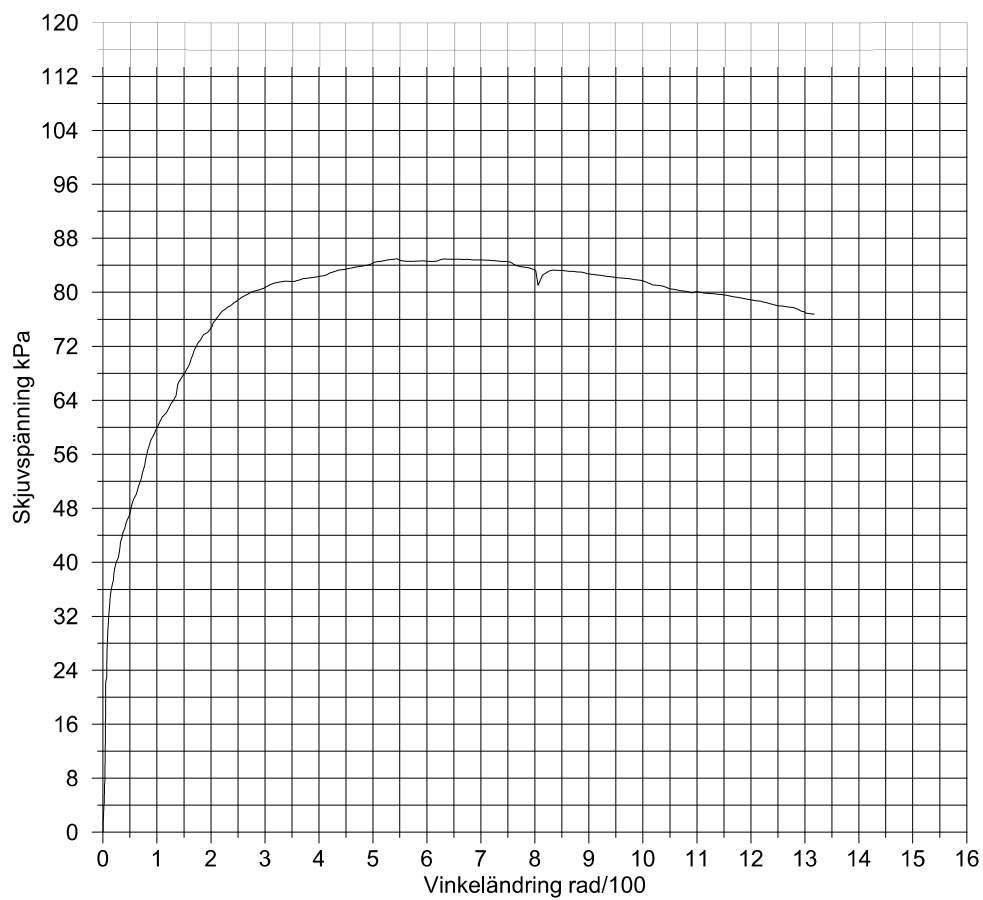


Figure A.22: Shear test



Projekt	E45 Lilla Bommen	Belastningshastighet	0,10mm/h
Datum	2016-02-29	Försöksmetod	odränerat
Borrhål	16GT07	Konsolideringsspänning	432(432)kPa
Beställare	PEAB	Vattenkvot före	56%
Uppdragsnr.		Skrymdensitet	1,70
Provtub	5226	Höjd	15,4mm
Djup:	70m	Diameter	50,0 mm
Utfört av	Peter Hedborg	Konsolideringstöjning	3,07%

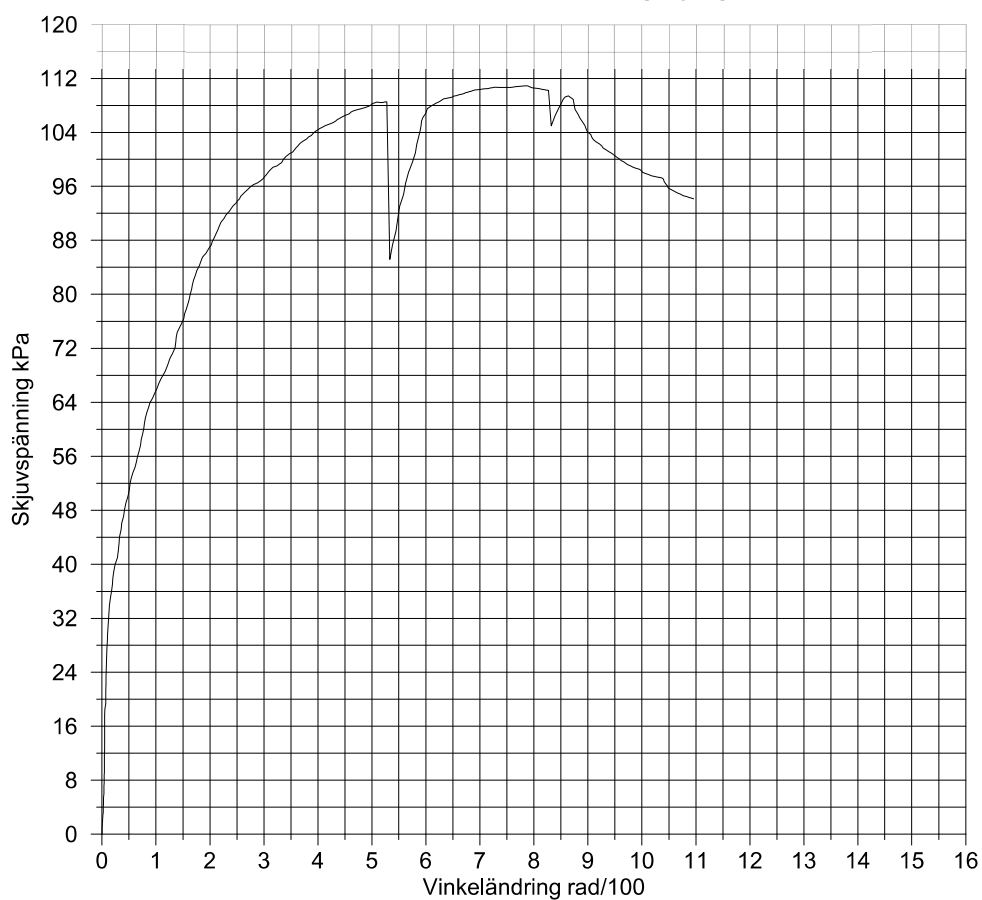


Figure A.23: Shear test

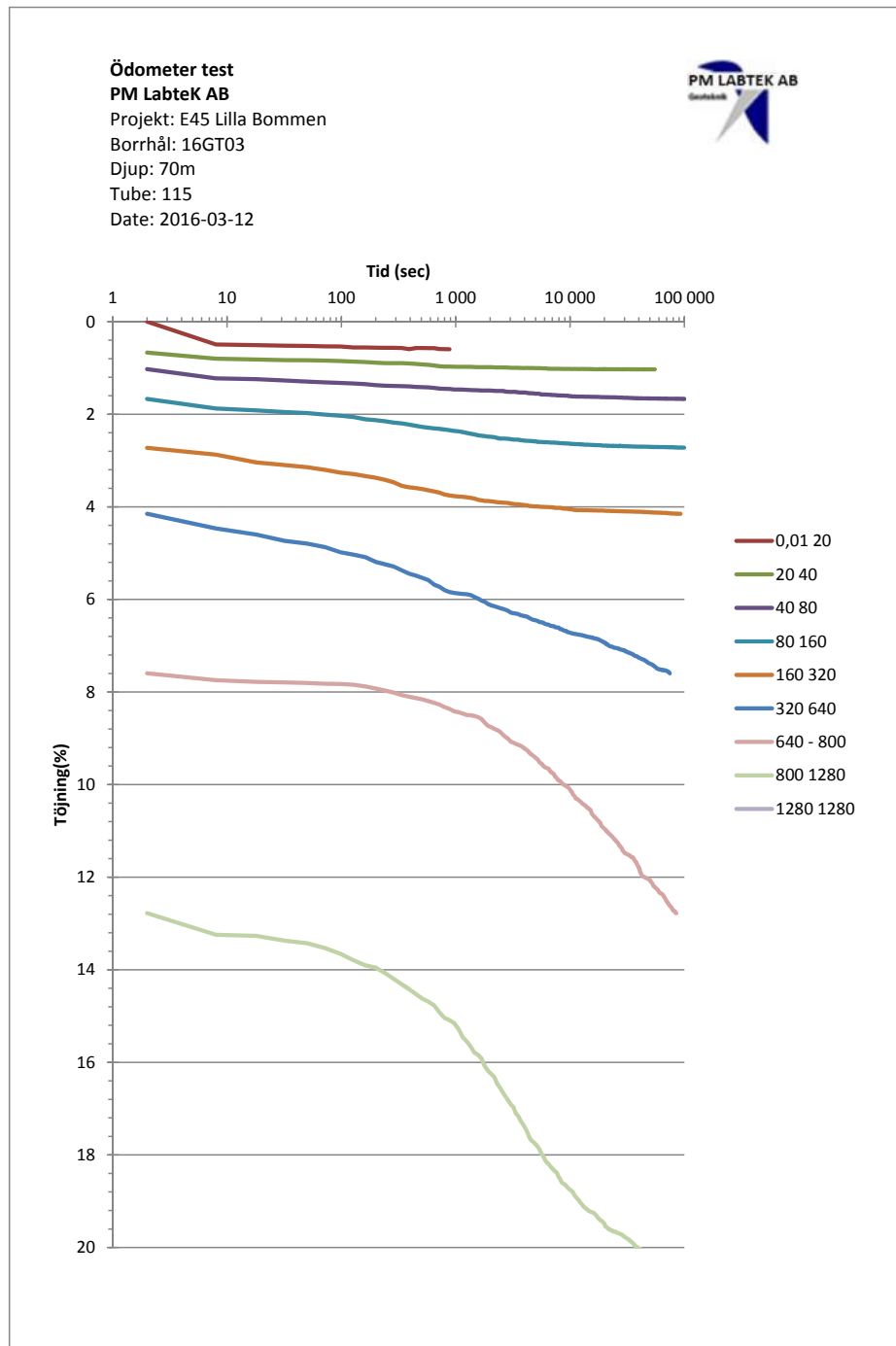


Figure A.24: Shear test

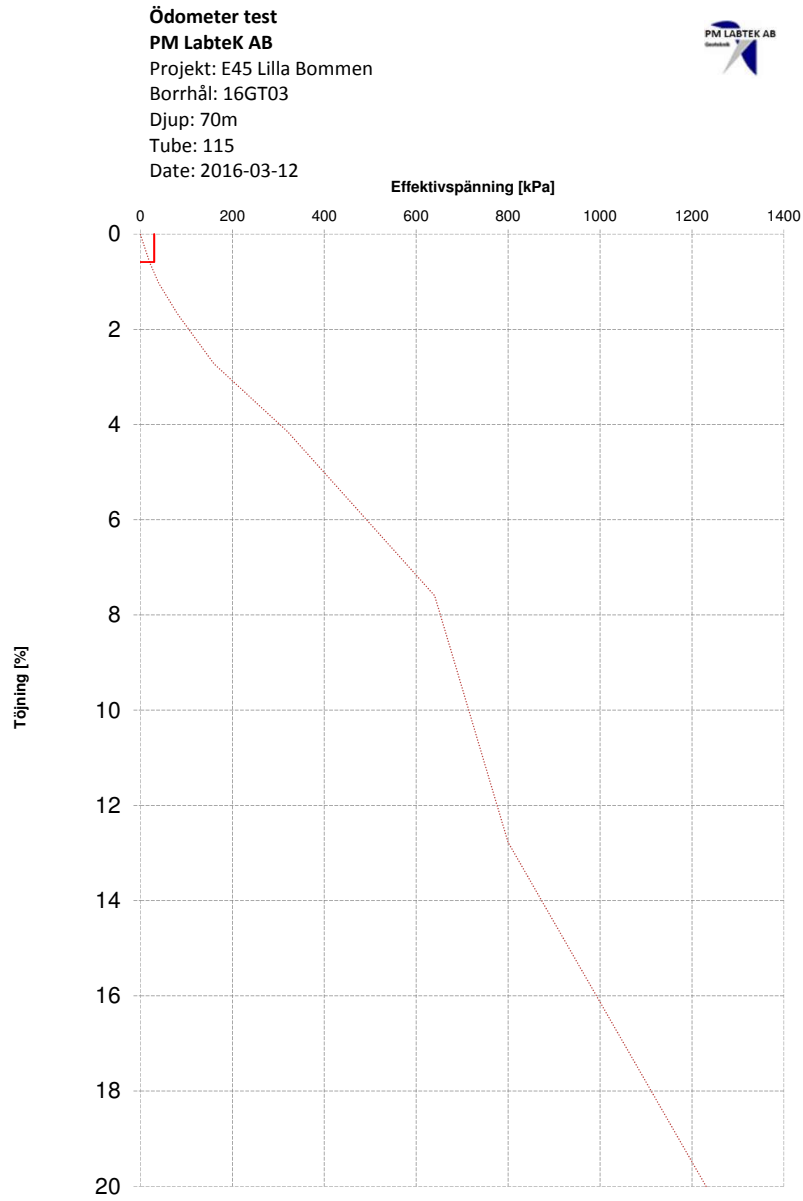


Figure A.25: Oedometer test

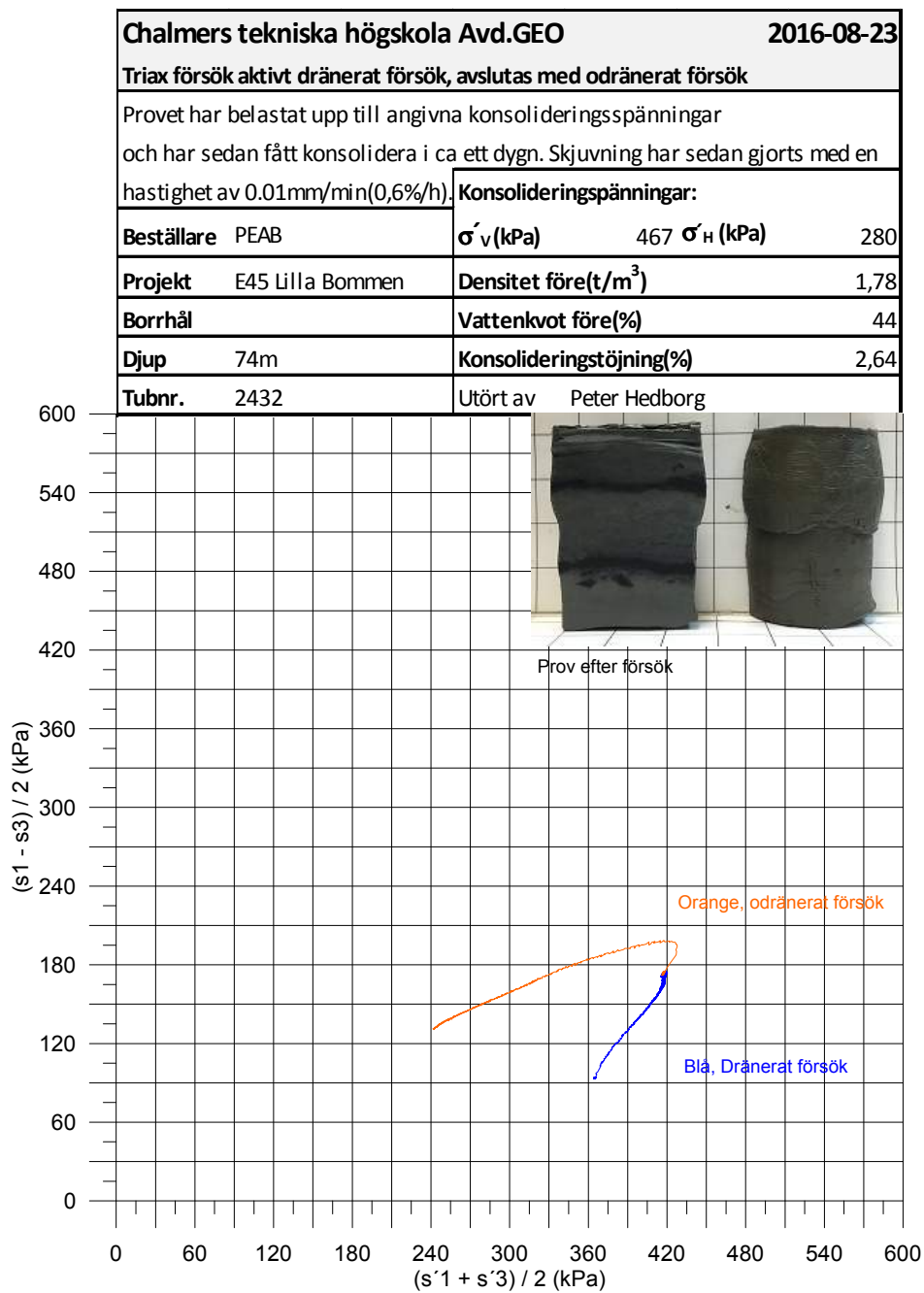


Figure A.26: Triaxial test

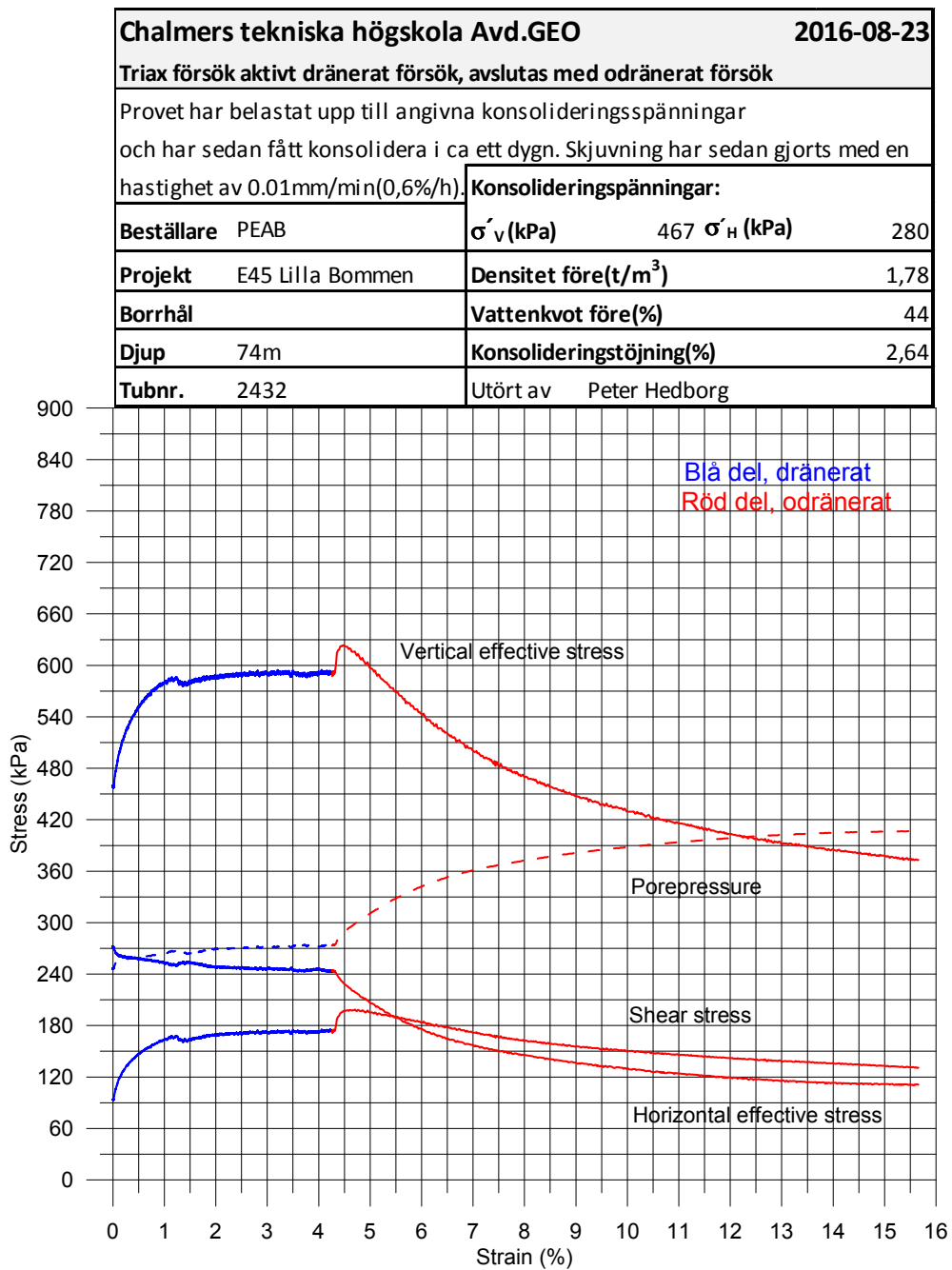


Figure A.27: Triaxial test

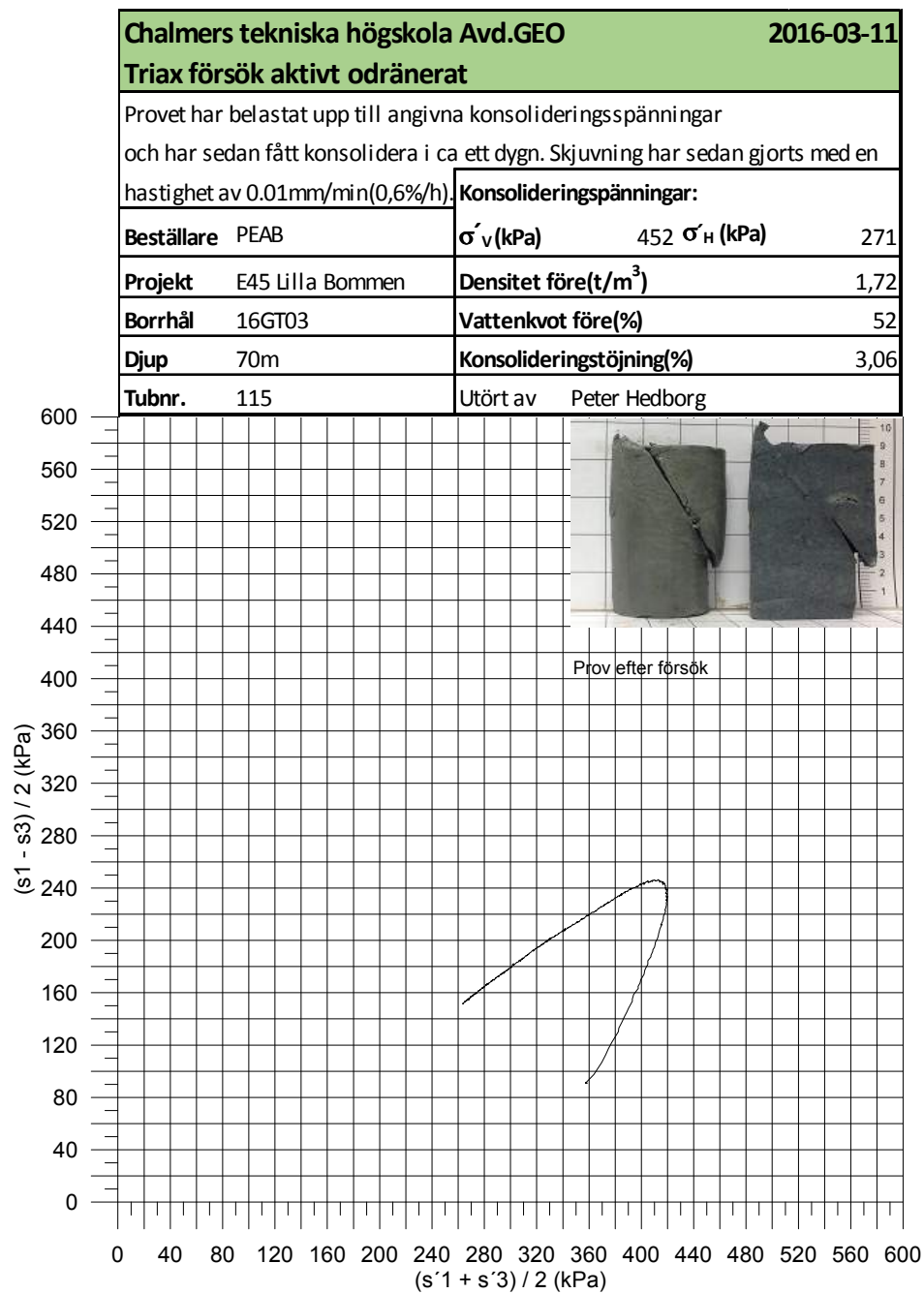


Figure A.28: Triaxial test

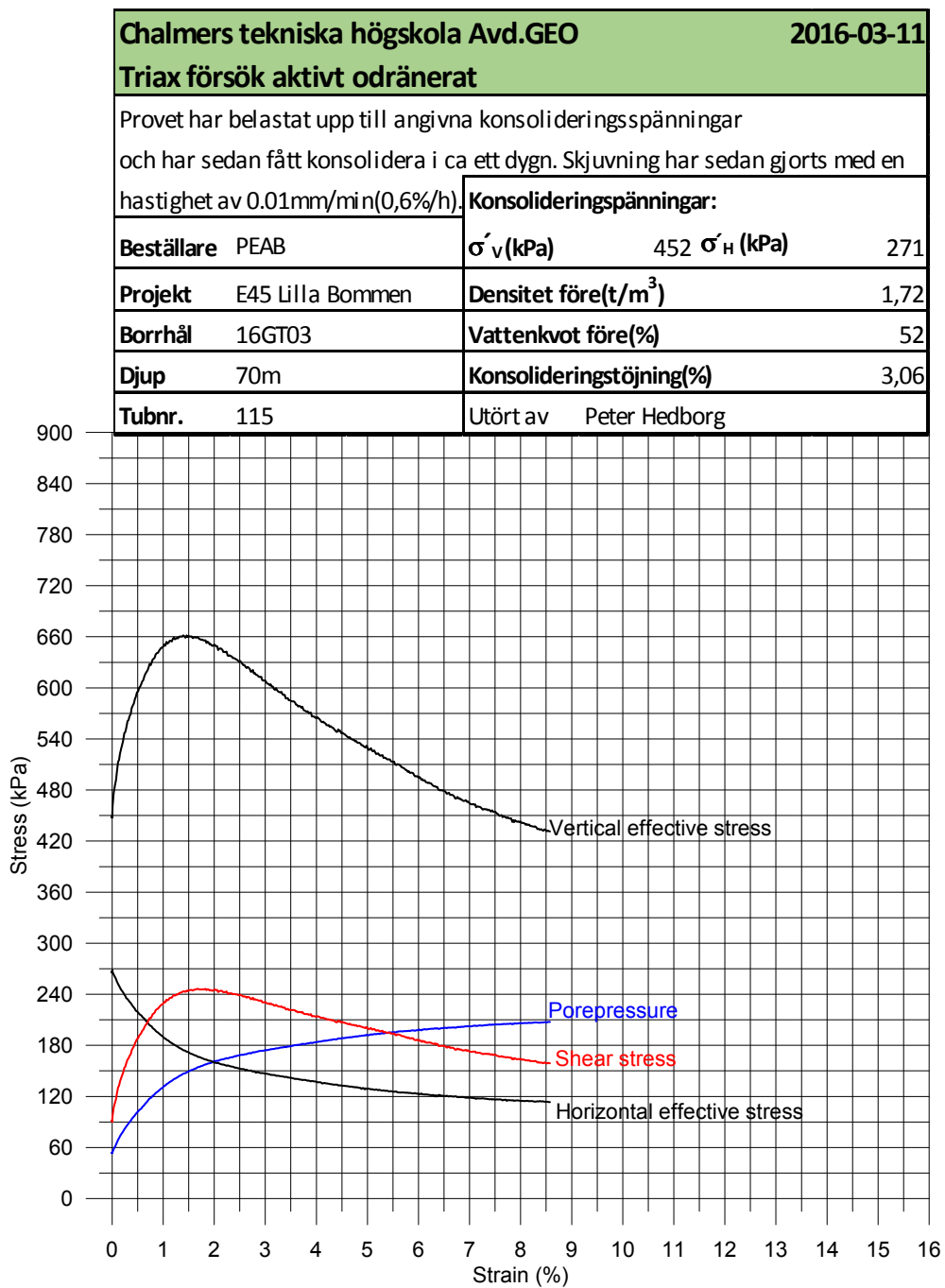


Figure A.29: Triaxial test

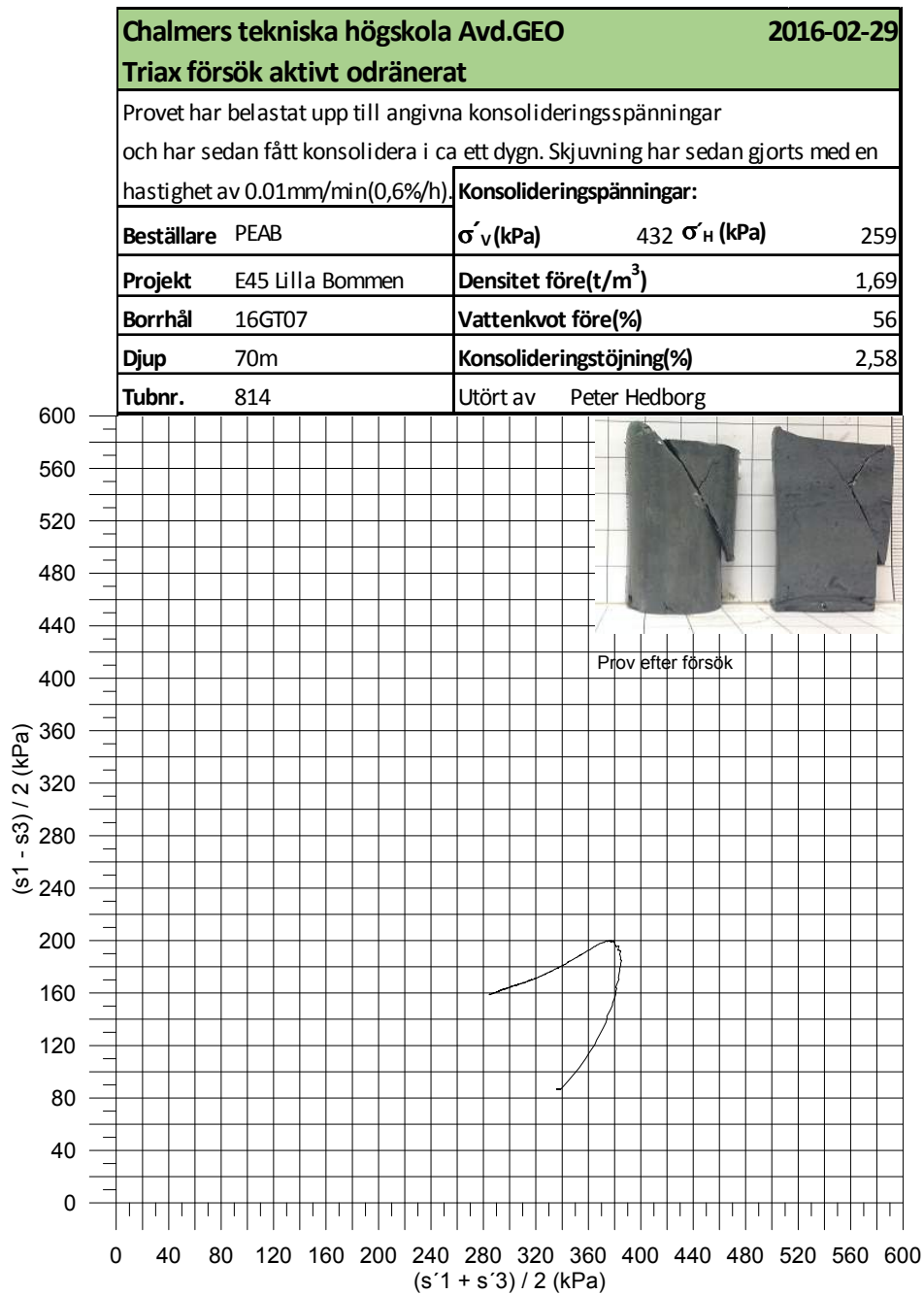


Figure A.30: Triaxial test

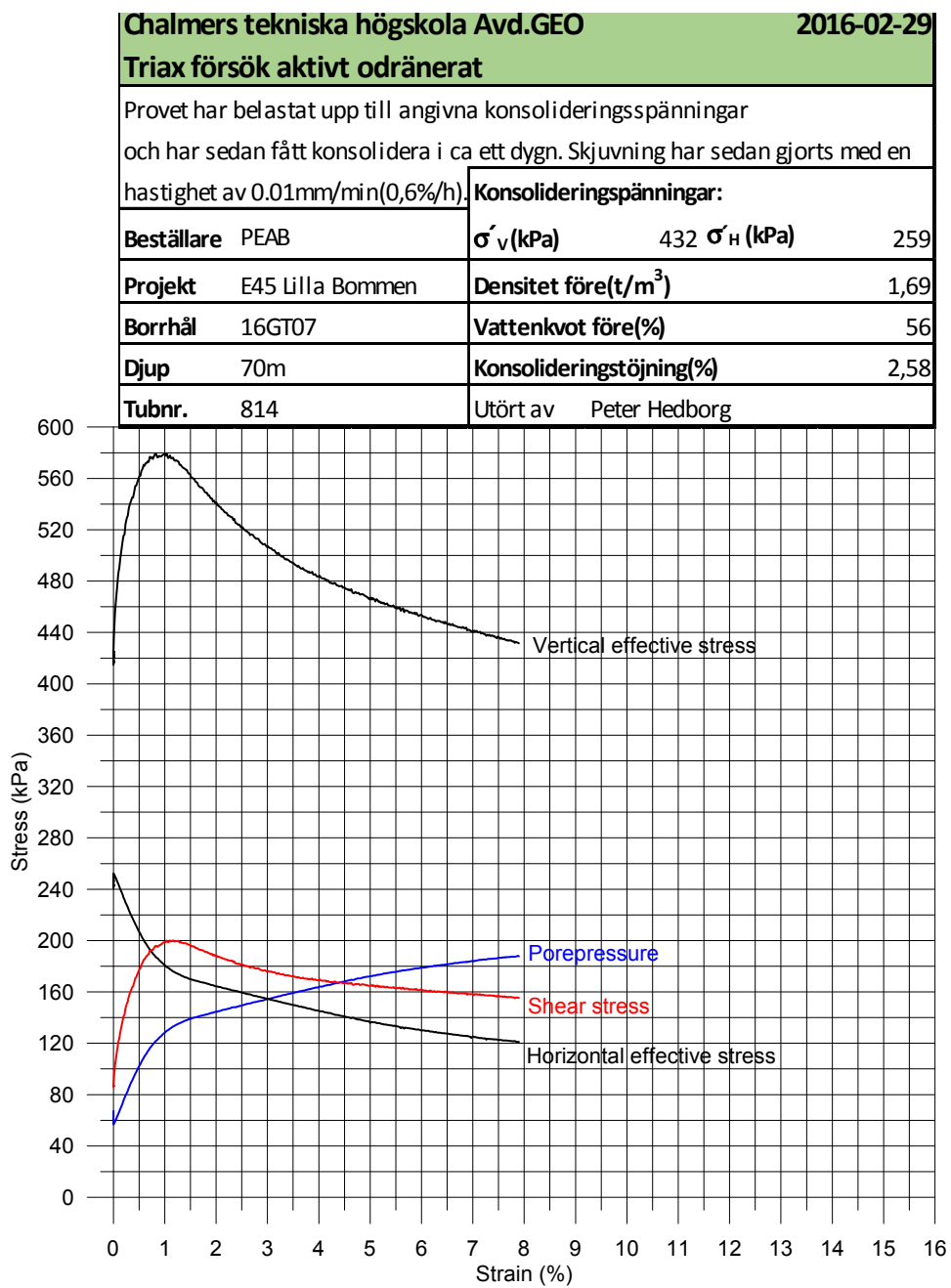


Figure A.31: Triaxial test

Chalmers tekniska högskola Avd.GEO		2016-03-14	
Triax försök passivt odränerat			
Provet har belastat upp till angivna konsolideringsspänningar och har sedan fått konsolidera i ca ett dygn. Skjuvning har sedan gjorts med en hastighet av -0.01mm/min(-0,6%/h)			
Beställare	PEAB	Konsolideringsspänningar:	
Projekt	E45 Lilla Bommen	σ'_v (kPa)	93 σ'_h (kPa) 56
Borrhål	16GT03	Densitet före(t/m^3)	1,67
Djup	10m	Vattenkvot före(%)	58
Tubnr.	565	Konsolideringstjöjning(%)	1,95
		Utört av	Peter Hedborg

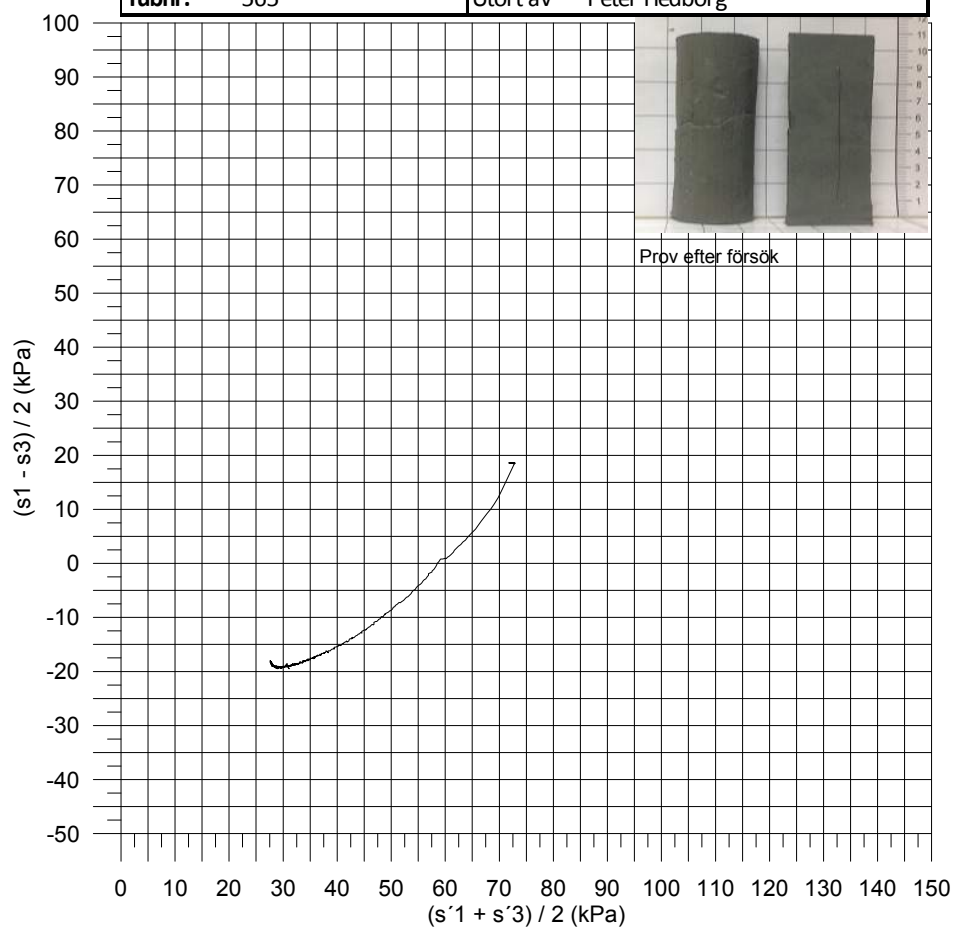


Figure A.32: Triaxial test

Chalmers tekniska högskola Avd.GEO		2016-03-14	
Triax försök passivt odränerat			
Provet har belastat upp till angivna konsolideringspänningar och har sedan fått konsolidera i ca ett dygn. Skjuvning har sedan gjorts med en hastighet av -0.01mm/min(-0,6%/h)			
Beställare PEAB		Konsolideringspänningar:	
Projekt E45 Lilla Bommen		σ'_v (kPa)	93 σ'_h (kPa) 56
Borrhål 16GT03		Densitet före(t/m ³)	1,67
Djup 10m		Vattenkvot före(%)	58
Tubnr. 565		Konsolideringstjöjning(%)	1,95
		Utört av	Peter Hedborg

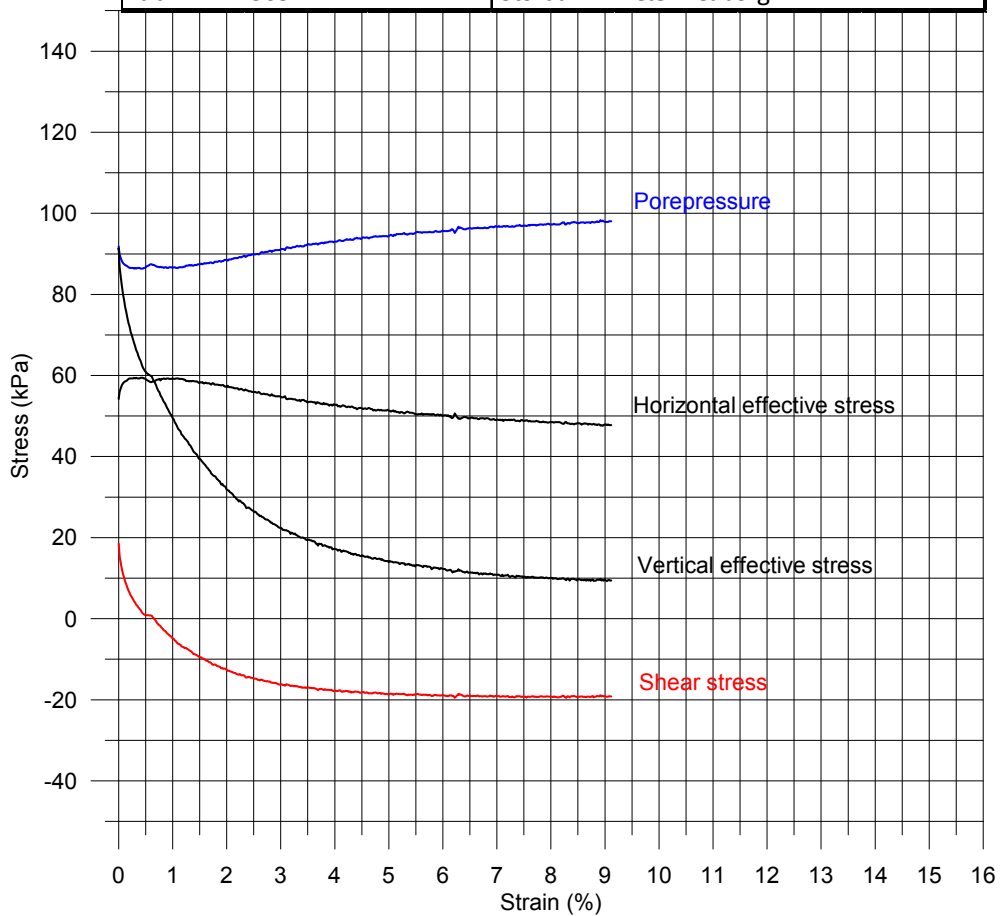


Figure A.33: Triaxial test

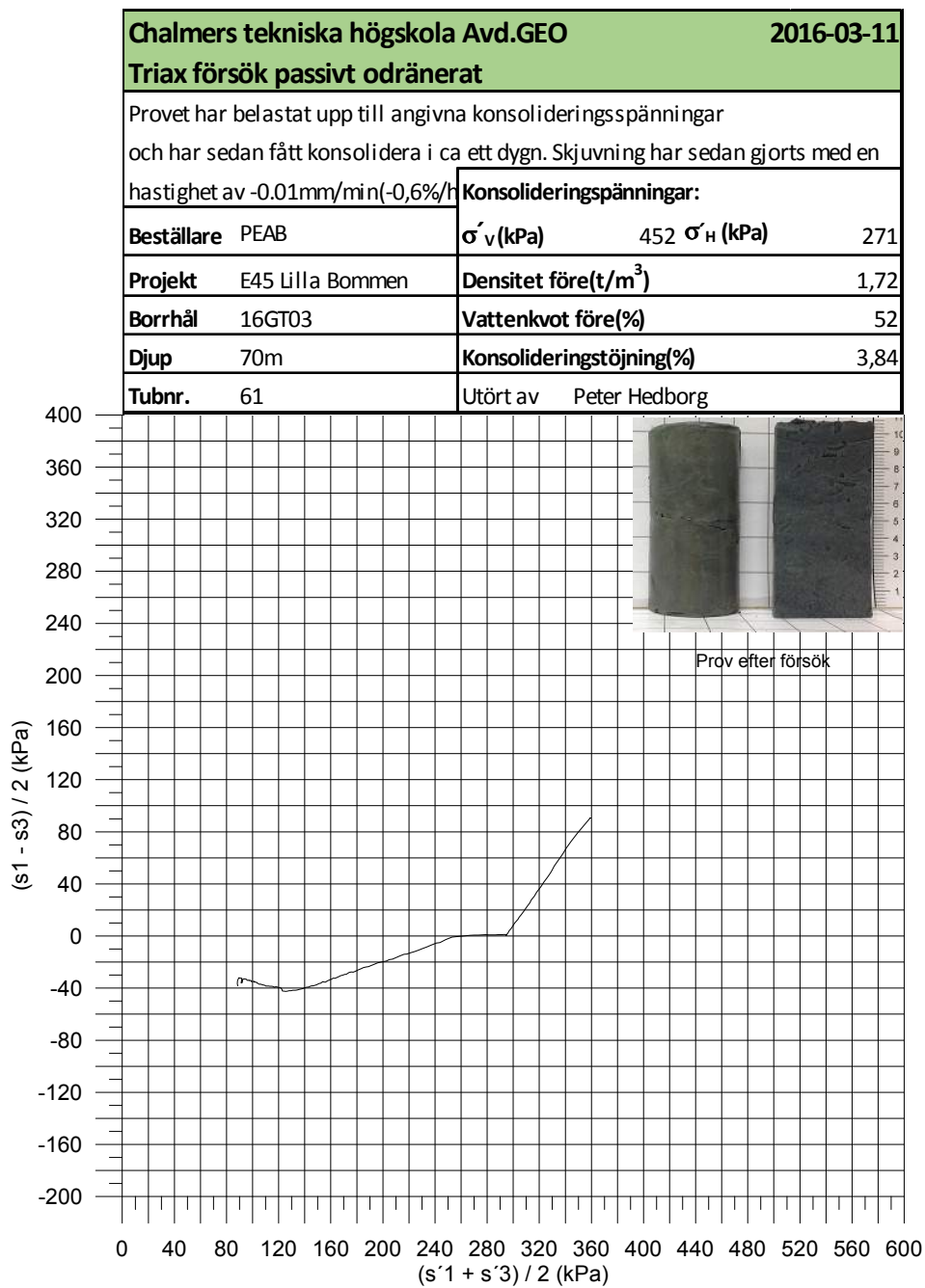


Figure A.34: Triaxial test

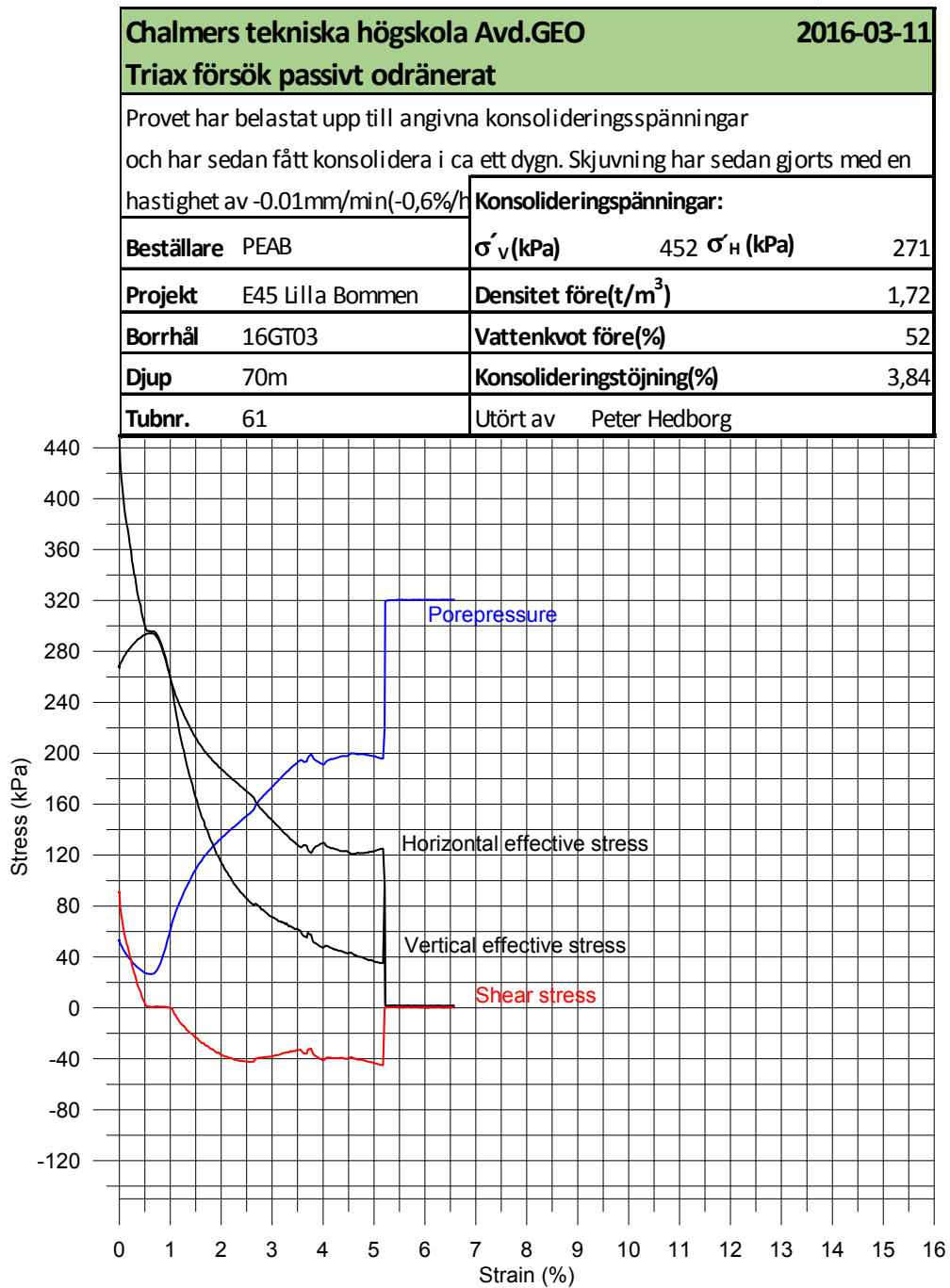


Figure A.35: Triaxial test

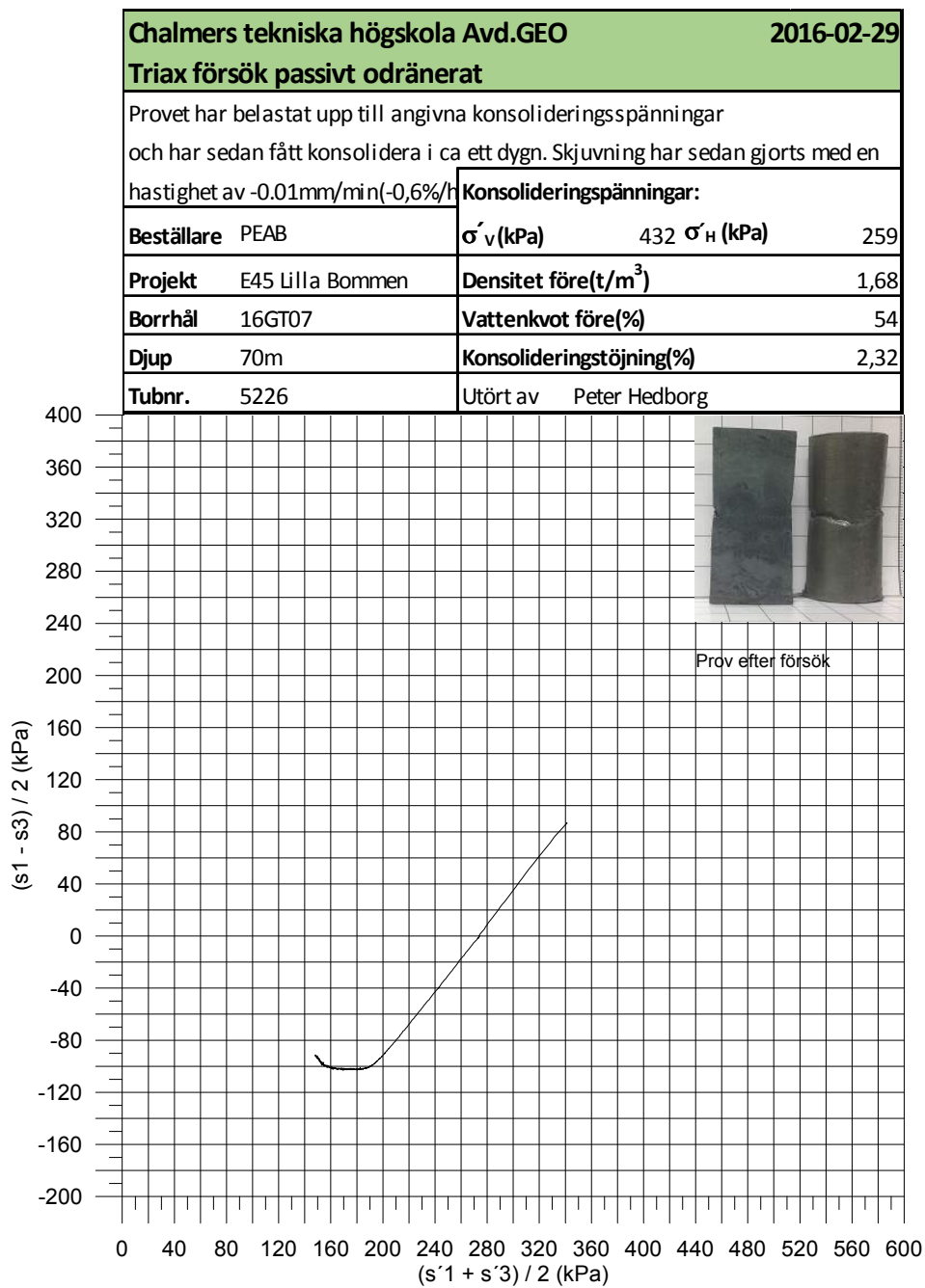


Figure A.36: Triaxial test

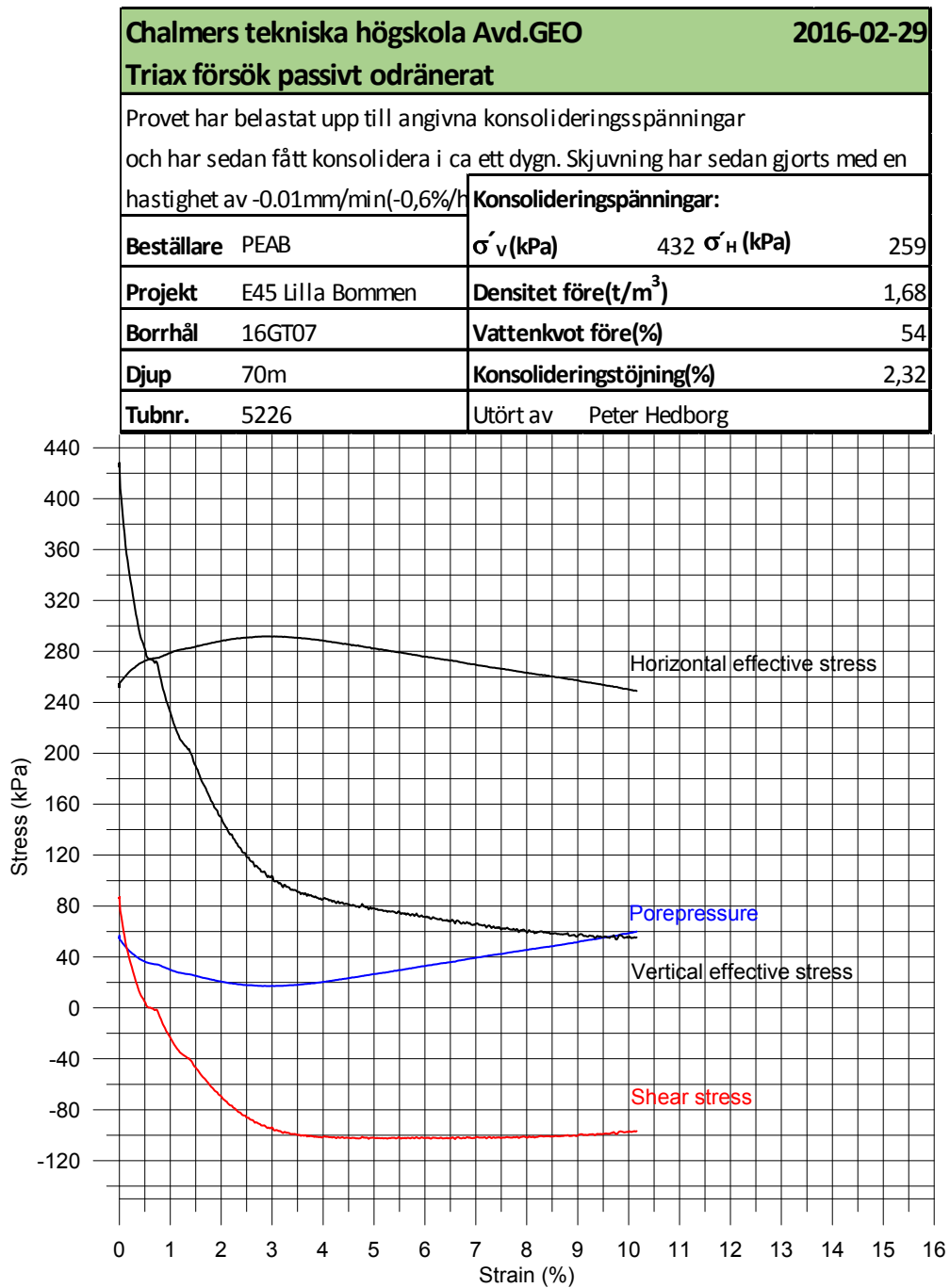


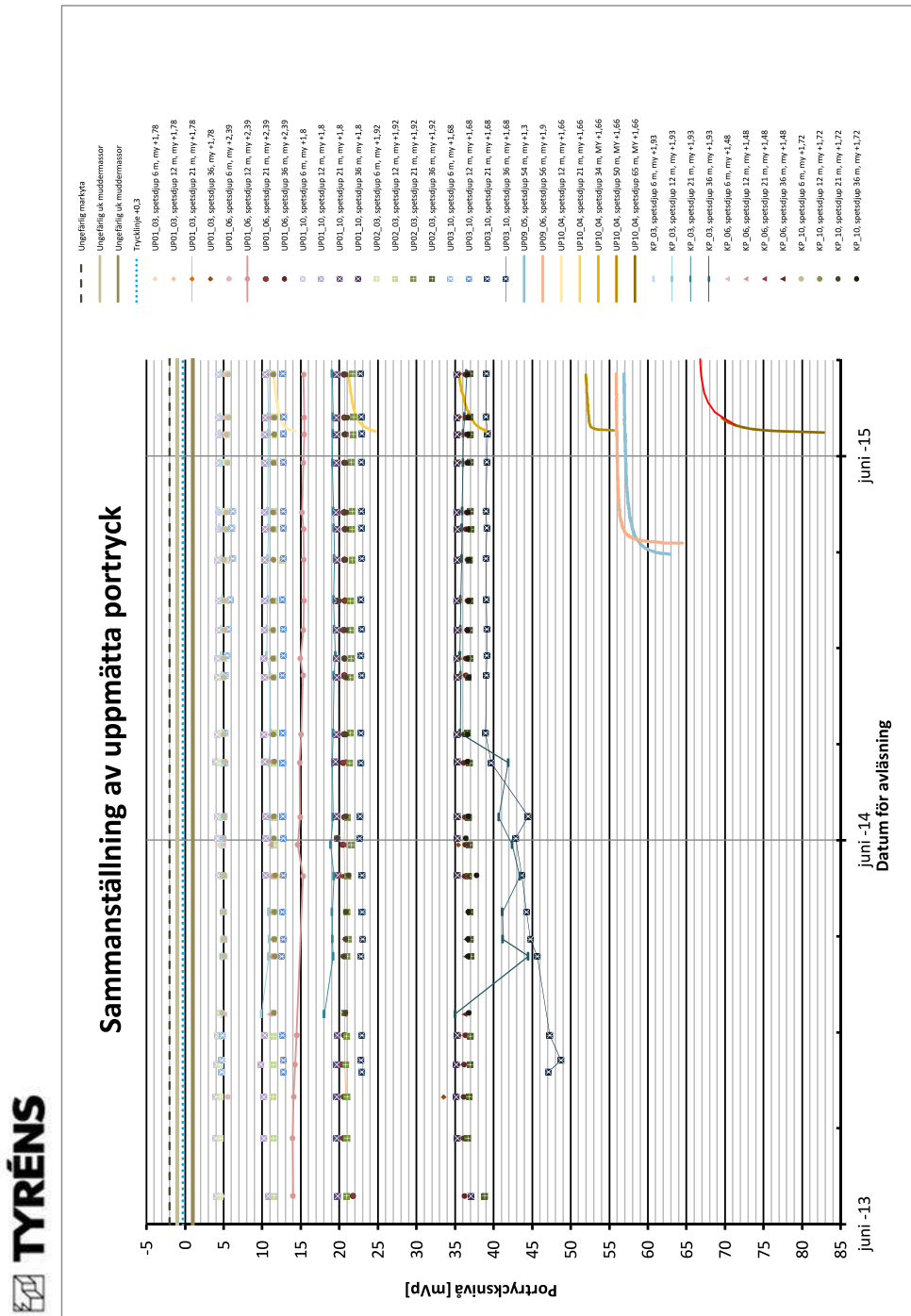
Figure A.37: Triaxial test

Sammanställning av Laboratorieundersökningar 2016								
 OSTÖRDA PROVER PM LABTEK AB Madångsvägen 11 43932 ONSALA Tel. 0704674666 Tel. 0708530383 peter.hedborg@labtek.se magnus.salmi@labtek.se		Projekt						
		E45 Lilla Bommen - Marieholm						
		Beställare PEAB						
		Uppdragsledare Michael B Svensson						
		Uppdragsnr						
		Borrhål 16GT03						
Fältundersökning gjord 2016-03-10, 16-03-11								
Labundersökning gjord 2016-03-13								
m.u.my.								
Sekt./BH	Benämning	Densitet	Naturlig	Konflyt	Sensivit	Omrörd	Plasticit	Skjuv-
			Vattenkvot	gräns		Skjuv-	etsgräns	hållfast
Djup (m)		t/m^3	W_N (%)	W_L (%)	$et S_t$	hållfast	W_P (%)	et
						et		(oreduce
								rad)
10,0	Grå LERA, inslag av få skalrester	1,68 1,70 1,68	61 62	65	9	2,67	33	24
20,0	Grå melerad, mörkgrå varvig LERA	1,53 1,54 1,54	86 81	82	23	1,43	29	33
40,0	Grå sulfidmelerad LERA	1,64 1,64 1,64	67 66	76	13	4,78	35	60
55,0	Grå sulfidmelerad varvig LERA	1,67 1,66 1,67	60 58	72	72	7,39	35	79
70,0	Grå sulfidmelerad LERA	1,75	53	63	8	9,9	31,0	82

Figure A.38: Laboratory evaluation

Sammanställning av Laboratorieundersökningar 2016								
 OSTÖRDA PROVER PM LABTEK AB Madängsvägen 11 43932 ONSALA Tel. 0704674666 Tel. 0708530383 peter.hedborg@labtek.se magnus.salmi@labtek.se		Projekt						
		E45 Lilla Bommen - Marieholm						
		Beställare				PEAB		
		Uppdragsledare				Michael B Svensson		
		Uppdragsnr						
		Borrhål				16GT07		
Fältundersökning gjord				2016-02-25				
Labundersökning gjord				2016-02-27				
		m.u.my.						
Sekt./BH	Benämning	<i>Densitet</i>	<i>Naturlig</i>	<i>Konflyt</i>	<i>Sensivitet</i>	<i>Omrörd</i>	<i>Plasticitet</i>	<i>Skjuv-</i>
			<i>Vattenkvot</i>	<i>gräns</i>		<i>Skjuv-</i>	<i>sgräns</i>	<i>hållfasth</i>
Djup (m)		<i>t/m³</i>	<i>W_N (%)</i>	<i>W_L (%)</i>	<i>S_t</i>	<i>et</i>	<i>W_P (%)</i>	<i>et</i>
								<i>(oreduce</i>
								<i>rad)</i>
20,0	Grå sulfidmelerad LERA	1,60	71	65	21	1,22	31	26
		1,66	62					
40,0	Grå sulfidmelerad LERA	1,62	69	79	18	3,06	36	56
		1,61	69					
55,0	Grå sulfidmelerad LERA	1,65	63	77	12	5,98	32	71
		1,66	62					
70,0	Grå svagt melerad LERA	1,70	57	73	9	11	34	96
		1,70	58					

Figure A.39: Laboratory evaluation



O:\GBG\253535\G\Utvärdering\Portryck.xlsx

Figure A.48: Pore pressure evaluation

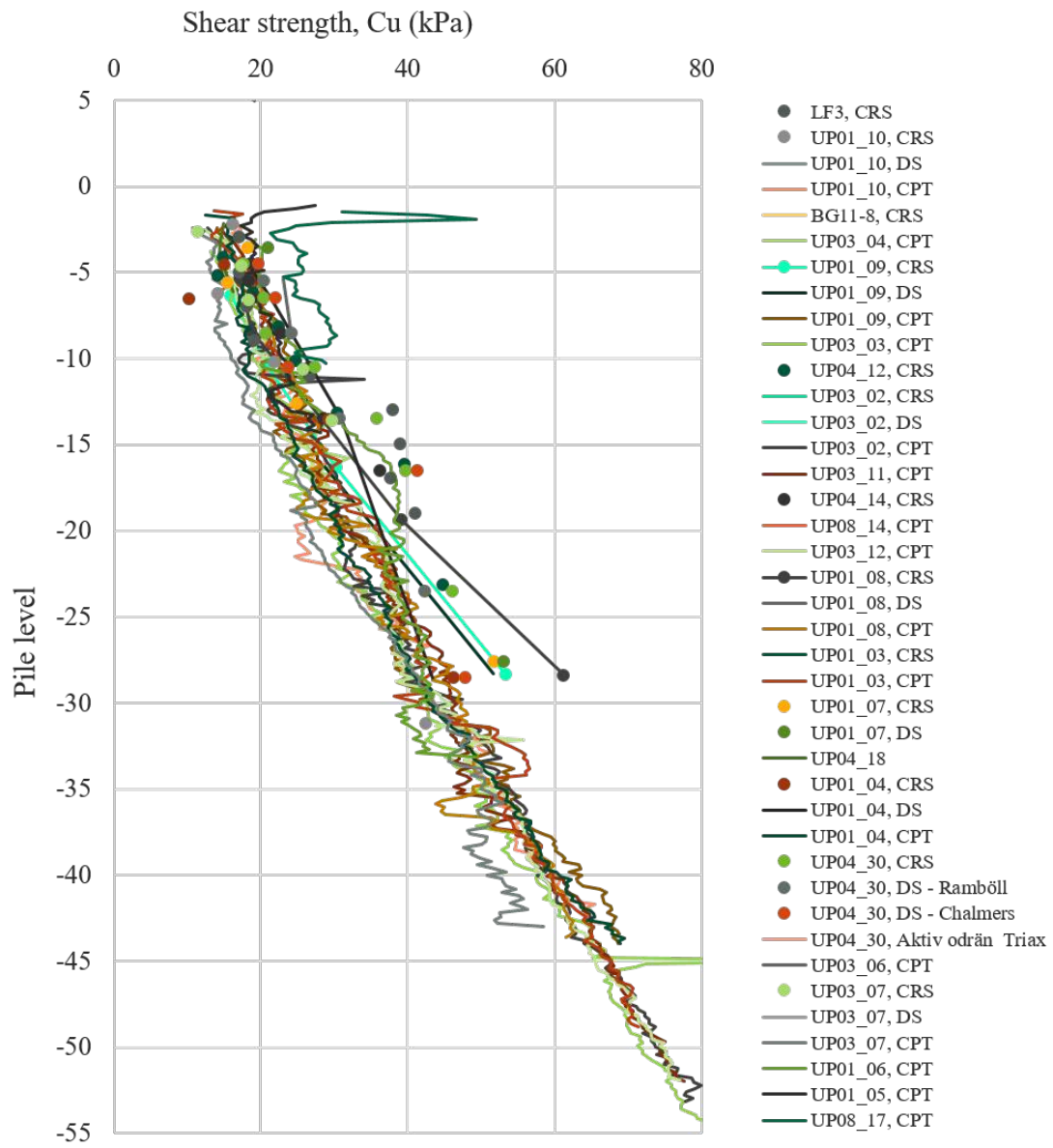


Figure A.51: Shear strength compilation

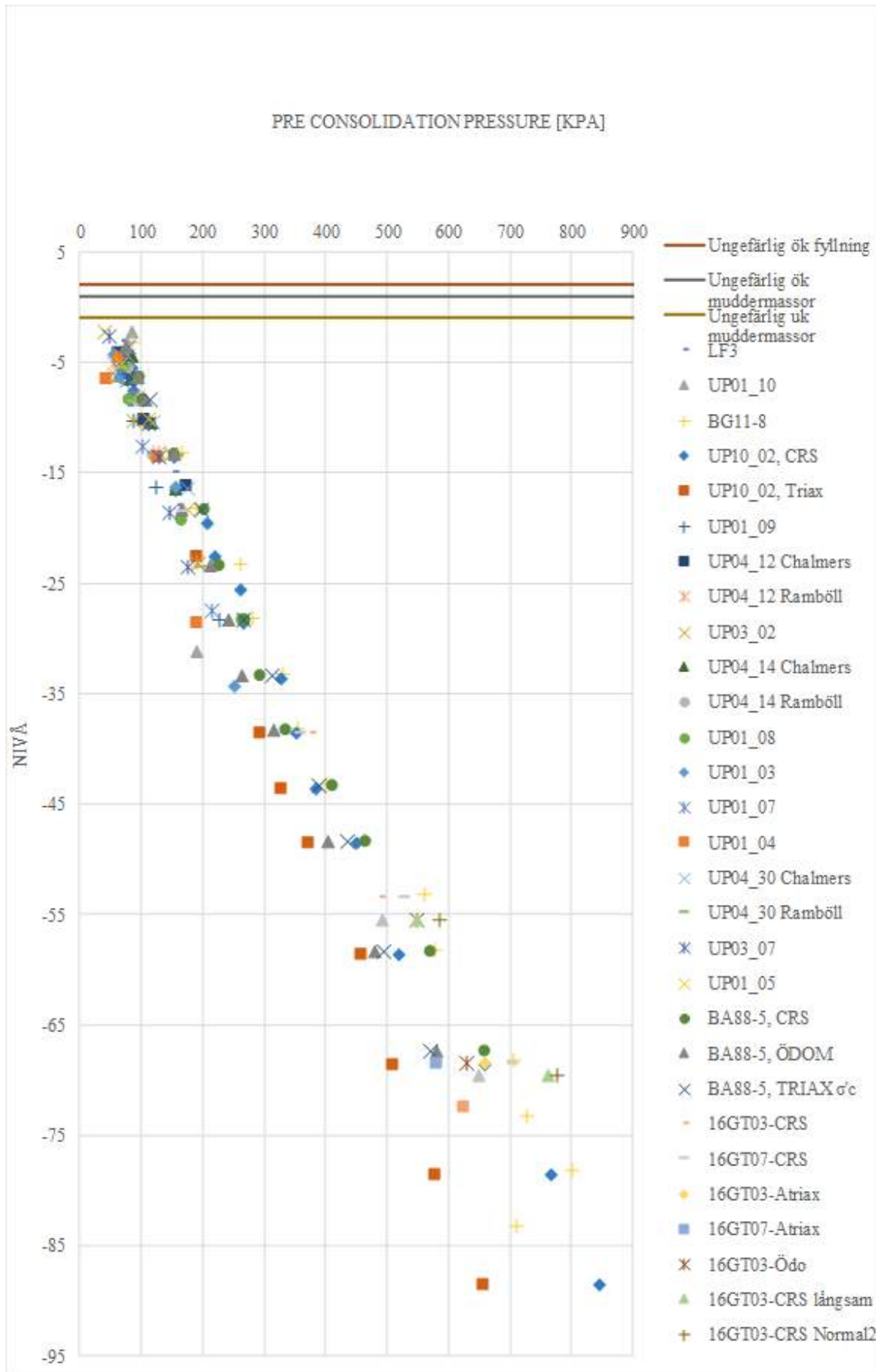


Figure A.52: Pre- consolidation compilation

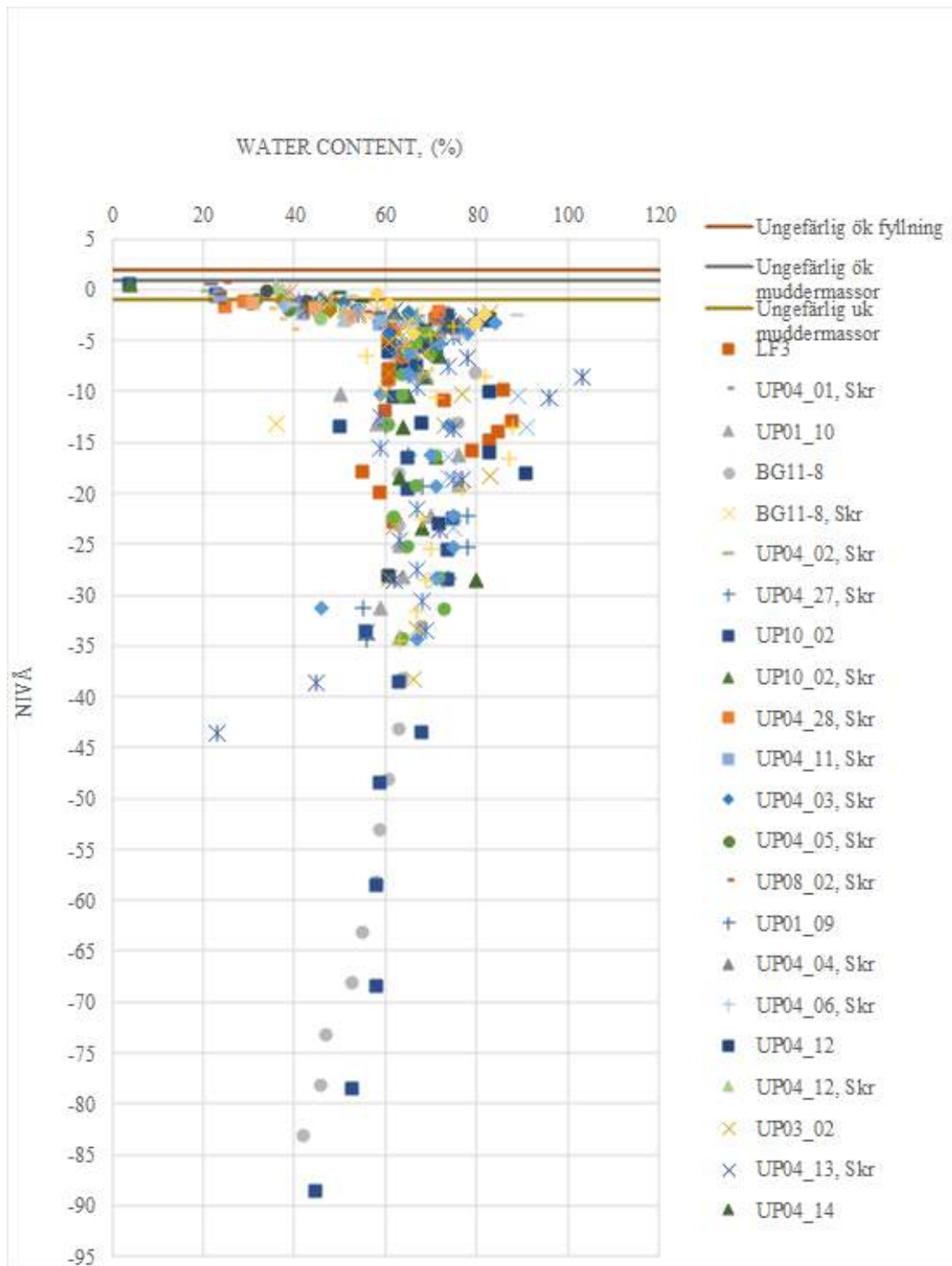


Figure A.53: Water content compilation

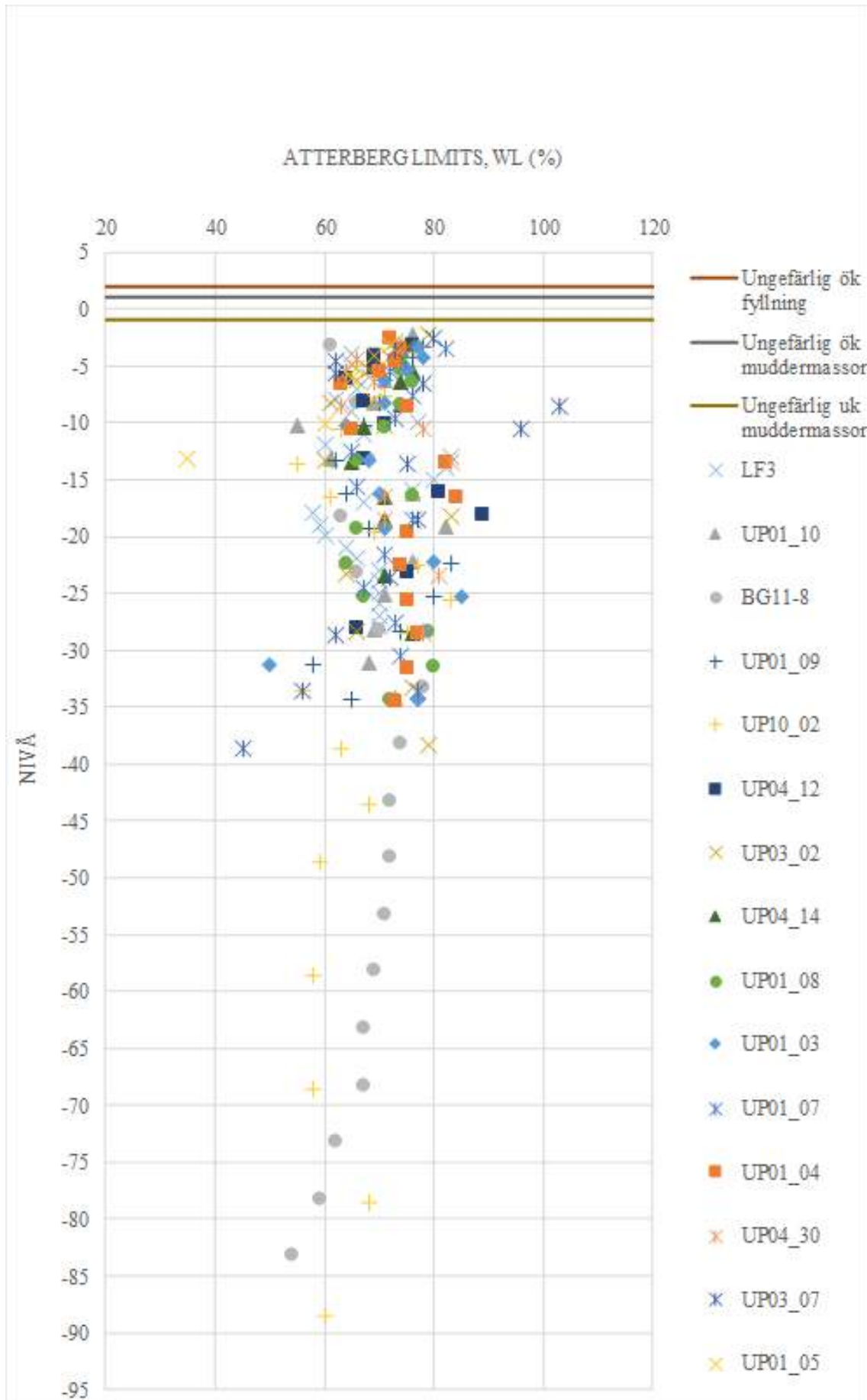


Figure A.54: Atterberg limits compilation

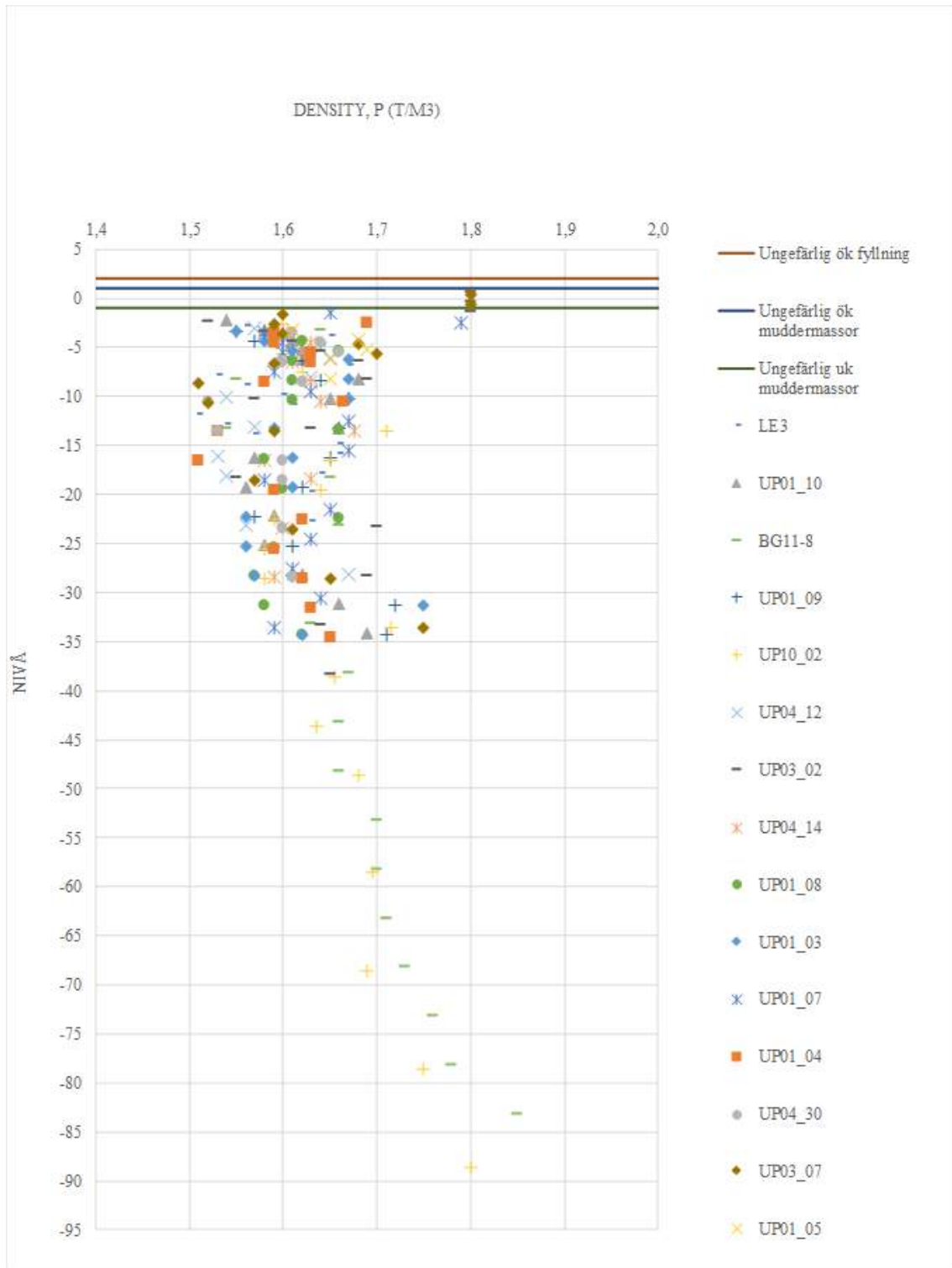


Figure A.55: Density compilation

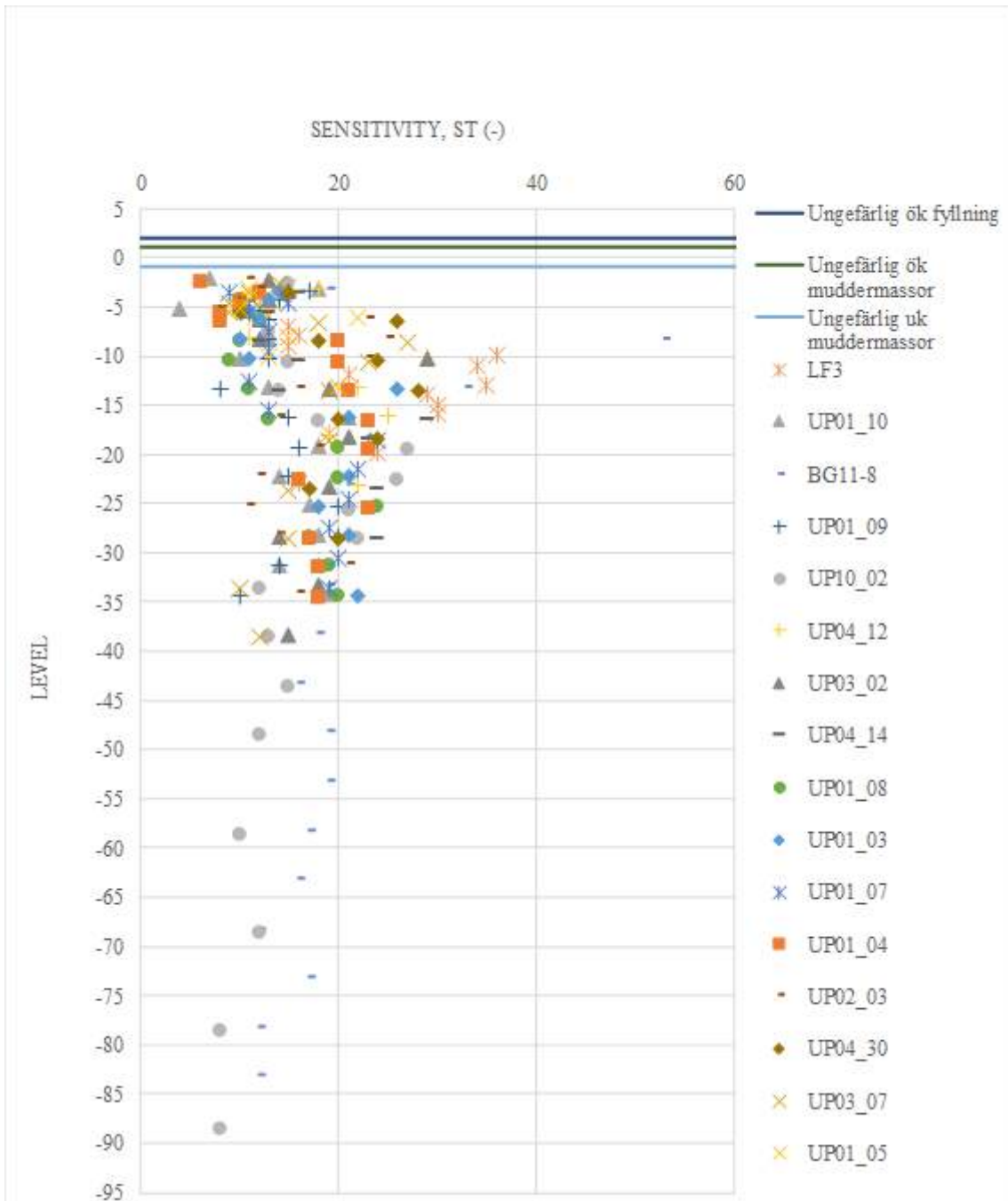


Figure A.56: Sensitivity compilation

A.4 Shear strength evaluation

The shear strength trend used in this thesis is based on the added red line in figure below. inclination is calculated manually from the graph.

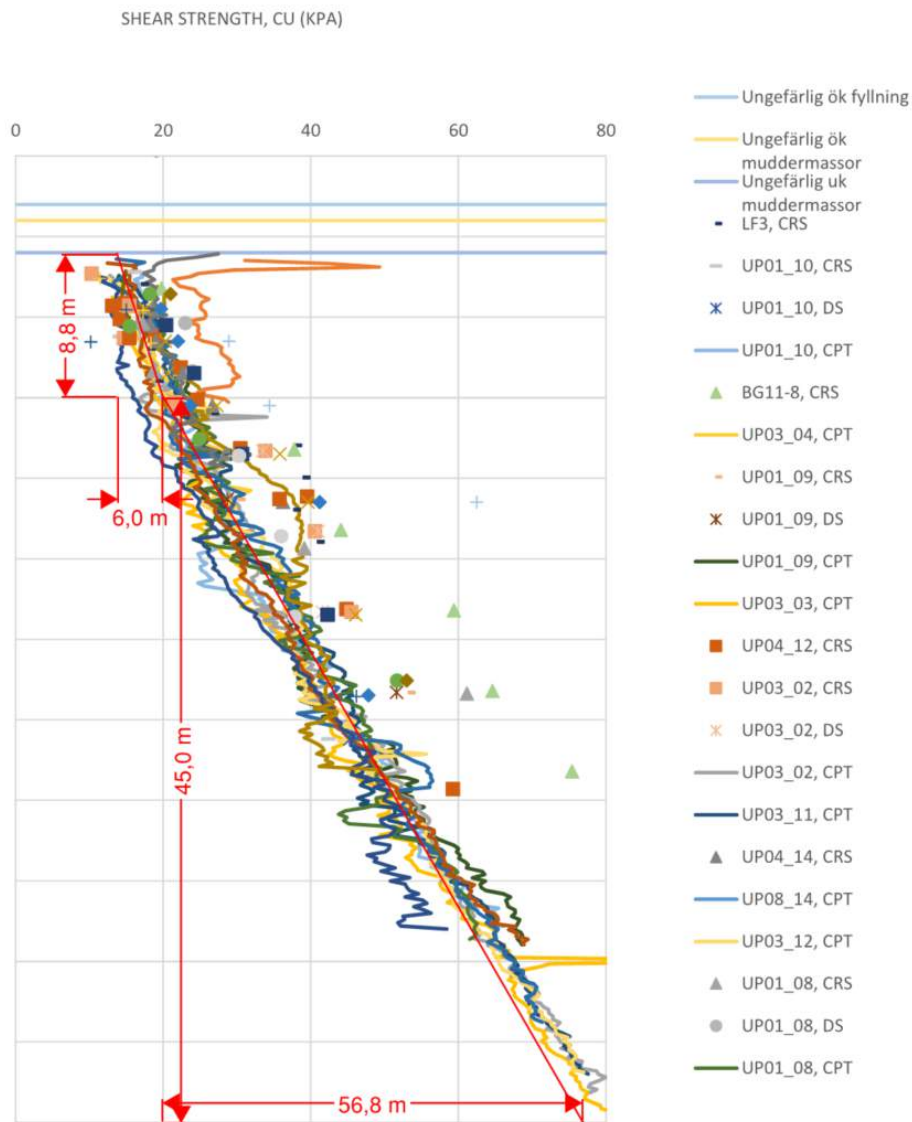


Figure A.57: Shear strength trend evaluation

A.5 Stress distribution evaluation

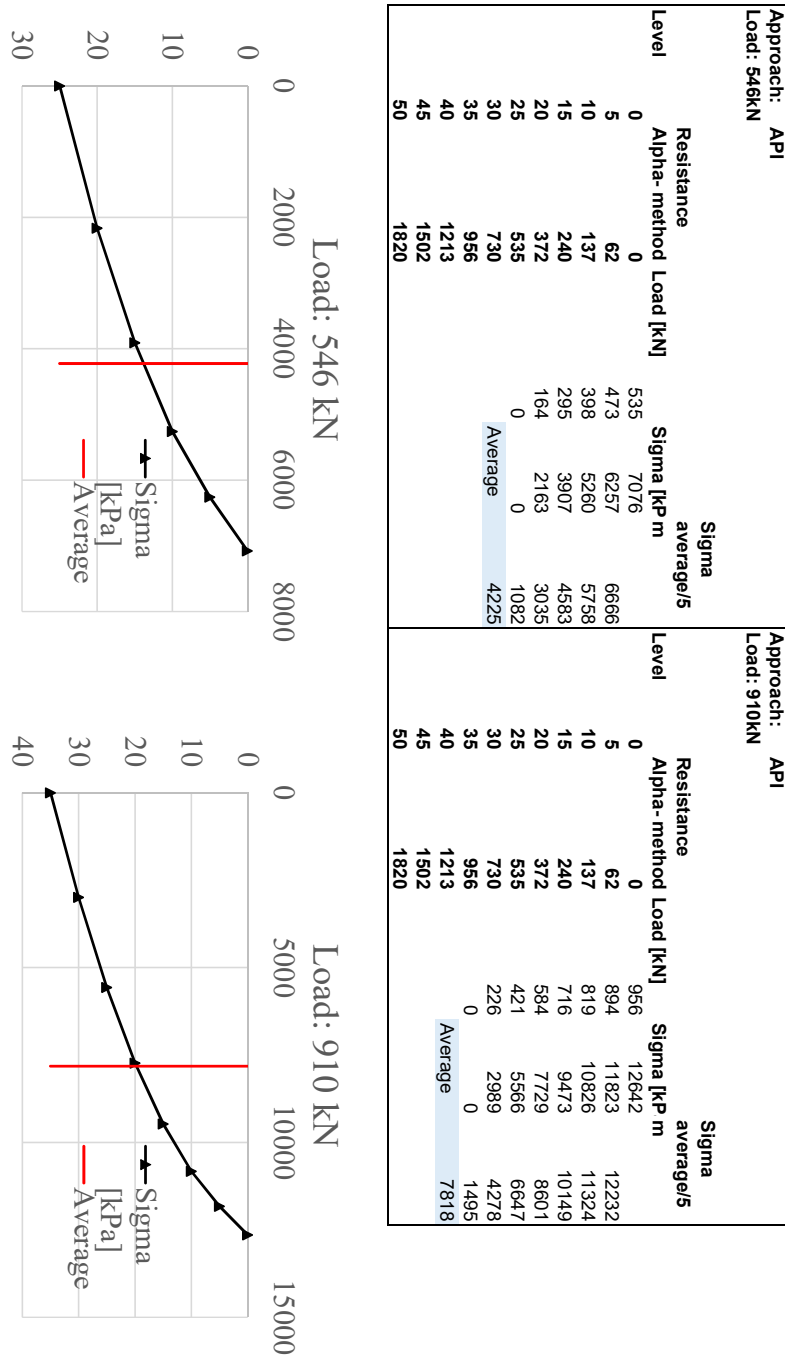


Figure A.58: Average stress evaluation for loading step 546 kN and 910 kN, API approach

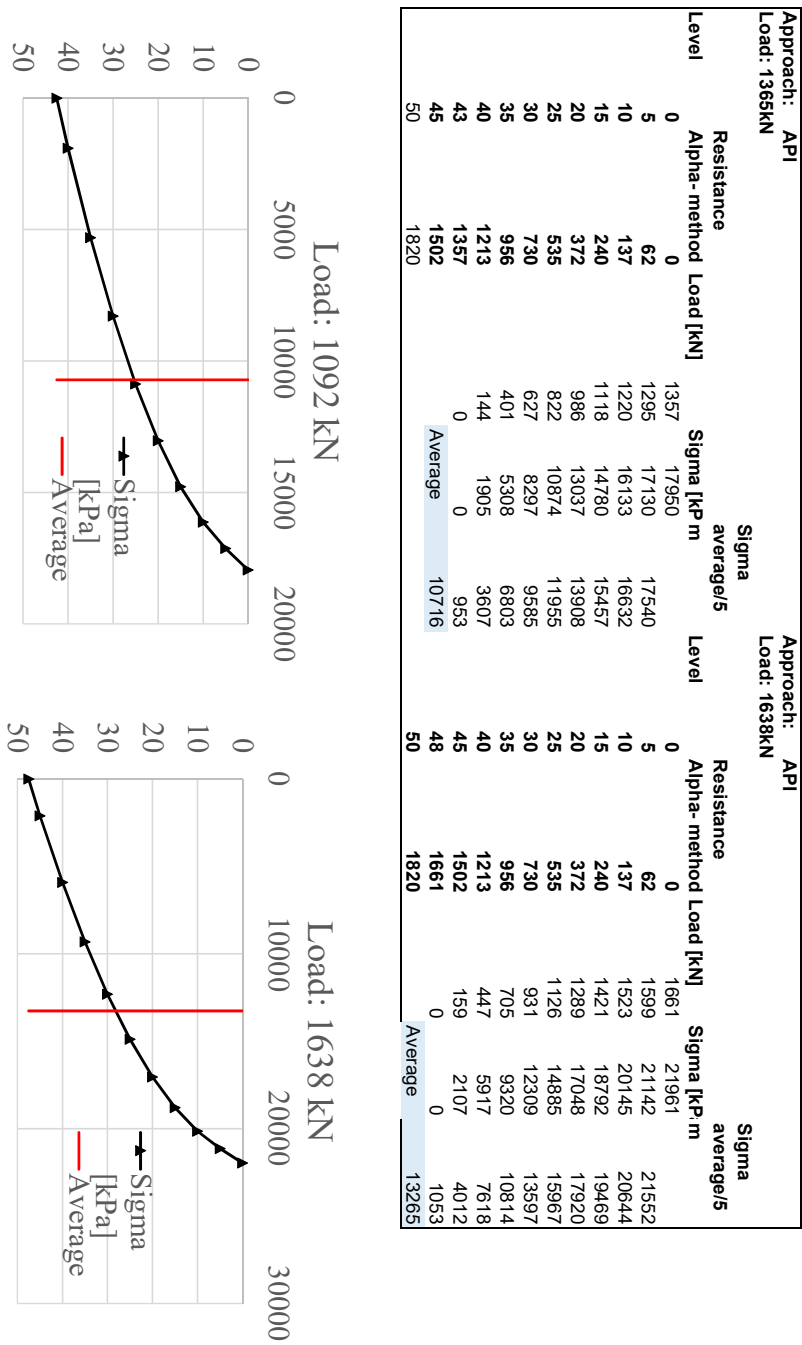


Figure A.59: Average stress evaluation for loading step 1365 kN and 1638 kN, API approach

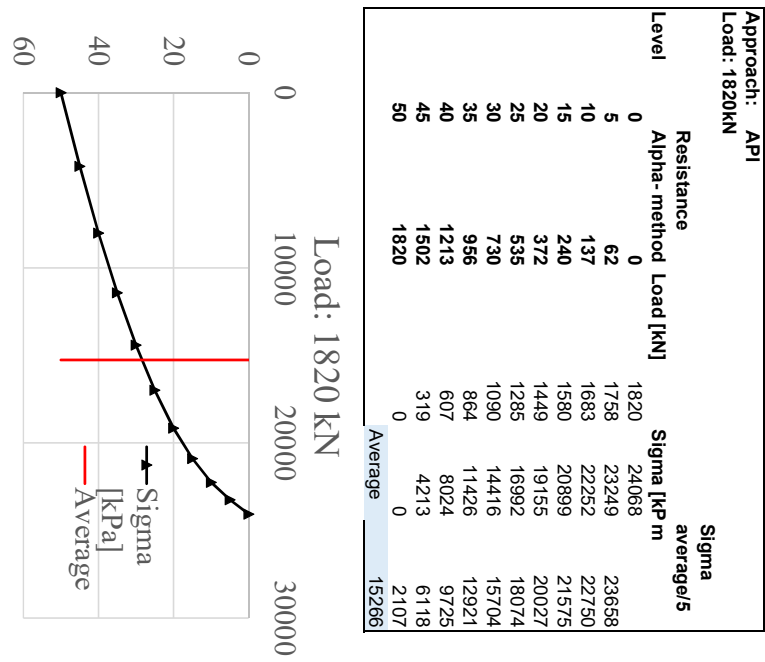


Figure A.60: Average stress evaluation for loading step 1820 kN, API approach

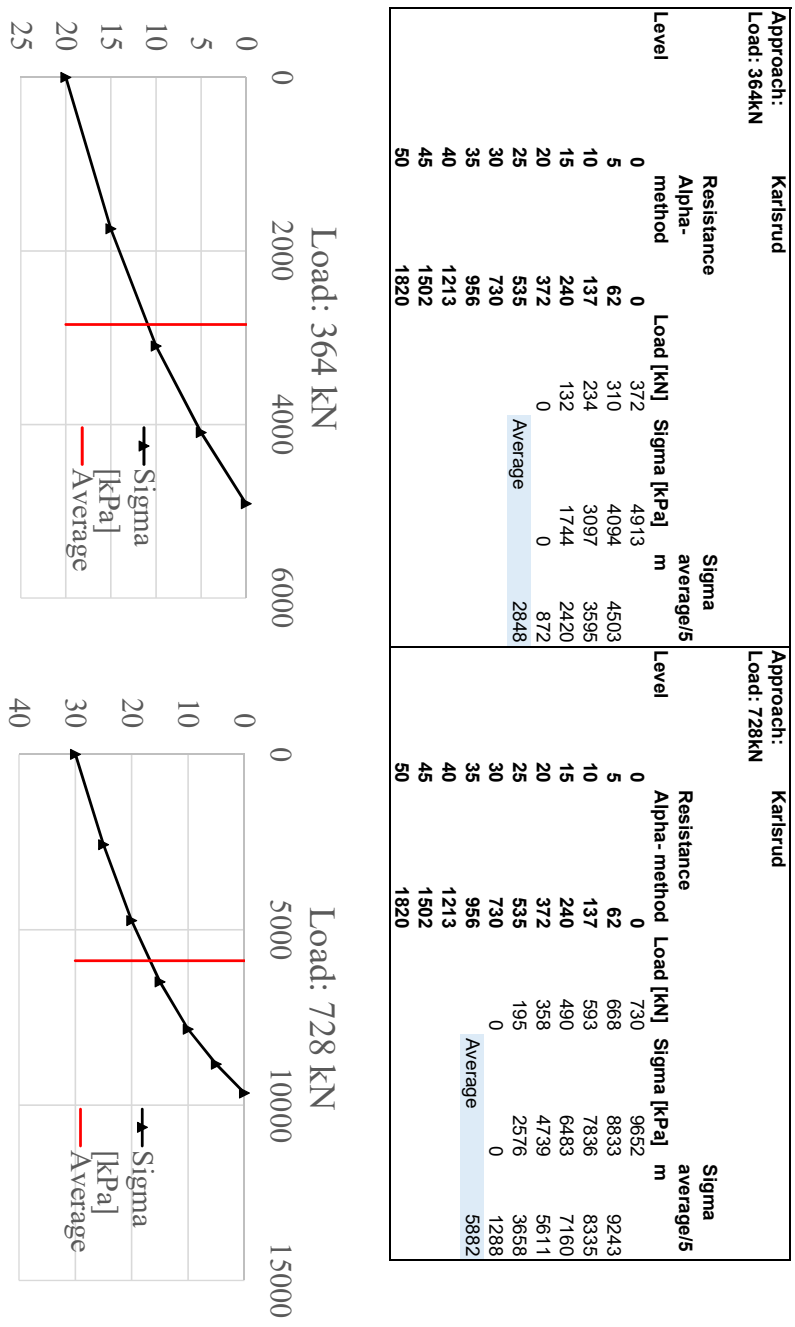


Figure A.61: Average stress evaluation for loading step 364 and 728 kN, Karlsruds approach

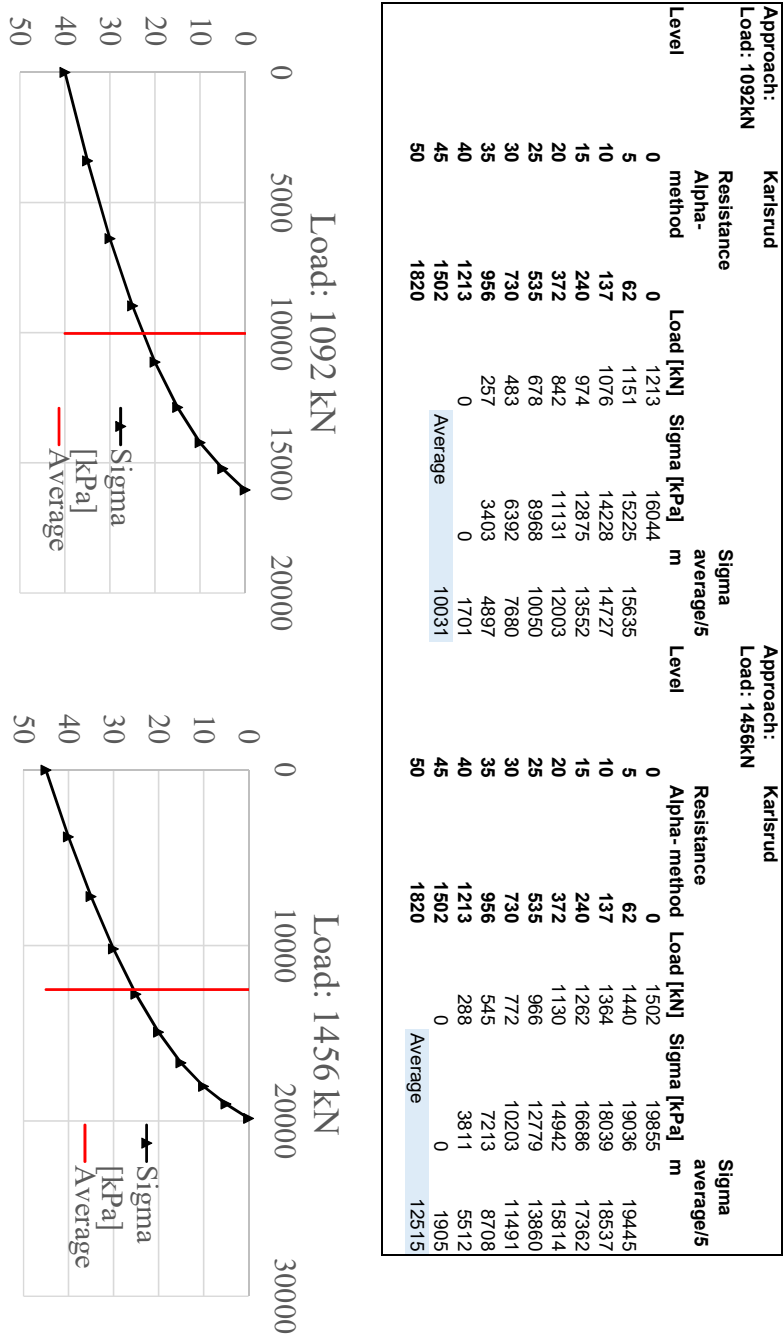


Figure A.62: Average stress evaluation for loading step 1092 and 1456 kN, Karlstruds approach

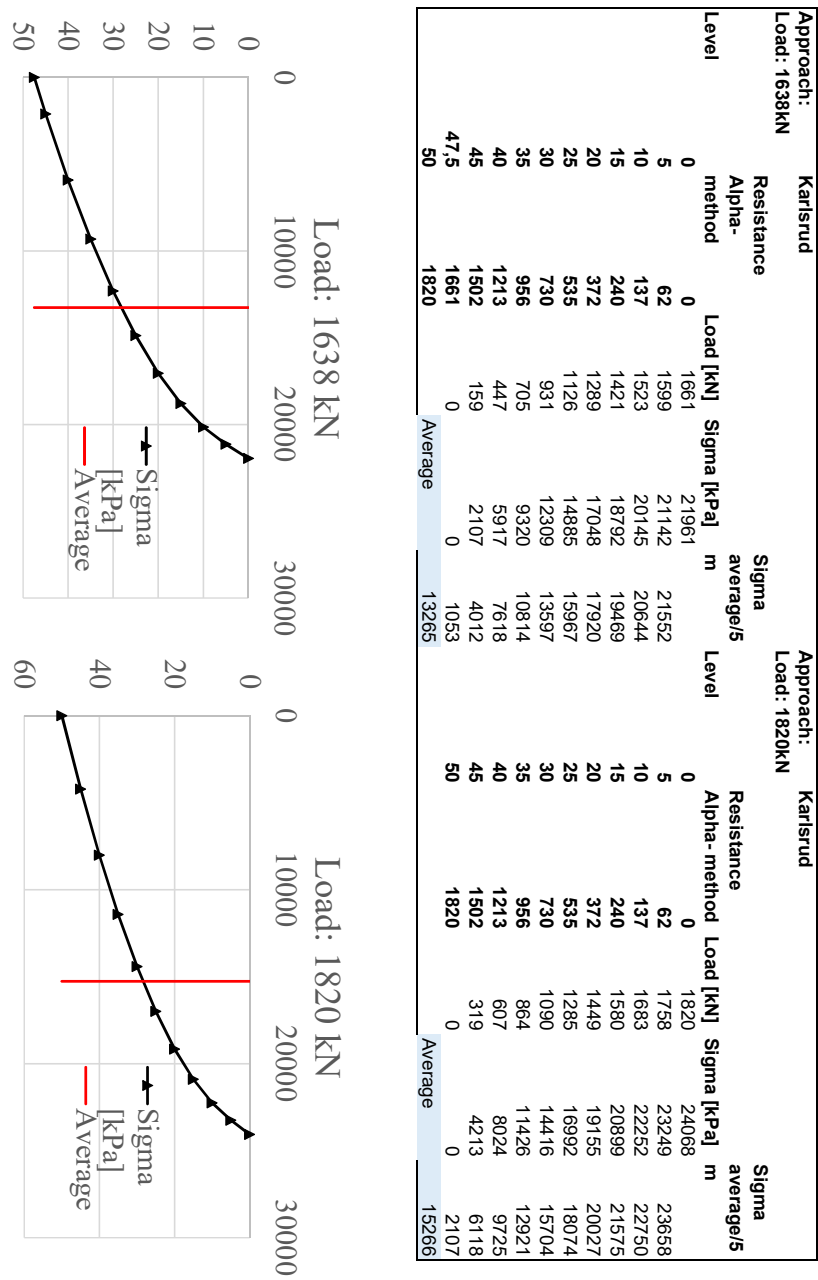


Figure A.63: Average stress evaluation for loading step 1638 and 1820 kN, Karlstruds approach